An-Najah National University

Faculty of Graduate Studies

FUNCTIONALIZATION OF ANTICANCER NATURAL COMPOUNDS (CITRONELLOL, *P*-COUMARIC ACID, *CIS*-JASMONE, AND THYMOL): PREPARATION, CHARACTERIZATION, AND CYTOTOXIC ACTIVITY

By

Nehaya Mohammed Yousef Salameh

Supervisors

Prof. Mohammed Al-Nuri

Prof. Nidal Jaradat

This Dissertation is Submitted in Partial Fulfillment of the Requirements for the Degree of PhD in Chemistry, Faculty of Graduate Studies, An-Najah National University, Nablus, Palestine.

2024

FUNCTIONALIZATION OF ANTICANCER NATURAL COMPOUNDS (CITRONELLOL, *P*-COUMARIC ACID, *CIS*-JASMONE, AND THYMOL): PREPARATION, CHARACTERIZATION, AND CYTOTOXIC ACTIVITY

By
Nehaya Mohammed Yousef Salameh

This Dissertation was Defended Successfully on 09/03/2024 and approved by

Prof. Mohammed Al-Nuri	
Supervisor	Signature
Prof. Nidal Jaradat	
Co-Supervisor	Signature
Prof. Orwa Houshia	
External Examiner	Signature
Prof. Ismael Warrad	
Internal Examiner	Signature
Prof. Mohyeddin Assali	
Internal Examiner	Signature

Dedication

I dedicate my thesis to the spirit of my deceased parents and the spirit of my deceased sisters, and I dedicate this work to my sisters and brothers and to everyone who contributed to the success of this thesis.

Acknowledgement

First, I would like to thank Almighty Allah, for letting me through all the difficulties. I have experienced your guidance day by day. You are the one who let me finish my degree. I will keep on trusting you for all of my life.

I would like to acknowledge and give my warmest thanks to my supervisor Prof. Mohammed Al-Nuri and co-supervisor Prof. Nidal Jaradat who made this work possible. Their guidance and advice carried me through all the stages of working and writing my thesis.

I would also like to thank Dr Mohyeddin Assali for his help searching for the novelty of the new compounds that were synthesized in this thesis.

I would also like to thank my committee members for letting my defense be an enjoyable moment, and for your brilliant comments and suggestions, thanks to you.

I would also like to give special thanks to my family as a whole for their continuous support and understanding when undertaking my research and writing my thesis. Your prayer for me was what sustained me this far.

I would also like to thank prof. Ismael Warrad, thank you for helping with the NMR analysis of some samples in Qatar.

I would also like to thank and Inas Bsharat, Renad Hamed, Saber Abo-Jabal for helping in NMR analysis in Jordan.

I would also like to thank Dr. Nawaf Al-mahariq for answering our questions in the laboratory

I would also like to thank Malak Daqqa, Ala'a Janem, Ebraheem Nassar, Tamara Zorba, Bahieh Abo Lil, Rasha Yaseen, Isra Qadi and all students who were being with me in the laboratory and through my study for my Ph.D degree.

I would also like to thank Ameed Ameereh, Rema, Mohamed Arar, Nafeth Dwekat, Ahamed Muosa, Mohammed Nabeel, Shruq Sobuh, and Abed El-Razeq Abweh for their help through my work on the thesis.

Declaration

I, the undersigned, declare that I submitted the thesis entitled:

FUNCTIONALIZATION OF ANTICANCER NATURAL COMPOUNDS (CITRONELLOL, *P*-COUMARIC ACID, *CIS*-JASMONE, AND THYMOL): PREPARATION, CHARACTERIZATION, AND CYTOTOXIC ACTIVITY

I declare that the work provided in this Dissertation, unless otherwise referenced, is the researcher's own work, and has not been submitted elsewhere for any other degree or qualification.

Student's Name: _____

Signature: _____

Date: 9.03.2024

List of Contents

List of Tables

List of Figures

List of Equations

List of Schemes

List of Appendices

FUNCTIONALIZATION OF ANTICANCER NATURAL COMPOUNDS (CITRONELLOL, *P*-COUMARIC ACID, *CIS*-JASMONE, AND THYMOL): PREPARATION, CHARACTERIZATION, AND CYTOTOXIC ACTIVITY

By
Nehaya Mohammed Yousef Salameh
Supervisors
Prof. Mohammed Al-Nuri
Prof. Nidal Jaradat

Abstract

Functionalizing of natural compounds exhibiting biological activity is one of the most efficient approaches for the synthesizing biologically active substances to improve their pharmacological effects or to investigate new therapeutic approaches.

This study aims to prepare new derivatives of bioactive compounds including citronellol, *p*-coumaric acid, *cis*-jasmone, and thymol by modification of their functional groups and to test their new biological activities whether there is an improvement or decline in these activities.

In our investigation, we follow the methods of preparing new compounds such as esters, amides, anhydrides and amines through condensation reactions of alcohols with carboxylic acids, and through Michael's addition methods. The new compounds were identified by FT-IR and NMR analysis. MTS assay was used to evaluate their anticancer activity. The broth dilution method was used to assess their antimicrobial activity.

Some of the new derivatives of natural products showed anticancer and antimicrobial activities more potent than the starting natural compound and others showed lower potency than the starting natural compound that was used to prepare new derivatives, but better preserving normal cell line.

The newly synthesized derivatives were successfully prepared, and their structures were verified by spectroscopic analysis. Their biological activities were tested against different cancer lines and microbial strains. Among the citronellol esters: - **J15** was the most potent against liver cancer Hep-G2. The *p*-CA ester **J14** was the most potent anticancer agent against CaCo-2, Hep-G2, HeLa, and MCF-7 cancer cell lines, **J14** also showed distinctively higher activity against all microorganisms except *Pseudomonas aeruginosa*.

The *p*-CA amide **J19** showed antimicrobial activity against *Escherichia coli*, *Proteus vulgaris*, *Pseudomonas aeruginosa*, and *Candida albicans*. The *p*-CA anhydride **N2** was the most potent against Hep-3B and MCF-7 cell lines while **N4** was the most potent against HeLa cell lines**.** Among the *cis*-jasmone amines, **N6** was the most potent against HeLa, and B16-F1cell lines. The amine **N8** showed distinctively highest antimicrobial activity against *Klebsiella pneumoniae, P. vulgaris*, *P. aeruginosa*, and *C. albicans*. The thymol ester **J16** was the most potent against CaCo-2, Hep-G2, HeLa, MCF-7, and skin cancer B16-F1 and showed distinctively highest activity against all microorganisms except against *E. coli* **J12** was the most potent.

Keywords: Natural anticancer compounds, Citronellol, Thymol, *cis*-Jasmone, *p*-CA.

Chapter One

Introduction

Functionalizing of natural compounds showing biological activity is one of the most effective methods for the synthesis of biologically active substances in order to improve their pharmacological effects or to investigate new therapeutic approaches. Actually, derivatizations are creative processes of finding new medication based on the knowledge of a biological target. Traditional methods of semi-synthesis of anticancer drug derivatives include the esterification of compounds or the addition of nucleophiles to α,β-unsaturated carbonyl compounds. Cancer is considered an important cause of death and an important obstacle to increasing the average period that a person may expect to live in every country in the world [1]. According to the World Health Organization (WHO) estimations in 2019, cancer is the first or second leading cause of death before the age of 70 years [2]. The Global Cancer Statistics 2020 **(**GLOBOCAN 2020) estimates that there were 19.3 million novel cases of cancer and almost 10 million deaths from cancer in 2020. The total of cancer cases reported in the West Bank in 2018 was 3,106 (corresponding to about 105 cases per 100,000 inhabitants). The number of cancer cases showed a steady increase between 2000 and 2018, at a level of about 6.5% per year. Data point out that radiotherapy and chemotherapy cost about $ 5 and $10 million, respectively [3]. Numerous researches have shown that natural products provide an wide range of biological activities such as antibacterial, antiviral, anti-inflammatory, antioxidant, immune system stimulation, anti-hepatotoxic, antiulcer, anticancer effects and anti-mutagenic [4]. In general, natural products contain a wide range of biologically active phytochemicals, including phenolic, glycosides, flavonoids, carotenoids, alkaloids and heterocyclic compounds that contain nitrogen, oxygen, and sulfur atoms, which have been shown to control early and late stages of cancer [5]. A number of important new marketable medicines have been made from natural resources, by structural changing of natural compounds, or by preparing new compounds that have been designed using the natural compounds as starting materials or models. The look for a better cytotoxic drug remains an important challenge in the finding of new antitumor drugs, achieved by molecular functional groups modification of the main compounds and capable of producing structural analogs with better pharmacological effect [6]. This study aims to prepare new derivatives of bioactive compounds by changing the groups having a special

activity of known natural anticancer substance and to test their new biological activities whether there is an improvement of biological efficiency and activity or there is a decline of such activity. In attempt to improve the biological effect of these substances, to reduce the ailment gravity, and to reduce societal and economic costs associated with healthcare. The following are anticancer natural products that have been functionalized and evaluated for their cytotoxicity.

1.1 Cancer

Cancer is defined as uncontrolled growth and spread of abnormal cells in the body and it can lead to death if left untreated. Cancer is mainly caused by endogenous factors like immune disorders, inherited genetic mutations, hormonal imbalances but mostly affected by the exogenous factors, for example unhealthy diet, tobacco smoke or chewing, environmental chemicals, certain organisms, and other different agents. Cancer can be treated by different methods like hormonal drugs, surgery, radiation therapy, antineoplastic chemotherapy, immune modulators and drugs specifically directed towards cancerous cells [7]. But no suitable result has been obtained from any of these methods. Therefore, there is a need to conduct research on the use of bioactive or synthesizing analog compounds in treating cancer. It is expected to provide a drug with more selectivity, lower toxicity, and higher activity. In latest years, plant extracts are used as chemo-preventive and chemotherapeutic compounds applied in the prevention of cancer because of their usefulness in research [6, 8].

Different types of cancer have been discovered, breast cancer is one of the primary and second most common malicious diseases that affect women across the world. In 2022, there were 2.3 million women detected with breast cancer and 670 000 losses universally. Breast cancer occurs in every country of the world in women at any age after teenage years but with increasing rates in later life. Female sex is the strongest breast cancer risk factor. Nearly 99% of breast cancers happen in women and 0.5–1% of breast cancers arise in men. Assured factors raise the risk of breast cancer including family history of breast cancer, increasing age, obesity, history of radiation exposure, harmful use of alcohol, postmenopausal hormone therapy, and tobacco use. Different types of treatment are used depending on the cancer stages, these treatments include surgery to remove the breast tumor, radiation therapy to reduce recurrence risk in the breast and nearby tissues and

medications to kill cancer cells and avoid spread, including chemotherapy, hormonal therapies, or directed biological treatments [9].

Colorectal cancer (CRC) can cause severe harm and death; it is a type of cancer that touches the rectum or colon (large intestine). It is one of the most common types of cancer global. People over 50 years old are susceptible to the risk of colorectal cancer that increases with age. The known symptoms include abdominal pain, diarrhoea, constipation, blood in the stool, low iron levels, fatigue and unexplained weight loss. Many people will not have signs in the early stages of the ailment. Staying physically active, eating a healthy diet and not smoking tobacco can reduce the risk of colorectal cancer. Regular screenings are crucial for early detection. Colon cancer is the second principal cause of cancer-related deaths global. In 2020, it was estimated that more than 930 000 deaths and higher than 1.9 million new cases of colorectal cancer have happened global. Different types of treatments for colorectal cancer are available and depend on the type and progression of the cancer and the person's medical history. Early detection of colorectal cancer can lead to better treatments and outcomes. These types of treatments consist of: surgery, radiotherapy (radiation), chemotherapy, targeted therapy and immunotherapy [10].

Cervical adenocarcinoma is the fourth most common cancer in women, with around 660 000 new cases in 2022 around the world. In the same year, about 94% of the 350 000 deaths caused by cervical cancer occurred in low- and middle-income countries. The risk factors include HIV occurrence and social and economic factors such as poverty, sex, and gender biases. Cervical cancer extremely affects younger women, and as a result, 20% of children who lose their mother due to cervical cancer. If cervical cancer is identified at a primary stage, surgery and/or radiotherapy are the main treatment choices and can provide long-term survival and/or cure. More progressive cases of cervical cancer are usually treated using a combination of chemotherapy and radiotherapy [11].

Hepatocellular carcinoma (HCC) generally called liver cancer (LC), is the second important cause of cancer-related death and its occurrence is increasing worldwide. Around 50% of patients with HCC receive systemic therapies [12]. HCC positions the fifth among common cancers in the world, which outcomes in poor diagnosis and no effective systematic management options available for patients at present. Unfortunately, it shows an annually increasing incidence universal and mainly in developing countries.

Along with reports, various risk factors could result in hepatocarcinogenesis, including cirrhosis, chronic hepatitis B virus (HBV) or hepatitis C virus (HCV) infections, carcinogen exposure (such as aflatoxin B1), a number of genetic and epigenetic alterations and excessive alcohol drinking. Since LC is considered as high chemoresistance, liver replacement or surgical resection may offer an early cure in LC, but still be unsuccessful to the majority of patients (>80%) with undetectable advanced disease. Hence, this highlights the need for looking for new compounds with greater activity and fewer side effects for chemoprevention and treatment [13].

Skin cancers are produced mainly by exposure to ultraviolet radiation (UVR), either from the sun or from synthetic sources such as sunbeds. Worldwide in 2020, over 1.5 million cases of skin cancers were detected and over 120 000 skin cancer-related deaths were stated. Extreme sun exposure in adolescents and children contributes to skin cancer in future life. A certain amount of UV exposure is beneficial to health, in particular for vitamin D. Effective and simple avoidance methods are obtainable [14].

Skin cancer is the most common kind of cancer global, and its occurrence continues to rise. It is generally divided into cancers originating from melanocytes (melanoma) and from the epidermally resulting cells (non-melanoma skin cancers). These sets represent the common of skin cancers (95%), with other skin tumours thus making up only a very slight percentage. Their high incidence and frequent occurrence makes them a main public health problem. The danger of developing skin cancer rises from a combination of environmental and genetic factors, the most common source being prolonged exposure to ultraviolet (UV) light [15].

The protective measures contain decreasing exposure to UV light and the sun. The primary finding of skin cancer significantly decreases both short- and long-term illness and death. The handling and follow-up with the doctor for melanoma patients may differ for the reason that the stage of the tumor and the primary lesion. The classic therapy for malignant melanoma is surgical removal, immunotherapy such as interleukin 2 (IL-2), biochemotherapy, and gene therapy [16].

The choice to make surgery can be affected by diverse thoughts including the co-illnesses of the patient and probable intolerance of the tissue, as well as the patient, for frequent courses of treatment. In some circumstances, topical treatment may be more suitable,

mainly when surgical intervention is prohibited by the patient or not possible. In fact, topical therapy is usually recommended for patients presenting with field cancerization or multiple clinical and sub-clinical injuries over a large anatomical area. Treatment with topical means may also allow for greater drug levels at site of the tumor, with possibly less toxicity to the patient than systemic agents [17].

Natural products, or compounds derived from natural products, have a massive possible for the improvement of chemotherapeutic means owing to the extensive structural diversity they show. Demonstration of this point is the fact that 49% of the total number of molecules agreed for use against cancer between 1981 and 2014 were produced directly from, or based on, natural products [18].

1.2 Functionalization of natural compounds

Functionalization of natural compounds having biological activities such as anticancer antimicrobial and antioxidants is attracting issue for researchers, as the production of new biologically active derivatives beginning from natural compounds is a skillful tool to increase their properties. Actually, functionalization is a appreciated policy to overcome natural compounds monoterpenoids phenols side effects for example low water solubility, toxicity, in addition to reduce their tough smells, that often limit their application. Furthermore, the synthesis of conjugate type compounds with the character of the multi-aim drug is an enormous hope in the treatment of civilization diseases such as infection and cancer [19]. For example, the olive oil in the Mediterranean diet is a healthy manner of living and eating these days. This type of diet has been greatly respected and is broadly known for being connected with many satisfactory properties, such as lower occurrence of different long-lasting ailments and extended long life. The phenols in olive oil despite their minor presence in olive oil they seem to be the part that responsible on olive oil bioactivity for example the antioxidant activity of tyrosol (2-(4-hydroxyphenyl)-ethanol) abundant in olive oil phenols can be reasonably improved by esterification of the alcoholic hydroxyl with different phenolic acids [20, 21]. The caffeic acid (3,4-dihydroxybenzoic acid) abundant in tea and coffee has anticarcinogenic, antioxidant, and anti-inflammatory activity. The esterification of caffeic acid to produce caffeic acid phenethyl ester improved the anti- inflammatory activity of caffeic acid for the treatment of severe lung harm [22]. Ursolic acid (UA) is a triterpenoid phytochemical that is enhanced in various plants. UA has showed anticancer activity through hindering

proliferation, destroying DNA replication, inducing Ca^{2+} release, and activating caspase (is a family of protease enzymes playing crucial roles in programmed cell death) in several cancers, including leukemia, breast carcinoma, melanoma, prostate cancer and hepatoma. Colorectal carcinomas often are linked with resistance to 5-fluorouracil. UA was able to inhibit the growth of altered cells, which are resistant to apoptosis, and of colorectal cancer cell lines independent of caspases. Studies conducted on UA explained that in combination with zoledronic acid, a third-generation, nitrogen-containing bisphosphonate active in the treatment of bone metastases, considerably prompted cell death in human osteosarcoma cells [23].

Quinolones and their derivatives have been the most widely studied heterocyclic compounds, regarding their recognized biological activity, strong safety profile, high bioavailability, and low degree of binding to plasma proteins. Many naturally plant-derived and synthetic quinolones have shown *in vitro* and *in vivo* anticancer activity, and few of them are currently used in clinical treatment. Quinolones represent a core source in drug development, having skeleton fortunate for the various structural modifications at almost any position of the quinolone ring, giving compounds with altered chemical and pharmacological properties. Several studies reported syntheses and characterization of organotin(IV) complexes with fluoroquinolones as ligands. Novel diphenyltin(IV) complexes were synthesized by merging two biologically active compounds into one single molecular skeleton, giving thus drugs with better pharmacological profile, which could be considered as potentially new anticancer agents. From them *bis*(3-(4-methyl-2-oxoquinolinyl-1(2H)-yl)propanoato)diphenyltin(IV) encourages apoptosis followed with strong blockade of cell division in colorectal carcinoma (HCT116) cells. Since the newcompound showed reactive oxygen species (ROS) and reactive nitrogen species (RNS) scavenging potential mentioned cytotoxicity [24].

1.3 Citronellol

Citronellol (Figure 1) is an acyclic monoterpenoid, colorless oily liquid with an antioxidant, antifungal, antimicrobial, anti-inflammatory, and possibly a chemo-preventive component [25-29]. Citronellol is the main ingredient of citronella oil [30]. Citronella oil is a bioactive substance extracted from the Lemongrass plant, related to *Cymbapogon* genus and to the *Poaceae* family [31]. Citronella oil is an important essential oils in world trade and is broadly used in the food, cosmetics, perfume, and drug

industries [32]. Citronellol has been reported to be active against cancer cell propagation, inhibition of DNA synthesis and encouraging the reactive oxygen species (ROS) generation, which cause damage to biological membranes through oxidative stress [29, 33]. Citronellol has been testified to possess strong antioxidant, anti-diabetes, anti-inflammatory, cardioprotective and anticancer activities [34-36]. Citronellol has been reported to show an anticancer effect against leukemia (HL60) at 50 µg/mL value of IC_{50} [37]. A study conducted by Rajendran *et al*., indicated that citronellol encourages apoptosis as evidenced by the loss of cell viability, increase ROS generation, and enhanced DNA damage. Citronellol encourages apoptosis in MCF-7 human mammary tumor cells by prompting oxidative damage and modulating the expression of various pro and anti-apoptotic proteins. And concluded that citronellol might be a potential therapeutic agent for the treatment of breast cancer [38]. Esters were synthesized from citronellol to improve its anticancer activity; Citronellyl isobutyrate (CIB) and citronellyl 2,2-dimethyl butyrate (CDB) have been prepared by using sodium hydroxide as a catalyst were reported to active against breast cancer cells (MCF7) at IC_{50} values of 2.82 and 4.75 µg/mL, respectively [39]. Furthermore, linking caproate synthesized from citronellol and caproic acid in palm kernel oil has also been stated to be effective in reducing *murine leukemia* (P388) cells growing through the increase of its cytotoxic activity. The IC_{50} of 38.49 and 10.63 µg/ml have also been found to inhibit 50% of *murine leukemia* (P388) cells growth [40].

Figure 1

Citronellol Structure

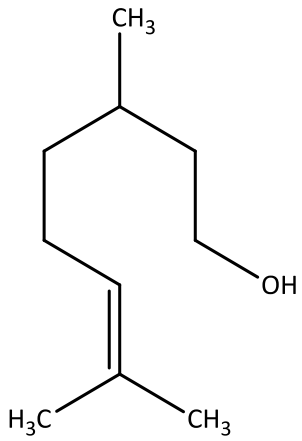

1.4 *p*-Coumaric acid

One of the hydroxy cinnamic acid derivatives is coumaric acid and is presented in three isomers; *ortho*- (*o*-), *meta*- (*m*-), and *para*- (*p*-) coumaric acids, *p*-coumaric acid *(p*-CA) is the most plentiful, (Figure 2) [41]. 4- Hydroxycinnamic acid is another name for *p*-CA [42]. Many cereals (coffee, maize, and wheat), fruits (strawberries, apples, and pears) and vegetables (tomatoes, carrots, and onions), contain *p*-CA [43, 44]. *p*-CA is free form or conjugated to other molecules, such as amines, organic acids, alcohols, and mono- or oligosaccharides, which are more abundant and have stronger biological activities than free *p*-CA in plants [44]. *p*-CA has concerned a great deal of attention due to its biological proprieties and pharmacological, counting antioxidant, cardioprotective, neuroprotective, antiplatelet, antiulcer, antimicrobial, chemoprotective, and anticancer activities. It has been confirmed that *p*-CA is a potential anticancer agent with fewer toxicity in human health. The physiological significance of *p*-CA lies in its availability for intestinal absorption and further interaction with target tissues. A collective proof from several studies showed that conjugated forms of *p*-CA are less available but more bioactive than free *p*-CA. The molecular mechanisms of *p*-CA as a potential CRC avoidance and treatment were studied *in vitro* and *in vivo*. These studies revealed that *p*-CA has a high bioavailability as related to other phenolic acids. *p*-CA can show anticancer activity by different mechanisms: oxidative stress and modulating inflammation, inducing apoptosis, stopping cell cycle progression, changing cellular proliferation pathways, and increasing sensitivity to chemotherapeutic drugs. Together, these properties make *p*-CA an encouraging nutraceutical applicant for phytochemical-based strategies to reduce CRC occurrence and morbidity [45]. The cytotoxic effects of *p*-CA have been clarified, against human colorectal carcinoma (CRC), while no significant effects were observed against healthy colon cells [46]. A study on *p*-CA, isolated from Brazilian green propolis extraction, showed efficacy on mouse tumor growth and progression [47]. *p*-CA also considerably reduces the creation of reactive oxygen species (ROS), which leads to lower the migration, incensement, and adhesion of the cancer cells [48]. *p*-CA with long-chain alkyl esters selectively stimulate apoptosis in cancer cells and are favorable structure for this task [49]. The bulky aromatic groups and electron-withdrawing substituents in esters and amides of *p*-CA derivatives were more potent in biological activities than other derivatives [50]. It was confirmed that an amide of *p*-CA containing isobornyl groups in *ortho*-positions relative to the phenolic hydroxyl with a morpholine part has the highest

antioxidant activity among other derivatives such as esters. The stated derivative significantly exceeded the reference substances *p*-CA, and 2,6-di-*tert*-butyl-4-methylphenol (BHT) known antioxidant agent [51].

Because the esterification of *p*-CA improved its activity as an antimelanogenic agent, a modifications on the carboxylic acid moiety of *p*-CA to generate more lipophilic and neutral ester analogs completely contribute to the gain in the cytotoxic and antiproliferative activity against the human and murine cancer cell lines. Moreover, the more lipophilic compound *n*-butyl *p*-coumarate rather than ethyl *p*-coumarate is underlined as a promising anticancer agent and a potential prototype for further modification to achieve more active compounds. The two new ester derivatives of *p*-CA were tested against the murine B16-F10 and the human SK-MEL-25 melanoma cells. While *p*-CA, at the concentration of 1 mM, unsuccessful to give a significant antitumor activity, the ethyl and butyl ester derivatives caused substantial tumor cell death at doses < 1 mM. Regardless of a reduction in their direct cytotoxicity at minor doses, both products controlled the melanoma growth by stopping the cell cycle. Besides, the *in vivo* experiments showed that the butyl ester derivative inhibited the lung B16-F10 problem, compared to the *p*-CA-treated mice. Thus, the esterification of *p*-coumaric acid enhanced the control over the proliferation of human and murine melanoma cells and can be well-thought-out an method for designing new anticancer agents [52].

Figure 2

p-CA Structure

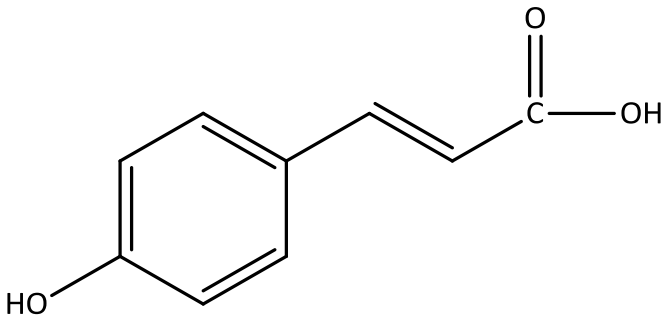

1.5 *cis*-Jasmone

cis-Jasmone is the most significant component among a hundred components in jasmine essential oil (Figure 3) [53]. Jasmone is a colorless to pale yellow volatile oil extracted from jasmine flowers. *cis* and trans-jasmone are two isomers of jasmone with differing geometry around the pentenyl double bond. *cis*-Jasmone is the only natural form, while synthetic jasmone can be obtained as *cis*- and trans forms, but *cis*-jasmone is the dominant one. Both forms have the same chemical properties and the same odor [54]. *cis*-Jasmone was originally discovered and characterized as a minor (3%) ingredient of jasmine absolute [55, 56]. Additionally, *cis*-jasmone odor is related to the odor of orange (*Citrus sinensis*), peppermint oil (*Mentha piperita*), tea (*Camila sinensis*), and, of course, Jasminum leaves [57]. *cis*-Jasmone is also released from leaves that have been crushed by animals, attracting the scientist's attention [58, 59]. *cis*-Jasmone attracts the pest's parasitoids and repel aphids [60, 61]. Furthermore, secondary metabolites selectively produced by the induction of *cis*-jasmone can decrease the pest's growth [62]. Perfumes and cosmetics largely contain jasmone so it has a commercial benefit [56]. *cis* -Jasmone is related to jasmonate stress hormones family that are produced by plants when are injured or attacked by insects [63], and *in vitro cis*-jasmone has been shown to reduce growth as well as induce apoptosis in leukemia and lung cells, as the jasmonate compounds have been specified to act directly on the mitochondria in T-lymphoblastic leukemia cells [64-66]. A study conducted by Tong *et al*., verified that *cis*-jasmone inhibited cell proliferation and encouraged apoptosis in SH-SY5Y human neuroblastoma cell line [67].

Progressive prostate cancer cells are normally hormone independent, unaffected to apoptosis and do not answer to chemotherapeutic agents. The capability of methyl jasmonate (MJ) and cisjasmone (CJ) to constrain growth in hormone independent prostate cancer cell lines, PC-3 and DU- 145, was assessed. CJ and MJ reduced cell growth, encouraged cell cycle capture and apoptosis. Comprehensive studies with the PC-3 cell line discovered that 2 mM CJ or MJ management resulted in caspase 3 stimulation and Tumor Necrosis Factor Receptor 1 (TNFR1) motivation, all hallmarks of apoptosis. These phytochemicals could be useful in the controlling of advanced prostate cancer [68].

Figure 3

cis- Jasmone Structure

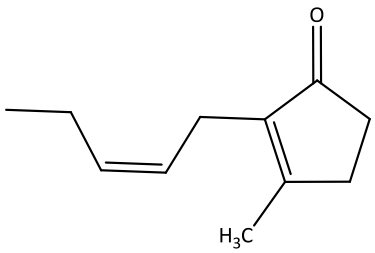

1.6 Thymol

Thymol (Figure 4) a natural compound is an isomer of carvacrol and a phenolic derivative of cymene. The main ingredient of the essential oils of a medicinal plant with several therapeutic properties' thyme (*Thymus vulgaris* L., Lamiaceae), is thymol (10-64%). The thyme plants are related to Mediterranean regions. They were used throughout history for food and medicinal purposes. These days, thymol and its plants are used in different fields of food, medicinal and cosmetic industries. Several studies have shown the various potential therapeutic uses of thymol in the treatment of different diseases that affect cardiovascular, respiratory and nervous systems in addition to antiviral, antibacterial proprieties, Anti-inflammatory, and antispasmodic activities, as well as a potential as a growth enhancer and immunomodulator [69-72]. Thymol, gained from thyme (*Thymus vulgaris*), has been proposed to sensitize certain cancer types to radiation, while defending against treatment side effects in the normal tissue. *In vitro* studies have established its radioprotective properties in lung tissue as a result of its anti-oxidant belongings. The taking of thymol prior to irradiation in hamster lung fibroblasts caused in a reduction of radiation-induced necrosis and apoptosis, facilitated through the prevention of radiation-induced DNA harm and mitochondrial membrane breakdown. In addition, thymol alleviated radiation-induced oxidative stress via a reduction in ROS levels and lipid peroxidation, as well as a hindrance of the radiation-mediated reduction of antioxidant enzymes [73]. Thymol extracts from thyme showed different anticancer activity against breast cancer with apoptosis percentage of 82.67; 80.98; 73.13; 72.28; 60.62; 27.74 and 98.43%, in different solvents of thyme extacts methanol, chloroform, ethyl acetate, ethanol, dichlorometane, n-Hexane and doxorubicin respectively. Among all extracts, methanol extract showed the highest apoptosis and caspase-3 activation

percentage. Thus all thyme extracts had anticancer properties in breast cancer cell line although efficacy of each solvent extract was differed [74].

Through different mechanisms, thymol shows anticancer activity; by lowering cell growth, producing reactive oxygen species (ROS) inside cancer cell and encouraging apoptosis [75, 76]. Sisto *et al*. demonstrated that the growth-lowering effect of cancer cells is not restricted to the effect of the free OH functional group of the phenolic terpenes but also chemical modifications can increase the anticancer effect[77]. Thymol derivatives containing furan exhibited promising antitumor activity[78]. The phenolic structure of thymol increases its antioxidant activity as the oxidation and reduction properties of thymol adsorb, neutralize free radicals and decompose peroxides. Many Thymol derivatives were investigated for structure-radical scavenging activity [79]. Functionalizing through the esterification of the thymol hydroxyl group with chloroacetyl chloride and *p*-CA exhibited a potent antioxidant activity with IC_{50} = 11.30 μM, which is lower than the standard IC_{50} = 24.20 μM of ascorbic acid [80].

Thymol touches various types of cancer cell lines, including colorectal cancer cells. However, the hydrophobic characteristics of thymol avoid its wider use. Therefore, novel derivatives (acetic acid thymol ester, thymol β-D-glucoside) have been produced with respect to hydrophilic characteristics. The new derivatives were evaluated against colorectal cancer cell lines HT-29 and HCT-116, genotoxic effect and ROS production. The new derivative of thymol derivatives (acetic acid thymol ester) has the potential to have a cyto/genotoxic effect on colorectal cancer cells, even at much lower (IC_{50}~0.08 μg/mL) concentrations than standard thymol (IC_{50}~60 μg/mL) after 24 h of treatment. The cytotoxic effect of the tested derivatives of thymol on the colorectal cancer cell lines was found to be both dose- and time-dependent. New derivatives of thymol considerably improved ROS making. The results established that the effect of the derivative on tumor cells is influenced by its chemical structure. However, thymol and its derivatives have great potential in the inhibition and management of colorectal cancer, which rests one of the most common cancers in the sphere [81].Other studies revealed that the presence of an unsaturated double bond in the new synthesized thymol derivatives was the chief factor that governs the antioxidant activity of the investigated compounds [82]. the thymol triphenylphosphine (TPP) conjugates, especially TPP-Thy3 conjugates are a chain of novel antibacterial means and could aid as a new therapeutic strategy for

combating antibiotic resistance. The extraordinary occurrence of methicillin resistant *Staphylococcus aureus* (MRSA) strains and the formation of non-growing, dormant tolerant cell "persisters" subsets help bacteria avoid antibiotic treatment and augment bacterial opposition, which produces a serious hazard to human health and life. It is crucial to find out novel antibacterial remedies active against MRSA tolerant cells. Thymol is a public nutraceutical with weak anticancer and antibacterial activities. A chain of Thymol triphenylphosphine (TPP) conjugates (TPP-Thy3) was considered and synthesized. These compounds displayed considerably enhanced inhibitory effect against Gram-positive bacteria compared with Thymol. Among them, Thy3d showed a little prospect of resistance selection and exhibited exceptional biocompatibility. Remarkably, Thy3d caused a fast murder result of MRSA tolerant cells (99.999%) at elevated concentration, and showed a powerful antimicrobial action by disturbing the solidity of the membrane of bacterial even the tolerant cell. Additionally, Thy3d showed great efficiency in a mouse model of subcutaneous murine MRSA infection. [83]. Thymol's antifungal activity against *Candida albicans*, *Candida tropicalis*, and *Candida krusei* strains was studied to explore its manner and synergistic effect when joined with a synthetic antifungal medication, nystatin. Thymol established antifungal action with a MIC of 78 µg/mL against *C. tropicalis* and 39 µg/mL against *C. krusei* and *C. albicans*. The antifungal action was unaffected by the incidence of sorbitol, but the occurrence of exogenous ergosterol caused thymol's MIC value against *C. albicans* to increase by eight times, from 39.0 to 312.5 µg/mL. The mixture of thymol and nystatin reduced the MIC values by 87.4%. The role of thymol in medicinal chemistry has encouraged many researchers to discover its widespread range of biological activities. Many thymol derivatives have been established and assessed for their biological characteristics; such as aldehydes, azo dyes, ethers, esters, formylation products, glucosides, and Mannich bases. The thymol moiety joined to pyridine, pyrazole, and isoxazole, topics formed compounds with encouraged antimicrobial activities [84]. Additional studies on natural compounds like thymol as leads for drug development against medically important bacterial pathogens are important. Thymol as a natural biological pattern can be improved chemically since the hydroxyl group makes it an applicant for structural alteration. Thymol was combined with triazole moiety to aid increasing its biological effectiveness. All the produced triazole-thymol products exhibited important but different antibacterial activity against the seven medically chief bacterial strains tested. The compound

4-((4-chloro-2-isopropyl-5-methylphenoxy)methyl)-1-(2-nitrobenzyl)-1H-1,2,3triazole confirmed a greater antibacterial action with a mean area of inhibition (38.7 mm) compared with ampicillin as the positive control which gave an area of inhibition 30.0 mm. Furthermore, the compound showed three-time strength than the original compound, thymol (11.0 mm) against MRSA at a concentration of 100 μg/ml [85].

Figure 4

Thymol Structure

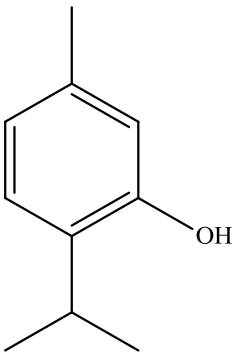

1.7 Esterification

Esters are among the utmost volume of industrial organic combinations produced. They are commonly used in different domestic and industrial practices. Esterification is one of the most important reactions in organic synthesis. The esters are found everywhere both as natural and artificial organic compounds. The most important examples of esterification merchandises are biofuels such as biodiesel, diluents such as methyl acetate and ethyl acetate, pharmaceuticals, paints and varnishes, coatings and plastics, and some are used as pesticides and herbicides. Esters are commonly used as preservatives and flavoring components in food industry, as essential perfume essences, in cosmetic and soap industries as smells or in personal care preparations [86].

In organic chemistry, an ester is a condensation of carboxylic acid with alcohol and this means typically an ester of carboxylic acid, except if some other kind of ester is identified. If the condensation reaction proceeds in acidic condition this is known as Fischer esterification Equation 1 [87].

Equation 1

Fischer esterification

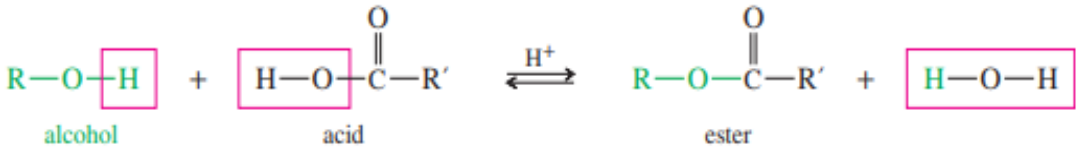

A large excess of alcohol or acid can be used in Fischer esterification to produce a good yield, because this type of reaction is in equilibrium or removes water which is one of the products by dehydrating agent drive reaction toward the product. The reaction is restricted by a low overall conversion due to the formation of thermodynamic equilibrium and slow rate of reaction. Fischer esterification is commercially so important; but it is costly with environmental effect [86].

Another method of producing ester is an exothermic reaction; an alcohol reacts with acid chloride in which unfavorable equilibrium is prevented, Equation 2 [87]. Acid chlorides, have lower commercial availability and high reactivity that causes the acylation reaction sometimes to yield a complicated mixture of products because they are sensitive to moisture [86].

Esterification can also be base-catalyzed. In this type of reaction, the stability of the alcohol C-OH bond and the steric hindrance of alcohol are two important factors; for that reasons, the tendency of esterification of primary alcohol increases [88].

Esterification can be used to enhance the bioactivity activity of natural compounds; Esterification of eugenol obtained new derivatives that were characterized by a high level of antioxidant activity estimated after 24 h of performing the experiment, which indicates durable protection against reactive oxygen species (ROS) in the profounder layers of the skin [89]. The synthesized cellulose amino acid ester showed different antibacterial activity and the bacteriostatic declining rate against *E. coli* can extent 99.5 % [90]. Esterification of drugs with fatty acids can modified the cellular uptake mechanisms of the drug and made it more active in human solid cancer models such as an elaidic acid ester (CP-4200) a derivative of azacytidine, effectively reduces DNA methyltransferase (DNMT) enzymes in all human cancer cell lines analyzed. In addition, CP-4200 showed a significantly improved *in vivo* efficacy when compared with azacytidine. Azacytidine is accepted for the treatment of myelodysplastic syndrome and has also been used

effectively for the clinical management of severe myeloid leukemia. Taken together, these results show a potent epigenetic regulatory activity for CP-4200 and propose that elaidic acid esterification of azacytidine rises the healing effectiveness of the drug [91].

Equation 2

Ester from the reaction of alcohol with acid chloride

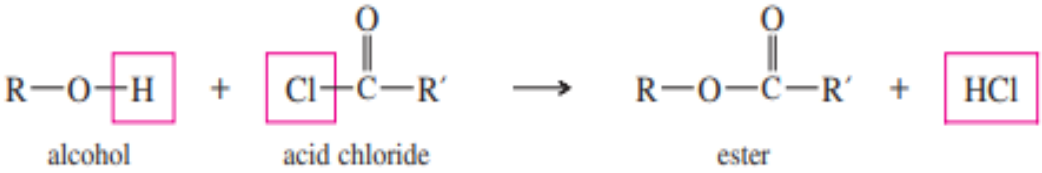

1.8 Michael Addition

Conjugate addition reactions are among the most significant carbon-carbon bond construction in organic synthesis and great progress has been made in the improvement of asymmetric Michael addition [92]. The Michael addition goes quickly at room temperature, offers short proceeding times, and includes less toxic precursors. Non-linear optical materials were also recognized using the Michael addition, which benefits from the lack volatile byproducts [93]. The Michael addition encompasses the addition of a nucleophile, also named a 'Michael donor,' to a stimulated electrophilic olefin, the 'Michael acceptor', causing in a 'Michael adduct'. Although, the Michael addition is usually considered the addition of enolate nucleophiles to stimulated olefins, a wide range of functional groups own enough nucleophilicity to perform as Michael donors. Reactions including non-enolate nucleophiles such as phosphines, amines, and thiols are usually mentioned as 'Michael-type additions. The Michael acceptor owns an electron withdrawing and resonance stabilizing activating group, which stabilizes the anionic intermediate. Michael addition acceptors are far more several and different than donors, because of the plethora of electron withdrawing activating groups that enable the Michael addition to olefins and alkynes. Acrylamides, acrylate esters, acrylonitrile, acrylamides, alkyl methacrylates, maleimides, cyanoacrylates and vinyl sulfones serve as Michael acceptors and are commercially obtainable. Less common, but equally essential, α,β-unsaturated aldehydes, vinyl ketones, nitro ethylenes, vinyl pyridines, vinyl phosphonates, acrylonitrile, azo compounds and even acetylene esters and β-keto acetylenes also function as Michael acceptors [94].

Michael addition is a conjugate addition of a nucleophile to α, β-unsaturated double bond of a carbonyl compound (or other electron-poor double bonds). Michael acceptor and Michael donor are terms used to indicate an electrophile that accepts a pair of electrons and a nucleophile that donates a pair of electrons respectively. Some examples of Michael donors are: carbanions between two strong electron-withdrawing groups such as carbonyl, cyano or nitro groups, enamines and lithium dialkyl cuprates. Some examples of Michael acceptors are: compounds that contain a double bond conjugated with a nitro group, carbonyl group or cyano group [87]. An example of Michael addition is adding lithium divinyl cuprate (Michael donor) to α, β-unsaturated ketone double bond (Michael acceptor). In this reaction, which is also named conjugate addition an enolate ion is formed as the vinyl group adds to carbon atom, then protonation at α carbon donates the Michael addition product as shown in Equation 3 [87].

Michael addition reaction has been used in drug discovery; the aimed covalent modification has appeared as a confirmed method to drug discovery with the recent FDA approvals of osimertinib, afatanib, and ibrutinib drugs that were planned to undergo an irreversible hetero-Michael addition reaction with a matchless cysteine residue of a specific protein. This strategy has extended the druggable setting by increasing the ligand binding selectivity for proteins in the same family and by enhancing the binding attractions for target proteins with surface binding sites. Moreover, compounds that function through aimed covalent inhibition mechanism have been shown to overcome drug resistance [95].

Between all the types of nanoparticles, dendrimers show numerous benefits, which make them perfect applicants for developed and targeted drug delivery in cancer investigation. Dendrimers can carry great amounts of drug into precise areas. In addition, they can be used for observing the development of the treatment process, with an exceptional theranostic capability. The innovation was obtaining these macromolecules by repeating a chemical procedure as follows: the most applied different synthesis of polyamidoamine (PAMAM) dendrimers begins with an amine functional principal unit that is reacted with methylacrylate by Michael addition chemical reaction. This performs in the synthesis of two new divisions per amine group with an ester-terminated dendrimer, which is known as a “half-generation” dendrimer. Additional amidation of the methyl ester with ethylene diamine gives “full-generation” amine-terminated dendrimers. Repeating of Michael

addition and amidation steps produce the next-higher group dendrimer with additions to its molecular weight, size, and number of terminal functional groups [96].

The maleimides which are used in bioconjugation have become advantaged chemical partners for the site-selective modification of proteins by thio-Michael addition of biothiols and, to a lesser extent,by Diels–Alder (DA) reactions with biocompatible dienes. Notable examples include immunotoxins and marketed maleimide-based antibody–drug conjugates (ADCs) such as Adcetris, which are used in cancer therapies [97].

The therapeutic influence of single reactive oxygen species (ROS) on cancer is limited, and joining with immunotherapy, chemotherapy, or other treatments is essential to improve the treatment efficiency. In order to precede these problems, researchers have discovered different ROS-generating platforms for ROS treatment. Hollow nanomaterials (*e.g.*, hollow manganese dioxide, hollow gold nanosphere, and hollow silica) have been broadly used in drug/gene delivery because of their great drug loading capacity. Dopamine (DA), as a bioactive molecule, occurs widely in living organism. Owing to its easy polymerization, good biocompatibility, and surface modification (*via* Michael addition or Schiff base reaction with amine or thiol), it has caught much attention in recent years. A Pt-embedded hollow polydopamine nanoparticle co-loaded with doxorubicin (DOX) and chlorine e6 (Ce6) as smart pH-responsive and mitochondrial-targeted nanoplatform was developed to realize enhanced combination therapy of chemotherapy and sonodynamic therapy (SDT) for cancer [98].

Diverse scenarios were found in the cases of crotonamide (–C=C–C(=O)–NH–) having inhibitors, namely pyrotinib, and neratinib which were testified for irreversible human epidermal growth factor receptor 2 negative (HER2) binding. The presence of the crotonamide group contributed to the irreversible HER2 binding via covalent bond formation. The crotonamide group can react with cysteine100 (Cys100) in the Adenosine triphosphate (ATP) binding domain via Michael addition. There was a carbon-sulfur covalent bond between neratinib and Cys100 in the ATP binding domain, in which the thiol group (-SH) and crotonamide operated as the Michael donor and acceptor, respectively. The irreversible binding of pyrotinib/ neratinib could extend and augment the action of HER2 inhibition, compared to reversible HER2 binding inhibitor [99].

Equation 3

Michael addition to α, β-unsaturated ketone

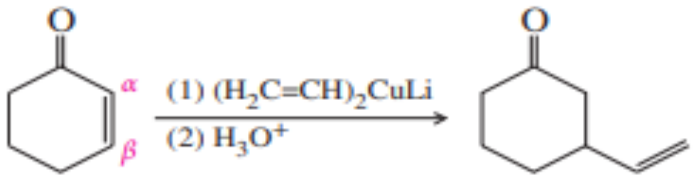

1.9 Amides

Reaction of 1^{o} and 2^{o} amines with acid chlorides or carboxylic acids using heat to drive off water forces reaction to end with amides. Initially ammonium carboxylate salt is formed by acid-base reaction between carboxylic acid and amine. Using heat above 100 °C evaporates water and produce amide Equation 4. This method is applicable for laboratory and industry [87].

Equation 4

Amide forming

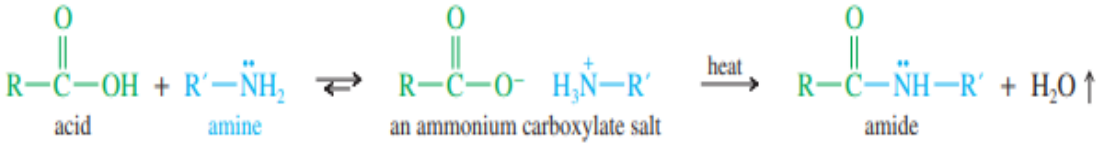

Amides play an important role in drug delivery in cancer treatment; developing of nanoparticles (NPs) by joining tumor-acidity-cleavable maleic acid amide (TACMAA) as a design feature. TACMAA is manufactured by the facile reaction of an amino group with 2,3-dimethylmaleic anhydride (DMMA) and its derivatives and can be cleaved under tumor acidity. By advantage of such characteristics, NPs having TACMAA enable size or surface charge switching at tumor locations so that they can overcome those delivery obstacles for enhanced drug delivery and cancer treatment. For example, the pH of blood is neutral, while the tumor extracellular environment structures an acidic pH ($pH_e \approx 6.5–7.0$) and the lysosome and endosome are more acidic (pH 5.5–4.5). The nanoparticles (NPs) should be capable to change their properties to adjust to each individual environment for effective and robust delivery. This request encourages the development and design of smart delivery transporters that can reply to endogenous and exogenous stimuli [100].

Lai *et al.* testified Doxorubicin loaded polyamidoamine dendrimer (DOX-loaded PAMAM dendrimer) conjugate for cancer treatment; DOX was conjugated with dendrimer through amide (PAMAM-amide-DOX) and hydrazone (PAMAM-hyd- DOX) as coupling molecules. Drug release study displays that at 4.5 pH (47% in 24 h) as-prepared PAMAM-hyd- DOX nanocarriers indicates faster drug release compared to at 7.4 pH (8% in 24 h), also PAMAM-amide-DOX confirms slower drug release compare to PAMAM-hyd-DOX at 4.5 pH. Cytotoxicity also approves that PAMAM-hyd-DOX nanocarrier has higher toxicity towards cancerous cells than PAMAM-amide-DOX nanocarriers [101].

Amide bond creation is the most straightforward way to link drug molecules to peptides. An amide bond is the most conventional and versatile method to peptide-drug conjugates of suitable biological and chemical stability [102].

1.10 Schiff bases

Schiff bases are a huge group of compounds described by the occurrence of a double bond connecting carbon and nitrogen atoms the specific structure of Schiff base is shown in Figure 5, and the general synthesis of Schiff bases is shown in Figure 6. The flexibility of Schiff bases is produced in the many ways to combine a range of alkyl or aryl substituents. Compounds of this type are both established in nature and synthesized in the laboratory. For years, Schiff bases have been greatly inspiring to many chemists and biochemists [103].

Many drugs have been raised up for cancer treatment and a sum of compounds has been industrialized in the pharmaceutical field. Schiff bases and their complexes enclose a vast area of many aspects of pharmaceutical and medicinal chemistry. Thus, universal research on Schiff bases and their complexes invite the researchers for effective treatment of cancer through Schiff bases. Schiff bases of heterocyclic compounds showed important anti-tumor activity. In this field, Schiff bases were made by the reaction of 4-amino-5-(pyridine-4yl)-4H-1,2,4-triazol-3-thiol with thiophene-2-carbaldehyde and furan-2-carbaldehyde and transition metal complexes of these Schiff bases were also prepared with Co(II), Ni(II) and Cu(II) metals. These complexes were tested against the human hepatocellular liver carcinoma cell line (Hep-G2) and human breast cancer cell line (MCF-7) and the results showed that all metal complexes exhibited reasonable to important cytotoxicity on cell lines HepG2 and MCF-7 [104].

In a study conducted by Hassan *et al*., a new series of Schiff bases was produced by the condensation of 5 amino-N-aryl-1H-pyrazole-4-carboxamides with aromatic aldehydes in refluxing ethanol with very high yields for evaluation of their antitumor activities against two human carcinoma cell lines (HepG-2 and MCF-7) using MTT assay. Most of Schiff bases showed improved antitumor effect than doxorubicin. Especially, the new Schiff base compound 5-(Benzylideneamino)-3-(4-methoxyphenylamino)-N-(4-methylphenyl)-1H-pyrazole-4-caroxamide (IC_{50} = 66.3 ± 4.9 μM) showed an exceptional antitumor activity when compared to doxorubicin (IC_{50} = 80.9 ± 2.1 μM) against HepG2 (liver) cell lines. In addition, the new Schiff base compound 5-(Benzylideneamino)-N-(4-chlorophenyl)-3-(4-methoxyphenylamino)-1H-pyrazole-4 carboxamide (IC_{50} = 60.8 ± 6.1 μM) showed a greater antitumor activity when compared to doxorubicin (IC_{50} = 65.6 ± 4.2 μM) against MCF 7 (breast) cell lines. These two new compounds were able to induce apoptosis in HepG2 and MCF-7, respectively [105].

Tetrahydrocurcumin (THC) is a metabolite of curcumin and a valued lead structure in medicinal chemistry owing to its curcumin-induced biological effects and its derivatives can be hopeful antitumor agents. A new series of Schiff bases of THC were produced by condensation of THC with different primary amines. Additionally, these compounds were tested against three human cancer cell lines comprising human breast adenocarcinoma (MCF-7, human epithelial lung carcinoma (A549), and human epithelial cervical cancer (HeLa). Most compounds showed reasonable to good anticancer activity against all three tested cell lines and are considerably more active than THC [106].

Figure 5

The specific structure fragment characteristic of Schiff bases

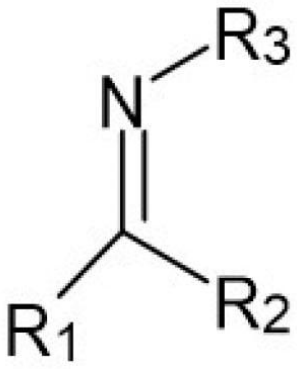

Note: Where R1, R2 and R3 are alkyl or (more often) aryl groups. R1 or/and R2 may also be hydrogen atoms

Figure 6

General synthesis of Schiff bases

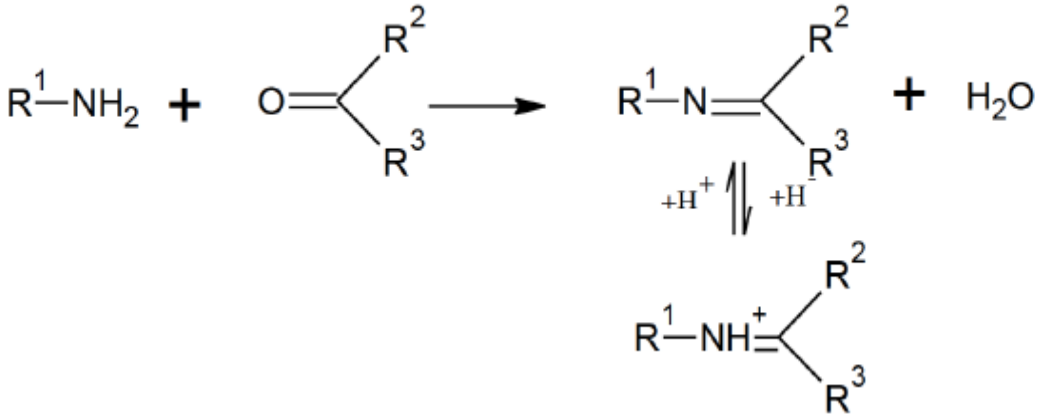

1.11 Objectives and Significance of the study

1.11.1 Objectives

The chief purpose of the study was the preparation of several derivatives of anticancer natural compounds, characterizing the structure of new compounds by various spectroscopic methods (IR, NMR) and testing their biological activity, *in vitro* screening of the potential anticancer activities and comparing those with the origin compounds. Table A1 Appendix A shows the structures of newly prepared derivatives. However, the specific objectives of the current thesis were to synthesize the following compounds:

1. 3,7-Dimethyloct-6-en-1-yl thiophene-3-carboxylate using condensation reaction of Citronellol with thiophene-3-carboxylic acid
2. 3,7-Dimethyloct-6-en-1-yl thiophene-2-carboxylate by esterification of citronellol and thiophene-2-carboxylic acid.
3. 3,7-Dimethyloct-6-en-1-yl-4-bromothiophene-3-carboxylate by esterification reaction of citronellol and 4-bromothiophene-3-carboxylic acid.
4. (E)-3,7-Dimethyloct-6-en-1-yl-3-(4-hydroxyphenyl)acrylate from the condensation reaction of citronellol and *p*-Coumaric acid.
5. (E)-2-Isopropyl-5-methylphenyl 3-(4-hydroxyphenyl)acrylate using condensation reaction of thymol and *p*-coumaric acid.
6. (E)-3-(4-Hydroxyphenyl)-N-(2-(piperazin-1-yl)ethyl)acrylamide by esterification of *p*-coumaric acid with 2-(piperazin-1-yl)ethanamine.

7. (E)-3-(4-Hydroxyphenyl)acrylic 4-methylbenzenesulfonic anhydride by esterification of *p*-Coumaric acid with 4-Toluenesulfonyl chloride.
8. 4-Methylbenzenesulfonic (E)-3-(4-(tosyloxy)phenyl) acrylic anhydride by esterification of *p*-Coumaric acid with 4-Toluenesulfonyl chloride.
9. (Z)-3-Methyl-2-(pent-2-en-1-yl)-3-((2-(piperazin-1-yl)ethyl)amino) cyclopentanone from *cis*-jasmone and 1-(2-Aminoethyl) piperazine using Michael addition method.
10. (Z)-3-Methyl-2-(pent-2-en-1-yl)-3-(2-phenylhydrazinyl) cyclopentanone by a condensation reaction of *cis*-jasmone with phenylhydrazine.
11. To use thymol as a precursor for 2-isopropyl-5-methylphenyl thiophene-3-carboxylate,
12. To condense thymol with furan-3-carboxylic to produce 2-isopropyl-5-methylphenylfuran-3-carboxylate.
13. To prepare 2-isopropyl-5-methylphenyl-4-bromothiophene-3-carboxylate by condensation reaction of thymol with 4-bromothiophene-3-carboxylic acid.
14. To produce 2-isopropyl-5-methylphenyl-5-bromothiophene-2-carboxylate using condensation reaction of thymol with 5-bromothiophene-2-carboxylic acid.

1.11.2 Significance

Previous studies suggested that citronellol, *p*-CA, *cis*-jasmone, and thymol have the potential anticancer activity. To our knowledge, no research explored the potential changes in these activities regarding the new compounds that were semi-synthesized in this study. This is the first study conducted on the new functionalization of natural compounds mentioned above. Consequently, the study may be a valuable tool to:

1. Explore the chemical and physical charterer of the newly synthesized derivatives.
2. Investigate their anticancer and antimicrobial activity.
3. It serves as a tool for choosing the suitable synthesized derivatives to be used for the treatment.

Chapter Two

Experimental part

2.1 Chemistry

2.1.1 Chemicals and Instruments

All chemicals and solvents were bought from Chemical Science Company and Sigma-Aldrich Company without further purification. Nuclear magnetic resonance spectra ^{1}H-NMR (500MHz, DMSO, ppm.) and ^{13}C-NMR (126 MHz, DMSO, ppm.) were recorded on Bruker-500MHz-Avance Ⅲ at the University of Jordan-Chemistry Department. Infrared spectroscopy (FT-IR) was recorded on a Fourier Transform Infrared spectrophotometer (Nicolet 1s5-Id3) at An-Najah National University-Chemistry Department. The glassware of the reactions was dried by using an oven. All reactions were done under inert conditions. Thin layer chromatography (TLC) plates were purchased from Sigma-Aldrich Chemical Company pre-coated with Merck Kiesel gel 60F254, and visualization was done using a UV lamp. To remove solvents rotary evaporator with a membrane pump at 30-50 mbar was used. Melting points were adjusted using Stuart Melting Point Apparatus (R00102618), silica gel was purchased from Sigma-Aldrich, with pore size 60Å, 230-400 mesh and 40-63 μm particle was used for performing flash column chromatography under 5 psi compressed air.

2.1.2 Synthetic procedures

The compounds prepared in this research were distributed into four groups depending on the natural starting materials (citronellol, *p*-CA, *cis*-jasmone, and thymol). Esters, anhydrides, amines and amides were prepared from these main compounds using different carboxylic acids for esters, tosyl chloride for anhydrides, 2-(piperazine-1-yl)ethanamine and phenyl hydrazine for amines and amides. The symbols of the compound of each group are not sequentially numbered because they were prepared separately. The names of groups and their compounds with their symbol are shown in Table 1.

Table 1

Name of group and symbols of their compounds

No	Group name	Compound symbols
1.	Citronellol	J3, J15, J13
2.	*p*-CA	N2, N4, J12, J14, J19
3.	*Cis*-jasmone	N6, N8
4.	Thymol	J10, J11, J12, J16

2.1.2.1 Synthesis of Citronellol Esters

A modified procedure from the assays of Wang *et al*., [107] and Pal *et al*., [108] was used. The synthesis of **J3**, **J15**, and **J13** compounds, the same procedure was followed but in different amounts, and Table A2 Appendix A shows the amounts used in each compound. In 50 ml RBF with a magnetic stirrer the required acid was dissolved or suspended in dry dichloromethane (DCM) to which oxalyl chloride in dry DCM was added drop-wise at 0 ℃ under inert conditions with constant stirring. Dimethylformamide (DMF) was added at 0 ℃ was added (only for **J13**); the reaction mixture was kept stirring at room temperature for 10 minutes and then refluxed for 3 hours. After that, the solvent was removed under vacuum. A solution of citronellol and triethyl amine (TEA) in dry DCM was added to a stirred mixture under inert conditions and kept stirring overnight. The reaction was monitored by TLC. After the completion of the reaction, distilled water was added to the reaction mixture and extracted with ethyl acetate (EAC). The upper organic film (density of EAC is 0.9 g/ml) was collected, dehydrated over anhydrous sodium sulfate (Na_2SO_4) and clarified. The solvent was removed under vacuum.

3,7-Dimethyloct-6-en-1-yl thiophene-3-carboxylate (J3)

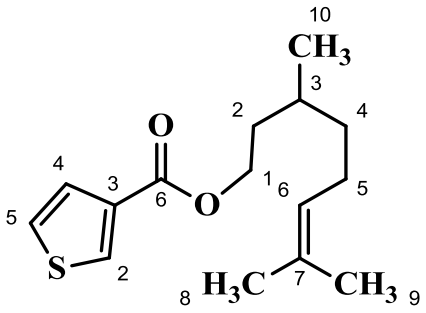

J3

The obtained sample **J3** was liquid with a 71.66% yield. The structure of **J3** was confirmed by spectroscopic analysis in Figures B1, B15, and B16 for **FT-IR**, **^{1}H-NMR**, and **^{13}C-NMR** respectively (shown in Appendix B). **FT-IR** (ν cm^{-1}): 3000.10 (C-H stretching alkene), 2914.13 (C-H alkane), 1717.19 (C=O carbonyl α,β-unsaturated ester), 1644.33(C=C), 1520.44 (C=C cyclic alkene), 1446.71, 1377.52, 1264.68, 1230.17, 1162.30 (C-O ester), 1048.34, 1024.32, 995.38, 918.60, 874.40, 833.12, 731.99. **^{1}H-NMR** (500 MHz, DMSO-d_6, ppm): δ 8.2576 (s, 1H (2 thiophene)), 7.6033 (d, *J* = 1.03 Hz, 1H (5 thiophene)), 7.4279 (d, 1H(4 thiophene)), 5.0684 (t, 1H (6 citronellol)), 4.2443 (d, *J* = 6.70 Hz, 1H (1 citronellol)), 4.0216 (d, *J* = 7.13 Hz, 1H (1 citronellol)), 3.4878 – 3.3545 (m, 4H (2,5 citronellol)), 1.9244 (s, 3H (8 citronellol)), 1.7591 – 1.6503 (m, 1H (3 citronellol)), 1.4903 (dt, 2H (4 citronellol)), 0.9052 (d, *J* = 6.57 Hz, 3H (10 citronellol)), 0.8361 (s, 3H (9 citronellol)). **^{13}C-NMR** (126 MHz, DMSO-d_6, ppm): δ 161.8789 (C=O, 6 thiophene), 134.5308 (4 thiophene), 133.3064 (2 thiophene), 132.9651(7 citronellol), 132.8328 (d, *J* = 2.99 Hz (3 thiophene)), 130.4341 (5 thiophene), 126.8958 (6 citronellol), 59.5868 (1 citronellol), 36.7536 (4 citronellol), 36.2840 (2 citronellol), 34.8127 (3 citronellol), 28.7608 (5 citronellol), 28.5347 (8 citronellol), 20.5508 (10 citronellol), 13.8964 (9 citronellol).

3,7-Dimethyloct-6-en-1-yl thiophene-2-carboxylate (J15)

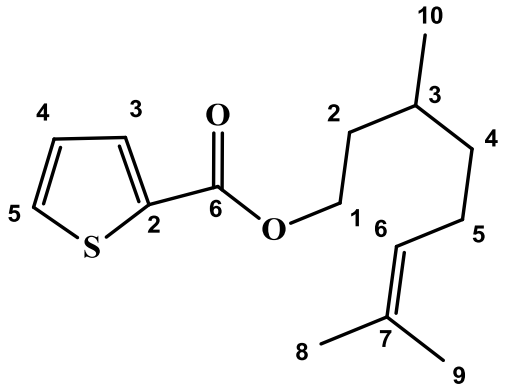

J15

J15 was cleaned by column chromatography silica gel to obtain liquid with output of 83.13%. Spectroscopic analysis is shown in Figures B2, B17, and B18 for FT-IR, ^{1}H-NMR and ^{13}C-NMR respectively in Appendix B. **FT-IR** ν cm^{-1}: 2960.93(C-H stretching alkene), 2915.35(C-H alkane), 1778.16, 1711.64 (C=O carbonyl α,β-unsaturated ester), 1525.86 (C=C cyclic alkene), 1417.77, 1376.28, 1358.59, 1260.71, 1233.59, 1203.51(C-

O stretching ester), 1095.50, 1045.90, 1006.59, 860.63, 751.14, 722.82. **^{1}H-NMR** (500 MHz, DMSO-d_6, ppm): δ 7.8937 (dd, 1H (3 thiophene)), 7.7410 (dd, *J* = 30.31, 1.25 Hz, 1H (5 thiophene)), 7.1853 (dt, *J* = 16.36, 3.76 Hz, 1H (4 thiophene)), 5.0567 (t, 1H (6 citronellol)), 4.2747 (td, *J* = 10.88, 5.38 Hz, 2H (1 citronellol)), 2.0299 – 1.9227 (m, 1H (5 citronellol)), 1.9441 – 1.7996 (m, 1H (5 citronellol)), 1.7020 (td, *J* = 13.66, 5.06 Hz, 1H (2 citronellol)), 1.6129 (d, *J* = 12.81 Hz, 3H (8 citronellol)), 1.5433 (d, *J* = 5.62 Hz, 3H (9 citronellol)), 1.4658 (ddt, *J* = 18.57, 12.25, 6.03 Hz, 1H (3 citronellol)), 1.2264 – 1.1244 (m, 1H (2 citronellol)), 0.9006 (d, *J* = 6.55 Hz, 2H (4 citronellol)), 0.8230 (d, *J* = 6.54 Hz, 3H (10 citronellol)). **^{13}C-NMR** (126 MHz, DMSO-d_6, ppm): δ 161.4860 (6 thiophene), 133.8676 (3 thiophene), 133.6026 (5 thiophene), 133.2264 (2 thiophene), 130.6822 (7 citronellol), 130.4198 (4 thiophene), 128.2433 (6 citronellol), 63.1574 (1 citronellol), 36.9222 (4 citronellol), 36.4089 (2 citronellol), 34.9164 (3 citronellol), 25.0109 (5 citronellol), 24.8854 (8 citronellol l), 19.4564 (10 citronellol), 19.3323 (9 citronellol).

3,7-Dimethyloct-6-en-1-yl 4-bromothiophene-3-carboxylate (J13)

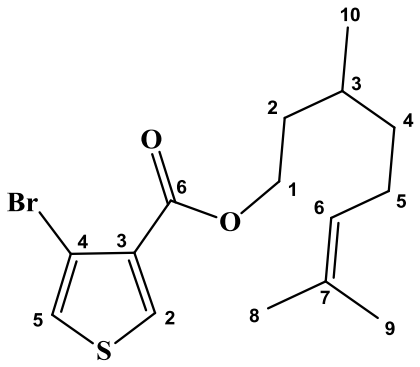

J13

The compound **J13** was cleaned by column chromatography silica gel to obtain a solid with melting point 115-117 ℃ and 56.92% yield. Spectroscopic analysis is shown in Figures B3, B19, and B20 for FT-IR, ^{1}H-NMR and ^{13}C-NMR respectively in Appendix B. **FT-IR** ν cm^{-1}: 3107.81 (C-H stretching alkene), 2960.51 (C-H alkane), 2926.49 (C-H alkane), 1727.56 (C=O conjugated ester), 1672.61, 1505.46 (C=C cyclic alkene), 1436.44, 1377.51, 1276.20, 1173.49 (C-O stretching ester), 970.81, 921.50, 885.75, 827.93, 769.36, 655.71. **^{1}H-NMR** (500 MHz, DMSO-d_6, ppm): δ 8.3599 (d, *J* = 3.56 Hz, 1H (2 thiophene)), 7.7617 (d, *J* = 3.54 Hz, 1H (5 thiophene)), 5.0658 (t, 1H (6 citronellol)), 4.1170 (t, *J* = 7.22 Hz, 2H (1 citronellol)), 3.4514 – 3.3894 (m, 2H (5

citronellol)), 2.3882 – 2.3112 (m, 1H (2 citronellol)), 1.9775 – 1.8977 (m, 1H (2 citronellol)), 1.6325 (s, 3H (8 citronellol)), 1.5561 (s, 3H (9 citronellol)), 1.2424 – 1.2064 (m, 1H (3 citronellol)), 1.1503 (dt, *J* = 13.50, 7.45 Hz, 2H (4 citronellol)), 0.8584 (d, 3H (10 citronellol)). **^{13}C-NMR** (126 MHz, DMSO-d_6, ppm): δ 162.2968 (6 thiophene), 135.6065 (2 thiophene,7 citronellol), 131.3452 (3 thiophene), 126.7301 (5 thiophene,6 citronellol,4 thiophene), 109.5036 (1 citronellol), 40.1117 (4 citronellol), 39.0196 (2,3,5 citronellol), 25.5245 (8 citronellol), 24.8630 (10 citronellol), 17.5283 (9 citronellol).

2.1.2.2 Synthesis of *p*-Coumaric Acid (*p*-CA) Derivatives

2.1.2.2.1 Synthesis of *p*-CA Esters

(E)-3,7-Dimethyloct-6-en-1-yl3-(4hydroxyphenyl)acrylate (*p*-CA) (J2)

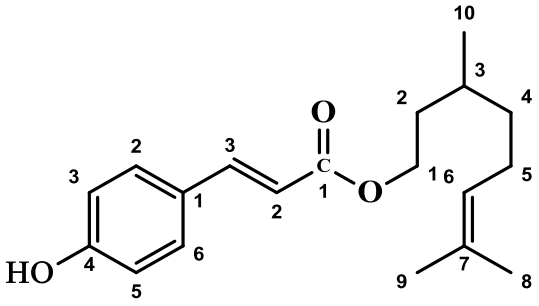

J2

Fischer esterification is a usual method to synthesize esters, wherein an alcohol is treated with a carboxylic acid in the presence of a catalyst of mineral inorganic acid. A modified procedure of Khatkar *et al*., [50] was used. In 50 ml RBF *p*-CA, one equivalent 0.13 g (1 eq., 0.0008 moles) with citronellol 1.16 g (9.3 eq., 0.0074 moles, 53 drops) in 5 ml EAC, concentrated H_2SO_4 as catalyst (1 ml) was added to the mixture drop-wise then the mixture was refluxed with heat and stirring for 48 hours**.** The reaction was checked by TLC. The reaction mixture was transferred in 200 ml ice-cooled water and neutralized by saturated $NaHCO_3$ (10 ml) then ether was used for extraction. The upper organic layer was collected (density of ether 0.7133 g/ml), dehydrated over a drying agent of Na_2SO_4 anhydrous, filtered and evaporated. The black thick liquid of **J2** was obtained with a 68.44% yield. Spectroscopic analysis is shown in Figures B4 and B21 in Appendix B for **FT-IR** and **^{13}C-NMR** respectively. **FT-IR** main functional groups ν cm^{-1}: 3435.17 (OH of *p*-CA), 2955.09 (C-H alkene), 2927.49 (C-H alkane), 2869.07 (C-H alkane), 2360.70 (CO_2), 1741.22 (C=O conjugated ester), 1633.47 (C=C conjugated alkene), 1458.56,

1366.25, 1217.90, 1171.67, 1118.02, 1047.20, 957.50, 735.10. **^{1}H- NMR** (500 MHz, DMSO-d_6, ppm): δ 7.9921 (d, *J* = 10.37 Hz, 1H,3 *p*-ca (d.b)), 7.9467 (d, *J* = 7.99 Hz, 2H, 2,6 *p*-ca), 7.5153 (d, 2H, 3,5 *p*-ca), 7.2077 (d, *J* = 26.11 Hz, 1H 2 *p*-ca (d.b)), 6.6279 (s, 1H OH *p*-ca), 6.4496 (t, 2H 1 citronellol), 5.0855 (t, 1H 6 citronellol), 2.1718 (t, 2H, 5 citronellol), 2.1134 (dt, *J* = 12.81 Hz, 4H, 2,4 citronellol), 1.8533 (s, 3H, 9 citronellol), 1.5504 (m, 1H, 3 citronellol), 1.3192 (d, *J* = 6.74 Hz, 3H, 8 citronellol), 0.9848 (d, *J* = 6.86 Hz, 3H, 10 citronellol). **^{13}C-NMR** (126 MHz, DMSO-d_6, ppm): δ 172.0224 (1C, C=O), 64.9332 (1C, 4 *p*-CA (C-OH)), 62.1613 (1C, 3 *p*-CA (d.b)), 58.8509 (3C, 2,6 *p*-CA, 7 citronellol), 38.6666 1C 1 *p*-CA), 36.4987 (1C 6 citronellol), 35.0282 (1C 1 citronellol), 29.2052 (1C 3 citronellol), 27.3759 (3C 3,5 *p*-CA, 2 d.b), 22.5642 (2C 2,4 citronellol), 22.4726 (2C 9, 5 citronellol, 21.0568 (2C 8, 10 citronellol).

(E)-2-Isopropyl-5-methylphenyl-3-(4-hydroxyphenyl)acrylate (J14)

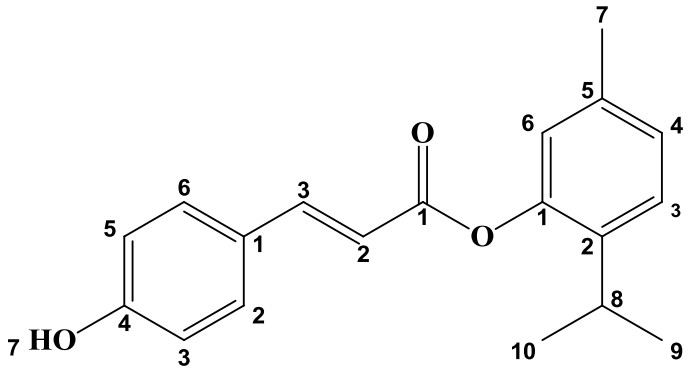

J14

A modified procedure from the assay of Wang *et al*., [107] and Pal *et al*., [108] was used. In 50 ml RBF with a magnetic stirrer, a mixture of *p*-CA 0.197 g (1.2 eq., 0.0012 moles) in methylene chloride (16 ml) was stirred at room temperature then heated and kept mixing for 10 minutes under inert condition until the acid powder was dissolved. Oxalyl chloride155 µL (1.8 eq. 0.2291675 g) in methylene chloride (5 ml) was added drop-wise to the mixture at 0 ℃ under inert condition with constant stirring, dimethylformamide (DMF) 100 µL (2 drops) was added to the mixture at 0 ℃, and the reaction mixture was kept stirring at room temperature overnight. After that, thymol 0.151 g (1 eq., 0.0010 moles) and TEA 0.152 g (1.5 eq., 0.0015 moles) in CH_2Cl_2 6 ml were to the mixture at 0 ℃. The mixture was stirred at room temperature for 10 minutes and then refluxed for 3 hours. The reaction was monitored by TLC. D.W was added to the mixture and extracted

with ethyl acetate (EAC). The organic upper layer (density of EAC 0.902 g/ml) was collected, dried over-drying agent Na_2SO_4, filtered, and evaporated. The crude product of **J14** was cleaned by column chromatography to furnish a brownish-yellow color liquid of **J14** with 69.15% yield, spectroscopic analysis was performed and shown in Figures B5, and B22 for **FT-IR**, and **^{13}C-NMR** respectively in Appendix B; **FT-IR** ν cm^{-1}: 3429.65 (O-H *p*-CA, 2961.92 (C-H alkene), 2926.65 (C-H alkane), 2866.49 (C-H alkane), 1753.09 (C-H overtone aromatic compound), 1704.32 (C=O carbonyl of conjugated ester), 1603.53 (C=C aromatic ring), 1585.71 (C=C alkene), 1513.64, 1457.17 (C-H bending methyl group), 1363.79 (C-H bending alkane gem dimethyl), 1327.70 (C-O aromatic ester), 1266.20 (C-O ester). **^{1}H-NMR** (500 MHz, DMSO-d_6, ppm) δ 7.7644 (d, *J* = 15.95 Hz, 1H (3 d.b)), 7.6495 (d, *J* = 8.55 Hz, 2H (6,2 *p*-CA)), 7.2420 (d, *J* = 3.57 Hz, 2H (5,3 *p*-CA)), 7.0492 (d, *J* = 8.05 Hz, 1H (3 thym)), 6.8746 (d, *J* = 1.64 Hz, 1H (4 thym)), 6.6563 (d, *J* = 15.88 Hz, 1H (6 thym)), 6.5700 (s, 1H (OH)), 6.5295 (d, 1H (2 d.b)), 2.9644 – 2.8990 (m, 1H (8 thym)), 2.2701 (s, 3H (7 thym)), 1.2382 (d, *J* = 2.82 Hz, 3H (9 thym)), 0.8673 (d, *J* = 4.57 Hz, 3H (10 thym)). **^{13}C-NMR** (126 MHz, DMSO-d_6, ppm) δ 165.6048 (C=O), 160.3037 (C-OH), 147.8014 (1 thym), 146.6899 (3 d.b), 136.8852 (5 thym), 136.1498 (2 thym), 126.8444 (6,2 *p*-CA), 126.3663 (1 *p*-CA, 3 thym), 124.9602 (4 thym), 122.4654 (6 thym), 113.0445(5,3 *p*-CA, 2 d.b), 26.6852 (9,10 thym), 20.3456 (d, *J* = 3.29 Hz (7,8 thym).

2.1.2.2.2 Synthesis of *p*-CA Amide

(E)-3-(4-Hydroxyphenyl)-N-(2-(piperazin-1-yl)ethyl)acrylamide (J19)

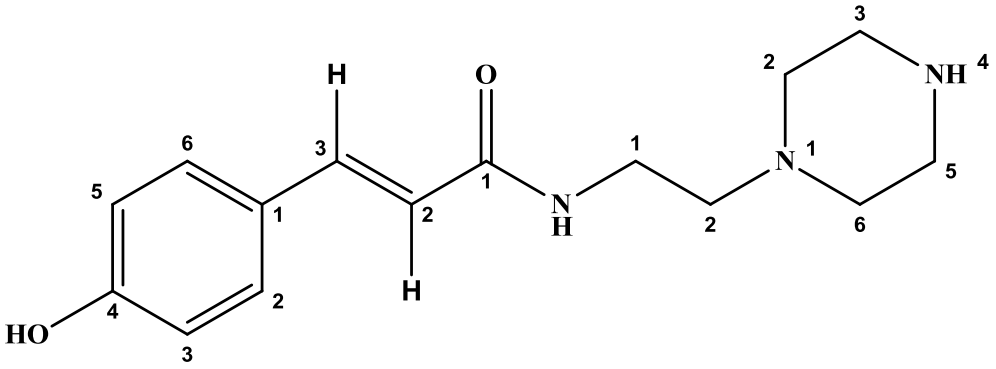

J19

A modification procedure of Khatkar, A., *et al*., [50] and Hanbali, G., *et al*., [109] was used. In 50 ml RBF 0.1 g (1.8 eq., 0.61 mmol) of *p*-CA ($C_9H_8O_3$) was stirred in 10 ml of

methylene chloride, and heated under inert conditions. Dimethylformamide (DMF) 7 drops were added drop-wise to the mixture at room temperature with constant stirring. Oxalyl chloride 3 ml was added to the mixture at 0 ℃. The mixture was kept stirring at room temperature for 3 hours a clear yellow solution was formed. The excess of oxalyl chloride was evaporated. A solution of 1-(2-aminoethyl)piperazine 99% ($C_6H_{15}N_3$) 0.1 g (1 eq., 0.33 mmol) in 5 ml methylene chloride was added drop-wise to the stirred mixture at room temperature, a thick yellow solution was formed, the mixture was kept stirring at room temperature for 24 hours. The completion of the reaction was checked by single spot TLC and IR. The solvent was decanted and a yellow crystal precipitate was separated. Solid was washed with methanol several times and then purified by recrystallization with alcohol. Spectroscopic data of sample **J19** is shown in Figures B6, B23, and B24 in Appendix B for **FT-IR**, **^{1}H-NMR**, and **^{13}C-NMR** respectively. Sample **J19** was solid with a melting point 240-243 ℃ and yield 97.35 %). **FT-IR** (neat): ν_{max} cm^{-1} 3387.52 (O-H and N-H), 3050 (C-H alkene), 2955.20 (C-H alkane), 1697.65(C=O conjugated amide), 1604.08 (aromatic ring), 1445.69 (C-N), 1386.60, 1302.98, 1161.82, 1060.81, 986.86, 843.80, 732.31(N-H, C-H aromatic), 668.33, 578.20, 563.16, 553.28, 539.40, 533.75, 521.81, 515.33. **^{1}H-NMR** (500 MHz, DMSO-d_6, ppm): δ 9.9698 (s, 1H (NH ethyl amine)), 8.4635 – 8.4275 (m, 6H (aromatic ring and d.b)), 3.8300 (s, 1H (OH)), 3.6594 – 3.6234 (m, 1H (NH piperazine)), 3.4305 (t, 2H (CH_2) (1 ethyl amine)), 3.3961 – 3.3601 (m, 8H (CH_2) (2,3,5,6 piperazine)), 3.2214 (t, 2H (CH_2) (2 ethyl anime)). **^{13}C-NMR** (126 MHz, DMSO-d_6, ppm): δ 34.1147(1 C (CH_2, 1 ethylamine)), 40.7539 (2C (3,5 piperazine)), 48.8104 (2C (2,6 piperazine)), 53.3339 1 C (2 ethyl amine)), 116.055 (2C (5,3 *p*-CA)), 120.64 (1C (2 d.b)), 127.915 (1C (1 *p*-CA)), 130.625 (2C (2,6 *p*-CA)), 141.79 (1C (3 d.b)), 157.44 (1C (4 *p*-CA)), 167.08 (1C (C=O)).

2.1.2.2.3 Synthesis of *p*-CA anhydride

A modified procedure from the assays of Sanmartin *et al*., [110] and Debasis *et al*., [111] was used. A solution of NaOH (15 ml of 5M NaOH) was added to a mixture of *p*-CA 0.75 g (1 eq., 0.005 moles) and *p*-toluenesulfonyl chloride (TsCl) 3.4 g (4 eq., 0.02 moles). The mixture was stirred at room temperature for 24 hours. The residue was treated with concentrated HCl for neutralizing, in an ice bath till litmus blue color paper converted to red color. The reaction run and completion were monitored by TLC. The solid was then filtered and washed with D.W and diethyl ether. The filter paper with

residue was placed in a desiccator for 72 hours for drying, and then the residue was recrystallized from ethanol. This sample was coded **N2**. Then in 100 ml RBF 0.062 g (1 eq., 0.000195 moles) of sample **N2** and 0.039 g (1.05 eq., 0.000205 moles) of TsCl in presence of 4-(dimethylamino)pyridine (DMAP) 0.025 g (1.05 eq., 0.000205 moles) in THF 2.5 ml were stirred at room temperature under inert condition for one hour. The formation of a new compound along with the formation of pyridinium salt was monitored by TLC then the reaction was stirred for 48 hours at room temperature under inert conditions. The sample was evaporated and coded **N4**, dissolved in a small amount of methylene chloride (2.5 ml), and purified via silica gel column chromatography.

Recrystallization from alcohol

Place the amount of solvent (ethanol) in an Erlenmeyer flask (EMF) size of 100 ml on a hot plate, when the solvent started to boil, an EMF with sample (**N2**) was put on a hot plate and directly added to a small amount of boiling solvent. The solution was mixed on a hot plate until all solid was dissolved while keeping contact with the hot plate; small portions of solvent were added until the entire solid was dissolved. Another EMF with funnel and filter paper was placed on a hot plate to filter the solution by gravity filtration. The filter paper was rinsed with a hot solvent. The filtrate was displaced from the hot plate and put on a bench to be cooled at room temperature. After 10 minutes, a precipitate developed, the filtrate was placed in an ice bath to complete recrystallization from ethanol, the precipitate was formed, and then the solid was decanted from solvent and put under inert condition for drying.

Synthesis of (E)-3-(4-Hydroxyphenyl)acrylic-4-methylbenzenesulfonic anhydride (N2)

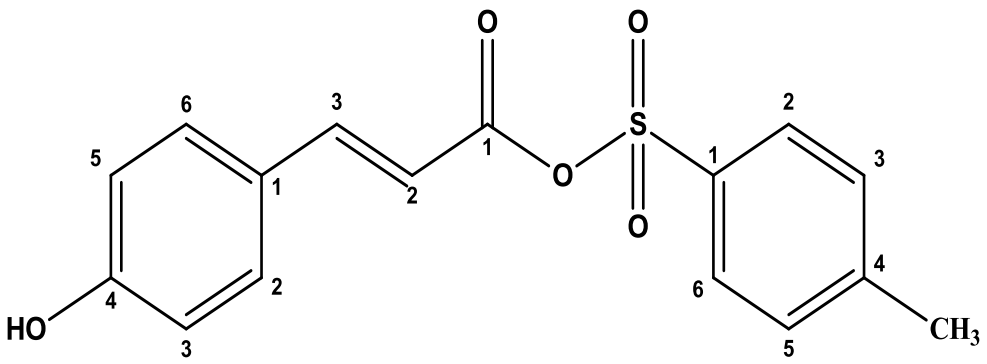

N2

The synthesis of compound **N2** is shown in Scheme 5. The melting point of the solid product **N2** is 203-205 ℃ and a 24.76 % yield. Spectroscopic data of sample **N2** is shown in Figures B7, B25, and B26 in Appendix B for **FT-IR**, **^{1}H-NMR**, and **^{13}C-NMR** respectively. **FT-IR**, ν cm^{-1}: 3724.61 (O-H stretching phenol), 2986.84 (C-H alkene), 2901.45 (C-H alkane), 1684.53 (C=O), 1630.05 (C=C), 1601.42 (aromatic ring), 1507.77, 1450.67 (C-H alkane bending methyl group), 1372.48 (S=O stretching sulfonate), 1314.38, 1284.68, 1244.92, 1212.54, 1175.36, 1156.74, 1093.57, 979.95, 945.69, 869.17, 851.39, 832.34, 757.38, 729.96, 684.90, 659.36, 577.05, 552.62. **^{1}H-NMR** (600 MHz, DMSO-d_6, ppm): δ 7.7092 (d, 2H (2,6 tosyl ring)), 7.6669 (d, 2H (2,6 *p*-CA)), 7.5014 (d, *J* = 16.02 Hz, 1H (3, C=C)), 7.4335 (d, 2H (3,5 tosyl ring)), 7.0095 (d, 2H (3,5 *p*-CA)), 6.4644 (d, *J* = 16.04 Hz, 2H (2, C=C and 4 (OH)), 2.3779 (s, 3H (CH_3)). **^{13}C-NMR** (151 MHz, DMSO-d_6, ppm): δ 167.2725 (1C, C=O), 149.8685 (1C (4,C-OH)), 145.8899, (1C (3, C=C)), 142.2202, (1C (1, *p*-CA)), 142.1407, (1C (4 tosyl ring)), 133.3827, 2C (2,6, *p*-CA)), 131.1559, (2C (3,5, tosyl ring)), 130.2544, (2C (3,5, *p*-CA)), 130.2105, 1C (2, C=C)), 129.7834, 2C (2,6, tosyl ring)), 129.7433, (1C (1, tosyl ring)), 21.1015, (1C, CH_3).

Synthesis of 4-Methylbenzenesulfonic(E)-3-(4-(tosyloxy)phenyl)acrylic anhydride (N4)

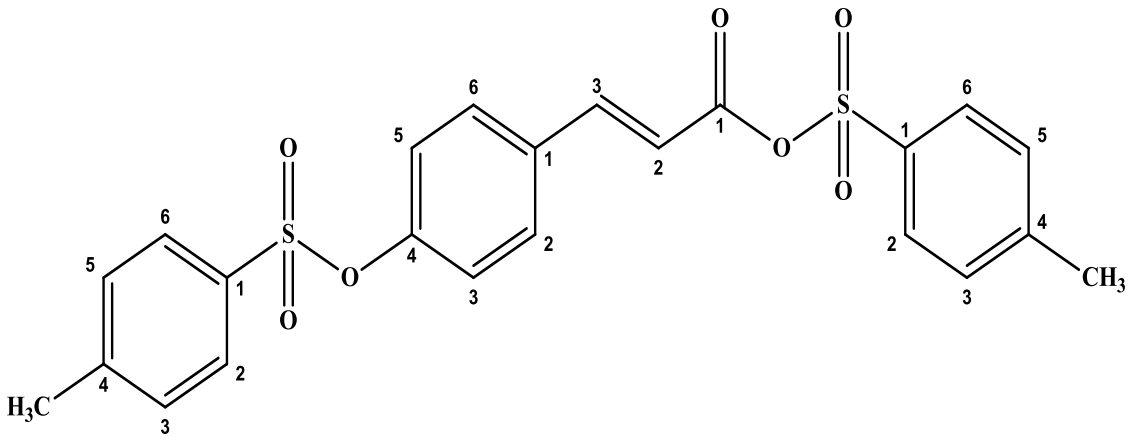

N4

The sample **N4** was purified via a silica gel column chromatography. The solid product of **N4** has a melting point of 199-201℃ and 90.19% yield. Spectroscopic data of **N4** is shown in Figures B8, B27, and B28 in Appendix B for **FT-IR**, **^{1}H-NMR**, and **^{13}C-NMR** respectively. FT- IR, ν cm^{-1}: 3075.20 (C-H alkene), 2924.57 (C-H alkane), 2848.58 (C-H alkane), 1681.38 (C=O), 1632.14 (C=C), 1596.52 (benzene ring), 1505.06, 1429.11,

1370.61, 1312.66, 1284.58, 1199.49, 1180.37, 1154.65, 1093.66, 982.48, 950.37, 868.47, 850.92, 813.38, 757.08, 729.28, 683.94, 657.78, 600.3, 576.23, 561.57, 551.87, 536.33, 508.36. **^{1}H-NMR** (500 MHz, DMSO-d_6, ppm): δ 7.8229 (d, *J* = 7.93 Hz, 2H (2,6 tosyl ring left)), 7.6321 (d, *J* = 8.26 Hz, 2H (2,6 right tosyl ring), 7.5874 (d, *J* = 7.86 Hz, 1H (3, D.B)), 7.5552 (d, *J* = 8.12 Hz, 2H (2,6 *p*-CA)), 7.3634 (d, *J* = 15.56 Hz, 2H (3,5, left tosyl ring)), 7.2112 (d, *J* = 7.73 Hz, 2H (5,3, right tosyl ring)), 7.0807 (d, *J* = 8.35 Hz, 2H (3,5, *p*-CA)), 6.5229 (d, *J* = 15.98 Hz, 1H (2, D.B), 2.3769 (s, 6H, $2CH_3$).**^{13}C-NMR** (126 MHz, DMSO-d_6, ppm): δ 149.4560 (1C (C=O)), 146.3408 (1C (4, *p*-CA)), 145.9506 (1C (3,D.B)), 138.2311 (2C (4,4 both tosyl rings)), 135.5114 (2C (1,1 both tosyl rings)), 131.89 (2C (2,6 *p*-CA)), 130.7390 (2C (3,5 left tosyl ring), (129.3208 (2C (3,5, right tosyl ring), 128.6956 (2C (2,6 right tosyl ring)), 128.5543 (5C (2,6 left tosyl ring, 1,3,5 *p*-CA ring)), 125.9907 (1C (2, D.B)), 21.2559 (2C (CH_3)).

2.1.2.3 Synthesis of *cis*-Jasmone amine

A modified procedure from the assay of Perdicchia *et al*., [112] was used. In 50 ml RBF equipped with a magnetic stir bar 2-(piperazin--yl)ethanamine 0.1.1233 g (1.74 eq., 0.0087 moles) or Phenylhydrazine 0.546 g (1 eq., 0.005 moles), and catalyst cinchona alkaloid (Dihydroquinidine (20%)) were dissolved in 5 ml toluene. *cis*-Jasmone 0.822 g (1 eq., 0.0050 moles) was added, and the solution was kept stirring at room temperature for 48 hours. Then, the mixture was refluxed for two hours while stirring. TLC monitored the reaction. The mixture was concentrated at low pressure.

Synthesis of (Z)-3-Methyl-2-(pent-2-en-1-yl)-3-((2-(piperazin-1-yl)ethyl)amino) cyclopentanone (sample N6)

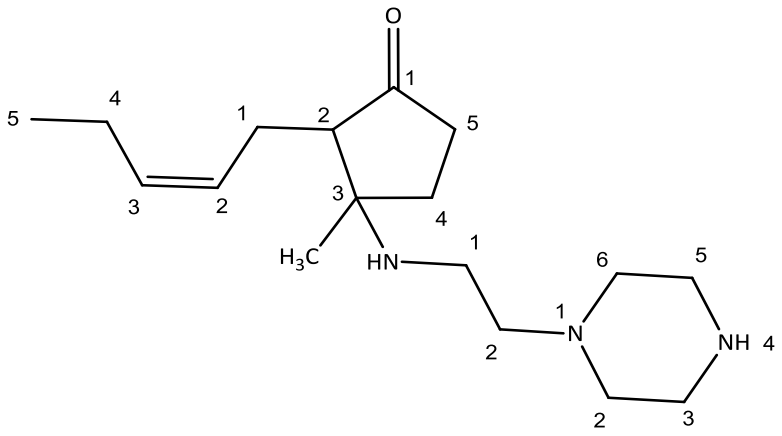

N6

Compound **N6** was cleaned by flash chromatography. The obtained product was solid with a melting point of 45-48 ℃ and 42.56% yield. Spectroscopic analysis for compound **N6** is shown in Figures B9 and B29 in Appendix B for **FT-IR**, and **^{13}C-NMR** respectively. **FT-IR** ν cm^{-1}: 3366.75 (N-H), 3280.98 (C-H alkene), 2945.43 (C-H alkane), 2822.69 (C-H alkane), 1659.59 (C=O), 1450.55, 1322.89, 1136.54, 1063.58, 1002.06, 939.81, 841.82, 618.67, 570.82, 545.94, 528.89. **^{1}H-NMR** (500 MHz, $CDCl_3$, ppm): δ 8.7217 (dd, 1H, (2 pentene)), 8.0397 (dd, 1H, (3 pentene)), 7.7428 (t, *J* = 4.53 Hz, 1H, (4, N-H piperazine)), 6.6416 (t, 2H (1 ethyl amine)), 6.2719 (t, 2H (2 ethyl amine)), 4.3815 (tt, 2H (5 cyclcopentanone)), 3.8536 (t, *J* = 40.64 Hz, 4H (3,5 piperazine)), 3.6587 (t, *J* = 9.59 Hz, 1H (2 cyclcopentanone)), 3.5172 (s, 1H (NH amine)), 3.3174 (t, *J* = 6.29 Hz, 4H (2,6 piperazine)), 2.8986 (dd, 2H (1 pentene)), 2.0543 (t, 2H (4 cyclcopentanone)), 1.9962 – 1.9146 (m, 2H (4 pentene)), 1.7923 – 1.5049 (m, 3H (CH_3 cyclcopentanone)), 0.9324 (t, *J* = 7.42 Hz, 3H (5 pentene)). **^{13}C-NMR** (126 MHz, $CDCl_3$, ppm): δ 161.2038 (C=O), 160.7197 (3 pentene), 158.2699 (2 pentene), 132.1173 (3 cyclcopentanone), 121.8260 (2 amine), 60.3107 (2 cyclcopentanone), 55.9974 (2C (2,6 piperazine), 53.4467 (2C (3,5 piperazine), 52.8192 (1 amine), 51.3583 (5 cyclcopentanone), 36.0371 (4 cyclcopentanone), 34.5150 (1 pentene), 24.8928 (CH_3 cyclcopentanone), 24.0087 (4 pentene), 20.6759 (5 pentene).

Synthesis of (Z)-3-Methyl-2-(pent-2-en-1-yl)-3-(2-phenylhydrazinyl) cyclopentanone (sample N8)

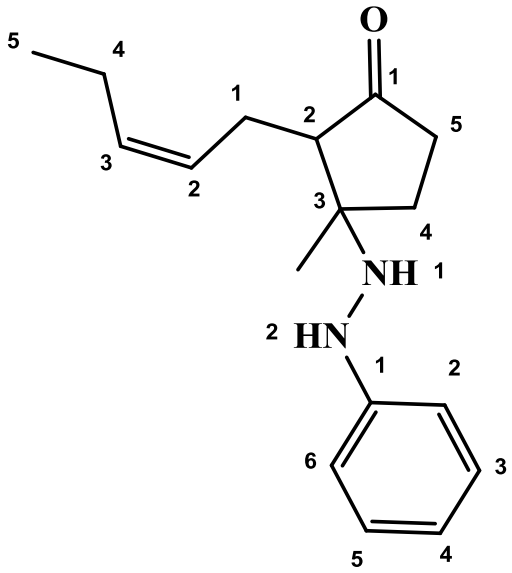

N8

Compound **N8** was purified by flash chromatography technique that furnished a solid product with a melting point of 115-124 ℃ and a 34.45% yield. Spectroscopic analysis is shown in Figures B10**,** and B30 in Appendix B for **FT-IR**, **^{13}C-NMR** respectively; **FT-IR** ν cm^{-1}: 3350 (N-H), 2966.16 (C-H, alkene), 1714.79 (C=O), 1590.40 (aromatic ring), 1553.43 (N-H). **^{1}H-NMR** (500 MHz, DMSO-d_6, ppm): δ 7.8793 (d, *J* = 7.79 Hz, 2H (3,5 aromatic)), 6.6250 – 6.5215 (m, 1H (4 aromatic)), 6.5169 (d, *J* = 7.65 Hz, 2H (2,6 aromatic)), 6.4550 – 6.3861 (m, 1H (2, N-H)), 6.3674 – 6.2623 (m, 1H (1, N-H)), 5.5318 (d, *J* = 7.74 Hz, 2H (2,3 pentene)), 2.6115 (s, 2H (5 cyclopentanone)), 2.0471 (s, 1H (2 cyclopentanone)), 2.0350 – 1.9455 (m, 2H (1 pentene)), 1.1317 (d, *J* = 12.34 Hz, 2H (4 pentene)), 0.7731 – 0.7037 (m, 2H (4 cyclopentanone)), 0.4911 – 0.3507 (m, 3H (CH_3 cyclopentanone)), 0.3372 (s, 3H (5 pentene)).**^{13}C-NMR** (126 MHz, DMSO-d_6, ppm): δ 207.9258 (1 cyclopentanone), 169.8254 1 aromatic), 158.9558 (3 pentene), 143.5309 (2 pentene), 140.5923 (4 aromatic), 130.0896 (3,5 aromatic), 127.9931 (3 cyclopentanone), 120.8765 (2,6 aromatic), 114.5854 (2 cyclopentanone), 38.7965 (4,5 cyclopentanone), 30.2836 (1 pentene, CH_3 cyclopentanone), 24.5359 (4,5 pentene).

2.1.2.4 Synthesis of Thymol Esters

A modified procedure by Khatar *et al*., [50], Wang *et al*., [107], Pal *et al*., [108], and Lazarevic *et al*., [113]. To synthesize compounds of **J16, J10,** and **J11**, the same procedure was followed but in different amounts, and Table A3 Appendix A shows the amounts used in each sample. The required acid was dissolved in DCM in 50 ml (R.B.F) with a magnetic stirrer, and oxalyl chloride was drop-wise added to the mixture at 0 ℃ under inert conditions with constant stirring. DMF was added and the reaction mixture was kept stirring at room temperature overnight under inert conditions. After that, the extra of oxalyl chloride was removed by an additional DMF. A mixture of thymol, and triethylamine (TEA) in CH_2Cl_2 was added to acid chloride under inert conditions, and kept stirring at room temperature under inert conditions overnight. Sample **J11** was refluxed for 3 hr. The reaction was checked by TLC. After the achievement of the reaction, the solvent was removed under low pressure. Distilled water (D.W) was added to the crude product and extracted with ethyl acetate. The upper organic layer was separated, dehydrated over Na_2SO_4 anhydrous, filtered and vaporized. If no separation was observed, the extraction was conducted with brine (saturated NaCl with D.W) such as in **J10.**

2-Isopropyl-5-methylphenylthiophene-3-carboxylate (J16)

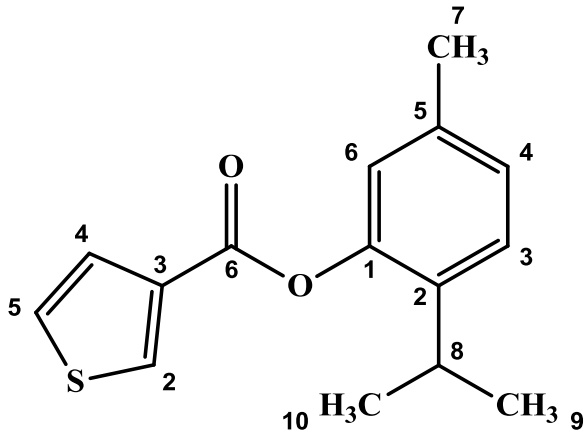

J16

The crude product was cleaned by column chromatography. The product was liquid with a yield of 72.80%. Spectroscopic analysis was performed and shown in Figures B11, B31, and B32 in Appendix B for **FT-IR**, **^{1}H-NMR**, and **^{13}C-NMR** respectively. **FT-IR**, ν cm^{-1}: 3072.20 (C-H alkene), 2956.10 (C-H alkane), 2924.05 (C-H alkane), 2853.91 (C-H alkane), 1710.24 (C=O ester), 1659.68 (C=C conjugated alkene), 1459.62 (C-H bending alkane methyl group), 1419.80, 1377.74 C-H bending alkane gem dimethyl. **^{1}H-NMR** (500 MHz, DMSO-d_6, ppm): δ 9.0412 (s, 1H (2, thiopene)), 6.9456 (d, *J* = 7.62 Hz, 2H (4,5, thiopene)), 6.5870 – 6.5049 (m, 3H (3,4,6, thym)), 3.1352 (hept, *J* = 7.00 Hz, 1H (8, thym)), 2.1561 (s, 3H (7, thym)), 1.1147 (d, *J* = 5.59 Hz, 6H (9,10, thym). **^{13}C- NMR** (126 MHz, DMSO-d_6, ppm): δ 154.1557 (6, thiopene), 135.2564 (1, thym), 133.5750 (2, thiopene), 131.1617 (2,5, thym), 125.6110 (3,5, thiopene), 119.6168 (4, thiopene, 3, thym), 115.5321 (6,4, thym), 26.0144 (8, thym), 22.6092 (9,10, thym), 20.6757 (7, thym).

Synthesis of 2-Isopropyl-5-methylphenyl-5-bromothiophene-2-carboxylate (J10)

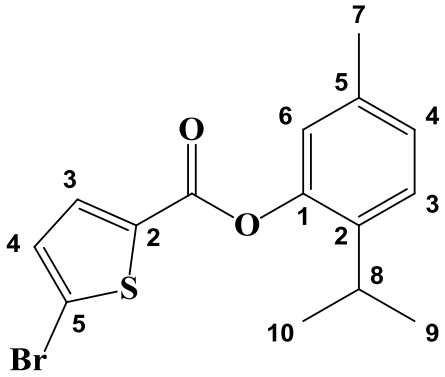

J10

The unfinished product was cleaned by column chromatography silica gel. The product was solid with a melting point of 118-124 ℃ and 86.05% yield. Spectroscopic analysis is shown in Figures B12, B33, and B34 in Appendix B for **FT-IR**, **^{1}H-NMR**, and **^{13}C-NMR** respectively. **FT-IR** ν cm^{-1}: 3100.63 (C-H alkene), 2962.58 (C-H alkane), 2869.64 (C-H alkane), 1731.00 (C=O ester), 1685.03 (C=C alkene), 1529.84 (C=C cyclic alkene), 1411.18 (C-H alkane methyl group), 1328.75 (C-H alkane gem dimethyl), 1277.59 (C-O aromatic ester), 668.87 (C-Br). **^{1}H-NMR** (500 MHz, DMSO-d_6, ppm): δ 8.1648 (d, *J* = 1.50 Hz, 1H (4, thiophene)), 7.9757 (d, *J* = 13.32 Hz, 1H (3, thym)), 7.6915 (d, 1H (3, thiophene)), 6.9483 (d, *J* = 7.83 Hz, 1H (4, thym)), 6.5531 (d, 1H (6, thym)), 3.8492 – 3.7025 (m, 1H (8, thym)), 2.0822 (s, 3H (7, thym)), 1.1572 (d, 6H (9,10, thym**)). ^{13}C-NMR** (126 MHz, DMSO-d_6, ppm): δ 162.9770 (C=O), 161.9383 (1, thym), 136.9320 (2, 5, thym), 133.5854 (4,3,5, thiophene), 131.8470 (3,4, thym), 118.5225 (6, thym, 2, thiophene), 26.055 (8, thym), 22.3662 (9,10, thym), 20.4910 (7, thym).

Synthesis of 2-Isopropyl-5-methylphenyl-4-bromothiophene-3-carboxylate (J11)

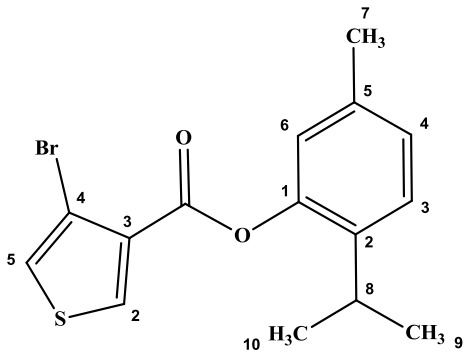

J11

The product was cleaned with column chromatography. The product had orange colored solid melting point of 164-167 ℃ with a yield 89.52%. Spectroscopic analysis was done in Figures B13, B35, and B36 in Appendix B for **FT-IR**, **^{1}H-NMR**, and **^{13}C-NMR** respectively. **FT-IR**, ν cm^{-1}: 2968.69 (C-H alkane), 1762.04 (C=O ester), 1490.28 (C-H bending methyl group), 1356.85 (C-H bending gem dimethyl), 1240.74 (C-O stretching aromatic ester), 1178.26 (C-O stretching ester), 667.41, (C-Br stretching. **^{1}H-NMR** (500 MHz, DMSO-d_6, ppm): δ 7.9734 (d, *J* = 3.38 Hz, 1H (2 thiophene)), 7.3684 (s, 1H (5 thiophene)), 7.2591 (d, *J* = 9.73 Hz, 1H (3 thym)), 7.0886 (s, 1H (6 thym)), 6.7809 (d, 1H (4 thym)), 2.9923 (q, *J* = 7.05 Hz, 1H (8 thym)), 1.3287 (s, 3H (7 thym)), 1.2205 (d, 6H (9,10 thym)). **^{13}C- NMR** (126 MHz, DMSO-d_6, ppm): δ 166.9959 (C=O), 154.7233 (1 thym), 131.6051(2 thym), 131.3311(5 thym), 129.1749 (2 thiophene), 128.6734(5 thiophene), 126.0595 (d, *J* = 10.28 Hz (3 thym)), 125.5614 (4 thym), 123.3387 (3,4 thiophene), 67.4218 (6 thym), 28.3705 (8 thym), 23.2552 (9 thym), 22.9375 (10 thym), 22.4058 (7 thym).

Synthesis of 2-Isopropyl-5-methylphenyl furan-3-carboxylate (J12)

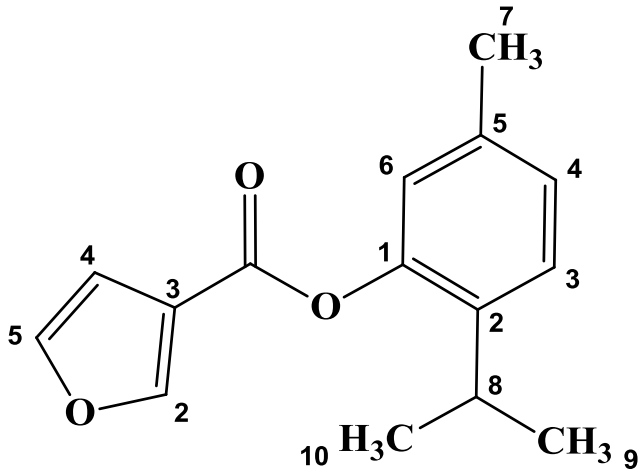

J12

Fischer esterification was applied, and a carboxylic acid reacts with alcohol with a catalyst of mineral inorganic acid. A modified procedure of the assay of Khatar *et al*., [50] was followed. In 50 ml RBF with a magnetic stirrer furan-3-carboxylic acid 0.117 g (1 eq., 0.001 moles) was mixed with thymol 1.445 g (10 eq., 0.010 moles) in CH_2Cl_2 10 ml and refluxed with concentrated sulphuric acid (H_2SO_4) 2.5 ml. The end of the reaction was checked by TLC. Then 20 ml ice-cooled D.W was added to the reaction mixture and

neutralized with sodium bicarbonate $NaHCO_3$ solution till blue litmus did not change its color followed by extraction of an ester with ether. The upper ether layer (density of ether 0.706 g/ml) was separated, dried over Na_2SO_4, filtered, and evaporated under vacuum. The product was cleaned with column chromatography to furnish a solid product with melting point of 133-134 ℃ with 38.43% yield. Spectroscopic analysis was done for sample **J12,** which is shown in Figures B14, B37, and B38 in Appendix B for **FT-IR**, **^{1}H-NMR**, and **^{13}C-NMR** respectively. **FT-IR**, ν cm^{-1}: 2965.51 (C-H alkene), 2922.01 (C-H alkane), 1713.81 (C=O), 1594.57 (C=C cyclic alkene), 1454.49 (C-H bending alkane methyl group), 1380.90 (C-H bending alkane gem dimethyl), 1259.59 (C-O stretching aromatic ester), 1186.57 (C-O stretching ester), 667.05 (C=C bending). **^{1}H-NMR** (500 MHz, DMSO-d_6, ppm): δ 8.1643 (d, *J* = 9.73 Hz, 1H (5, furan)), 7.7788 (s, 1H (2, furan)), 7.7296 – 7.6350 (m, 1H (3, thym)), 7.4418 – 7.3902 (m, 1H (4, furan)), 7.1408 (d, *J* = 7.86 Hz, 1H (6, thym)), 6.6503 (s, 1H (4, thym)), 3.1935 (p, *J* = 7.00 Hz, 1H (8, thym)), 2.4640 (s, 3H (7, thym)), 2.0445 – 1.9261 (m, 6H (9,10, thym)).**^{13}C-NMR** (126 MHz, DMSO-d_6, ppm): δ 159.8485 (C=O), 158.5856 (1, thym), 141.9807 (2, furan), 135.7697 (5, furan), 133.0601 (2, thym), 129.6586 (5, thym), 128.6312 (3, thym), 127.7619 (4, thym), 125.5053 (6, thym), 118.4223 (3, furan), 115.0676 (4, furan), 26.5694 (8, thym), 22.1085 (7, thym), 18.9474 (9,10, thym).

2.2 Biological part

2.2.1 Materials and Instrument

a. Anticancer activity

The *in vitro* cytotoxic evaluation was done using the MTS assay against six cancer cell lines:- including hepatocellular carcinoma (Hep3B (ATCC HB-8064) and HepG2 ((ATCC HB-8065)), cervical adenocarcinoma (HeLa, CRM-CCL-2 ATCC), breast carcinoma (MCF-7, ATTCC HTB-22), skin cancer cell line (B16-F1, CRL-6323 ATCC), colorectal carcinoma (CaCo-2, CRL-2102 ATCC) cell line in addition to the normal cell line (LX-2, ATCC SCC064). All the chemicals were bought from biological industries, but the **MTS** reagents were bought from SIGMA Company (USA). All of the six cancer cell lines were bought from ATCC.

b. Antimicrobial activity

The materials and instruments used: Spectrophotometer for preparing McFarland, micropipette, laminar flow, an incubator at 37 ℃, tips, 96 wells plates, falcon tubes, Muller Hinton broth (M.H.B), Brain heart infusion broth (B.H.I) for *Candida albicans*, normal saline, All material and tool must be sterile and to sterile sample using a UV light for 20 minutes. The antibacterial and antifungal activities were tested against fresh bacteria cultures: MRSA (clinical sample), *Staphylococcus aureus* (ATCC#25923), *Klebsiella pneumonia* (ATCC#13883), *Escherichia coli* (ATCC#25922), *Proteus vulgaris* (ATCC#8427), *Pseudomonas aeruginosa* (ATCC#9027), and *Candida albicans* (ATCC#90028) as antifungal activity.

2.2.2 Methodology

2.2.2.1 *In-vitro* Anticancer Activity Analysis

a. Preparation of Cancer Cells Line

A modified procedure of Widiyarti *et al*., [39], Hawash *et al*., [114] and Jaradat *et al*., [115] was used. The cells were cultivated in Roswell Park Memorial Institute (RPMI 1640) enhanced with 10% Fetal Bovine Serum (FBS) and 1% penicillin-streptomycin (Pen-Strep) antibiotic, 1% L-glutamine, phosphate buffer solution x1 (PBs) and enzyme trypsin 0.25% proteolytic enzyme that is used to detach cells from the adherent substrate [116]. Dulbecco's Modified Eagle Medium (DMEM) was used for normal cell culture (LX-2). Cells were seeded by 100 µL of $1x10^4$ cells per well in a 96-well plate and incubated at 37 ℃ in a humidified atmosphere with 5% CO_2. After that the media was discarded. After 24 h, cells were confluent, the media was changed and cells were incubated with 100 µL of different concentrations of the samples in duplicate for 72 h at 37 ℃ in a moistened atmosphere with 5% CO_2. After that the samples were discarded.

b. MTS Assay

The metabolic function of mitochondrial enzymes which are formed by live cells that change3- (4,5-dimethylthiazol-2-yl)-5- (3-carboxymethoxyphenyl)-2- (4-sulfophenyl)-2H- tetrazolium (MTS) a yellow colored liquid to a brown colored formazan yields that are directly soluble in cell culture medium allows to a quantitative assessment of the viability of cells. The intensity of the color (at 490 nm) due to formazan is proportional to the number of live cells [117]. Cell viability was assessed by CellTiter 96® Aqueous

One Solution Cell Proliferation (MTS) assay agreeing to the manufacturer's instructions (Promega Corporation, Madison, WI). At the end of the management, 80 μL of media (pink color) and 20 μL of MTS were added to every well and protected at 37 °C for 2-4 h. Absorbance was measured at 490 nm using an ELISA plate reader. Wells with culture media, cells, solvent (DMSO) and without samples in the same plate were left as controls, and wells with media were only left blank. Percent inhibition was calculated as in Equation 5.

Equation 5

Calculation of inhibition%

Inhibition%=(1-(absorption of special concentration/absorption of control))*100%

The IC_{50} value was a measure of the effectiveness of a compound in inhibiting the biological function of the active sample, was calculated by linear regression analysis between percent [39].

2.2.2.2 Antimicrobial Analysis

a. **Preparation of Mueller Hinton broth (MHB) media**:

A modified procedure of Leber [118] was used, and MHB media was prepared by dissolving 8.4 g from MHB powder in 400 ml of distilled water. This solution was heated by stirring with a magnetic stirrer until it dissolved completely, then it was autoclaved for 20 minutes to ensure its sterilization.

b. Preparation of McFarland turbidity standard No.0.5

The standard McFarland turbidity was prepared by mixing 9.95 ml of 1% (v/v) sulfuric acid and 50 μl of a 1.175% (W/V) barium chloride dihydrate ($BaCl_2.2H_2O$) solution. The tube which had the 0.5 McFarland standard, was then sealed with parafilm to avoid vaporization and stored in the dark at room temperature. The 0.5 McFarland standard was strongly mixed on a vortex mixer before use. A 0.5 McFarland standard is comparable to bacteria suspension $1.5x10^8$ colony forming units (CFU/ml) [119].

c. Preparation of the bacterial and fungal suspension:

A sterile swab of 6 kinds of fresh bacteria cultures (MRSA (clinical sample), *Staphylococcus aureu*s (ATCC#25923), *Klebsiella pneumonia* (ATCC#13883),

Escherichia coli (ATCC#25922), *Proteus vulgaris* (ATCC#8427), *Pseudomonas aeruginosa* (ATCC#9027), and one type fungal culture fresh *Candida albicans* (ATCC#90028) were taken from each culture and dissolved gently in a separable sterile tube containing 4-5 ml of normal saline. The turbidity of each solution was measured by a spectrophotometer at 620 nm. The turbidity for all the bacterial suspension was adjusted into McFarland standard of 0.08-0.12 (the blank is normal saline). The concentration of bacteria should be $1.5*10^8$ CFU/ml (CFU=colony forming unit), and the optical density for the candida should be 0.12-0.15. Six other sterile tubes were marked with each type of bacteria and filled with 100 µl of each prepared bacteria suspensions in its new tube followed by adding the media of Mueller Hinton broth till the final volume reached 10 ml in each tube. Another tube was filled with 100 µl of *Candida* suspension followed by adding the media of Mueller Hinton broth till the final volume reached 10 ml in each tube. A collection of seven 96 well microplates were marked, 6 for the bacteria (each one for the fourteen samples) and the 7th for candida.

d. Determination of minimum inhibitory concentration (MIC)

MIC of samples was determined by the broth microdilution method in sterile 96-wells microplates according to the CLSI [120]. The 600 µg/ml samples of 10% DMSO and 10% DMSO (negative control) were two-fold-serially diluted in nutrient broth in the wells of plates in a final volume of 100 µL. 50 µl from the prepared media of Mueller Hinton broth were filled in columns 1-12 of the column (including the last row H of the well). Followed by filling the first column with 50 µl from each sample (also here the last row H was included). From this first column, a serial micro dilution using a multichannel pipette was started by taking 50 µl from this sample and mixing it then diluting until column 10. This was made for all types of samples. Then 50 µl from each type of bacteria inoculum of 10^4 CFU/ml was filled in its specific row for columns 1-11 (excluded row H). The microtiter plates were then enclosed and protected at 37 ℃ for 24 h. The same steps for the other types of bacteria were repeated for *Candida*. Each sample was run in duplicate. Well number 11 was positive (+ve) control (bacteria and broth), well number 12 was negative (-ve) control (broth only), and row H was control (broth and sample) to know if there was contamination or not. The MIC was considered the lowest concentration in the sample, which inhibited the bacterial growth.

Chapter Three

Result and discussion

3.1 Chemistry

3.1.1 Citronellol Esters

Three esters from citronellol were synthesized following a literature method with minor modifications [107, 108]. In this procedure, acid chloride was first prepared, and then citronellol was added with triethylamine (TEA) and refluxed at room temperature. TLC checked the progression of the reaction. In the reaction of preparing acid chloride 4-bromothiophene-3-carbonyl chloride a capillary amount of DMF was used and some reactions requisite more reflux time than others (**J13**). The following procedure produced only the predictable product; some starting materials were also detected in some reactions, as in the case of preparation of (**J13**). Different yields were obtained the highest in3,7-dimethyloct-6-en-1-yl thiophene-2-carboxylate (**J15**) 83.26% and the lowest in **J13** 56.92%. Flash column chromatography was used for the purification of the compounds' products except for the compound **J3**. Cleaned products were analyzed using different analytical and spectroscopic procedures, such as melting point, FT-IR, ^{1}H-NMR, and ^{13}C-NMR. In all cases, results are coordinated with the estimated structures. The structures and the experimental part for the prepared citronellol esters are summarized in Scheme 1, the general mechanism of the reaction of DMF with oxalylchloride then with carboxylic acid is shown in Figure 7, and the citronellol esters characterization data are shown in Table A4 in Appendix A.

Scheme 1

Citronellol esters prepared from reacting citronellol with different substituted thiophene carboxylic acid

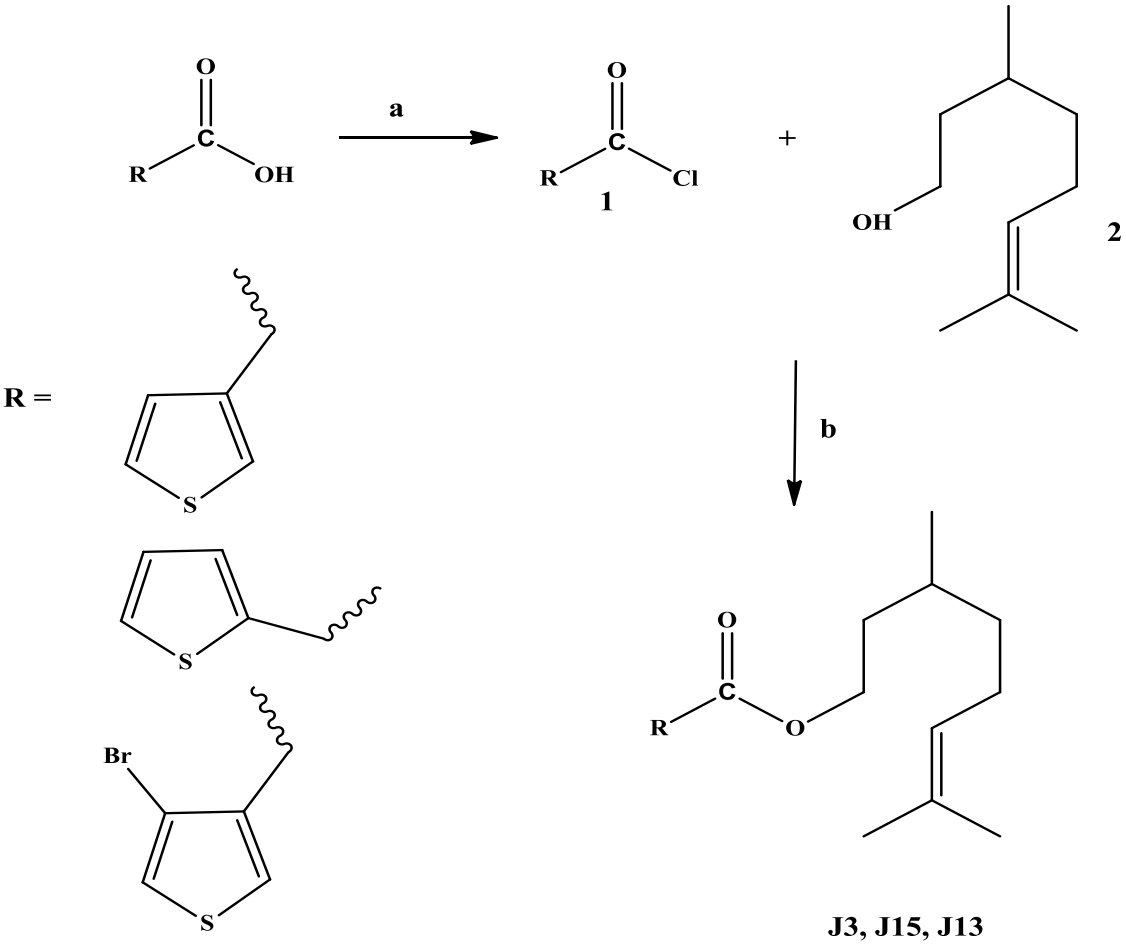

Figure 7

Mechanism of oxalylchloride with DMF and carboxylic acid

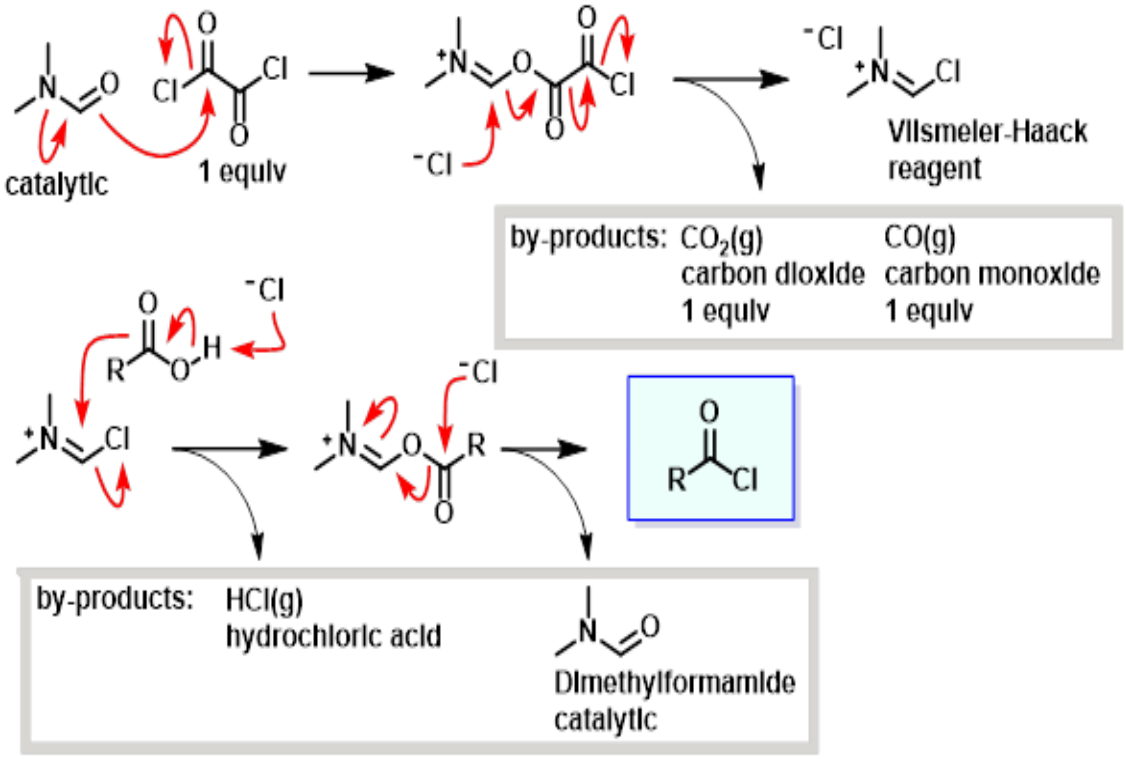

3.1.2 *p*-Coumaric acid (*p*-CA) derivatives

p-CA Esters

Compound **J2** was prepared by Fischer esterification through condensation of *p*-CA (1 eq.) with citronellol (9.3 eq.) and a catalytic amount of conc. H_2SO_4 which resulted in a thick black liquid with a yield of 68.44%. The chemical structure of **J2** was recognized by spectroscopic techniques using FT-IR and ^{13}C-NMR, Figures B4, and B21 in Appendix B. All spectral data indicated the successful synthesis of **J2.** Scheme 2 shows the synthesis of compound **J2.**

Scheme 2

Synthesis of J2

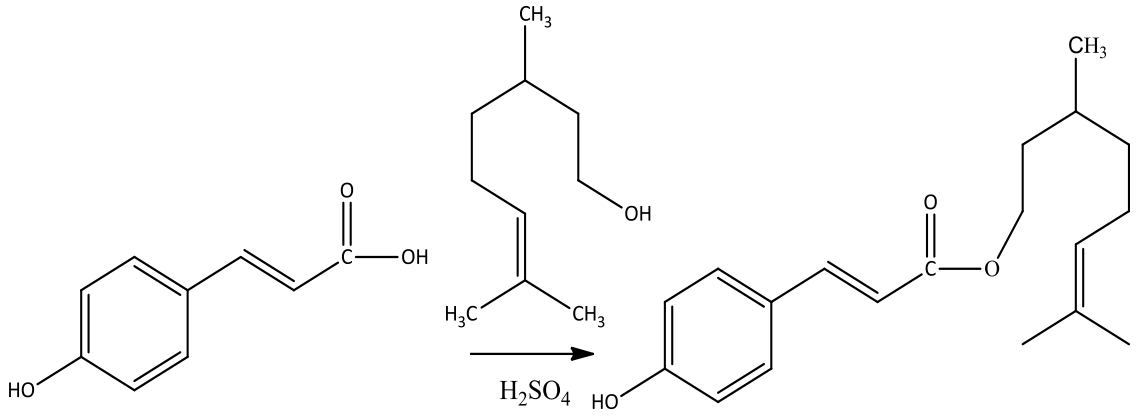

J2

p-CA ester with thymol compound **J14** was prepared by condensation (1.2 eq.) *p*-CA with (1 eq.) of thymol and (1.5 eq.) of TEA, resulting in a liquid product with 69.15% yield. The structure of **J14** was recognized by spectroscopic analysis: FT-IR, and ^{13}C-NMR which are shown in Figures B5, and B22 in Appendix B**,** respectively, and Scheme 3 shows the synthesis of compound **J14.**

Scheme 3

Synthesis of J14

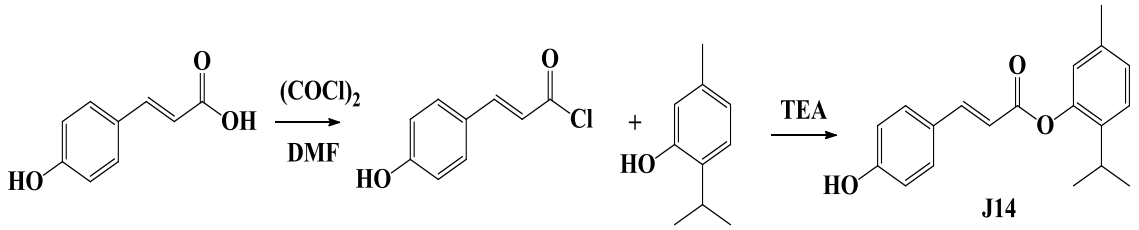

p-CA Amide

p-CA (1.8 eq.) was refluxed with aminoethyl piperazine to produce **J19**, which was yellow crystals with a 97.35% yield. Scheme 4 shows the mechanism of preparation of **J19**. The structure of **J19** was recognized by spectroscopic analysis: FT-IR, ^{1}H-NMR, and ^{13}C-NMR which are shown in Figures B6, B23, and B24 in Appendix B, respectively.

Scheme 4

Synthesis of J19

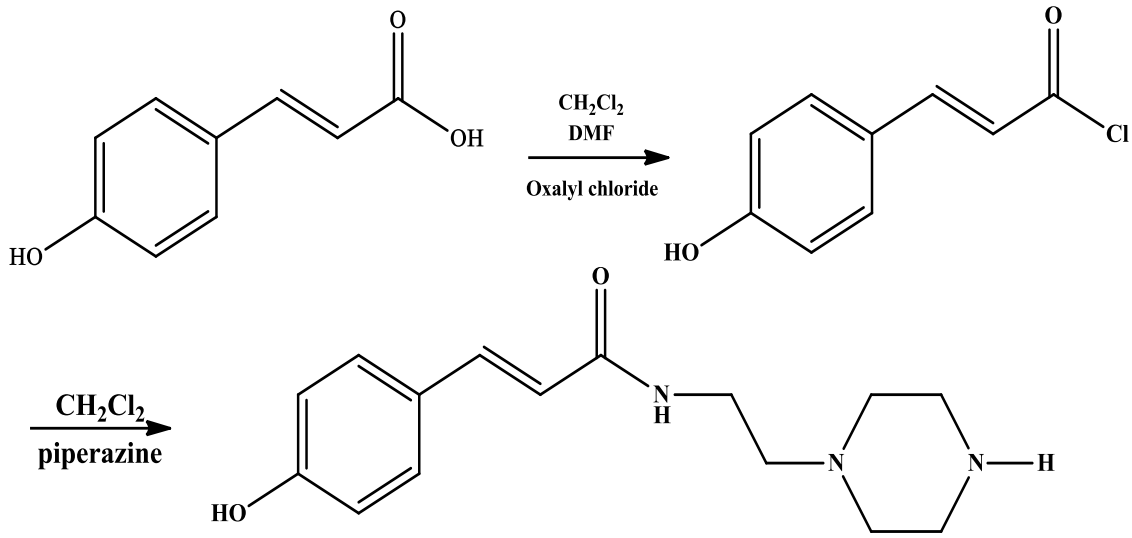

J19

p-CA Anhydride

p-CA(0.25 eq.) was mixed with TsCl (1 eq.) in basic condition 5M NaOH to produce sample **N2** with 24.76 % yield. The mechanism of the reaction is shown in Scheme 5. The structure of **N2** was recognized by spectroscopic analysis: FT-IR, ^{1}H-NMR, and ^{13}C-NMR which are shown in Appendix B, Figures B7, B25, and B26 respectively.

Scheme 5

Synthesis of N2

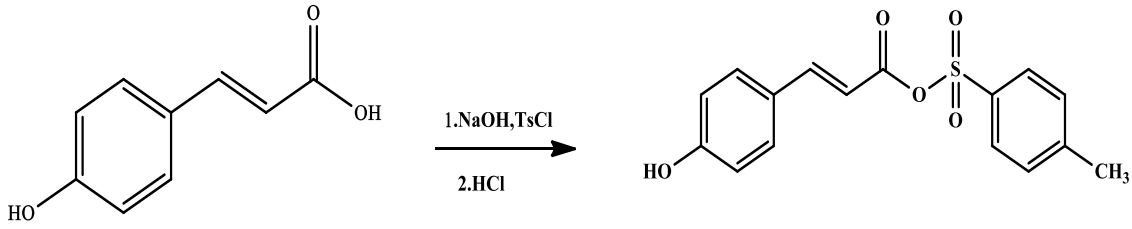

N2

Sample **N4** (90.19% yield) was prepared by mixing 1 eq. of sample **N2** and 1.1 eq. of TsCl in presence of 4-(dimethylamino)pyridine (DMAP) 1.1 eq. The mechanism of the reaction is shown in Scheme 6**.** The structure of sample **N4** was known by spectroscopic analysis: FT-IR, ^{1}H-NMR, and ^{13}C-NMR shown in Figures B8, B27, and B28, respectively in Appendix B.

Scheme 6

Synthesis of N4

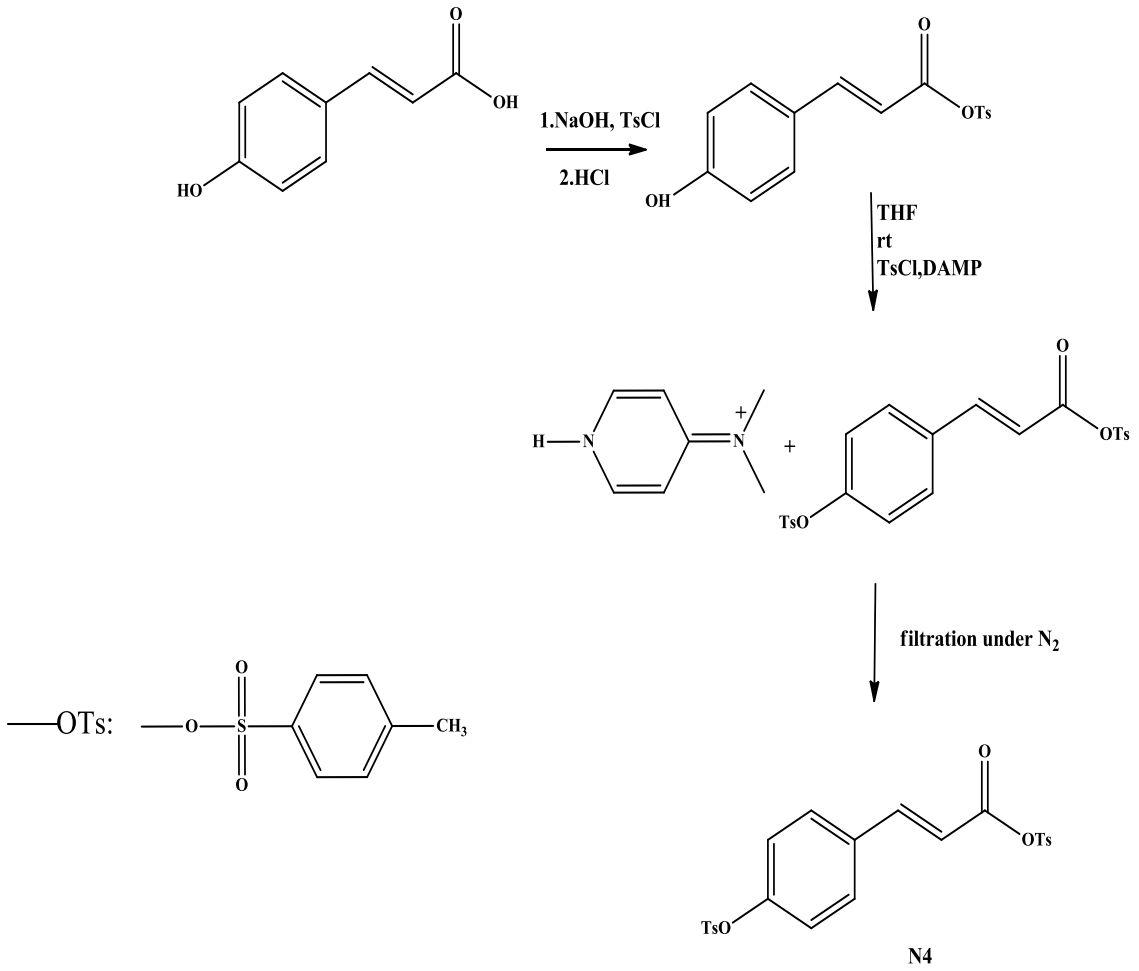

3.1.3 *cis*-Jasmone amine derivatives

cis-jasmone 1 eq. was reacted with 2-(piperazin-1-yl)ethanamine 1.7 eq. to produce **N6** with yield 42.56%. The equation and the mechanism of the reaction are shown in Scheme 7 and Figure 7 respectively**.** The low yield may be attributed to the possibility of the formation Schiff base according to Equation 6 or to the attack of cyclic secondary amine of 2-(piperazin-1-yl)ethanamine as in Equation 7. The structure of **N6** was proven by spectroscopic analysis: FT-IR, and ^{13}C-NMR. All spectral data showed that amine of *cis*-jasmone with 2-(piperazin-1-yl)ethanamine had been produced effectively. The spectroscopic analyses are shown in Figures B9 and B29 in Appendix B.

Scheme 7

Synthesis of N6

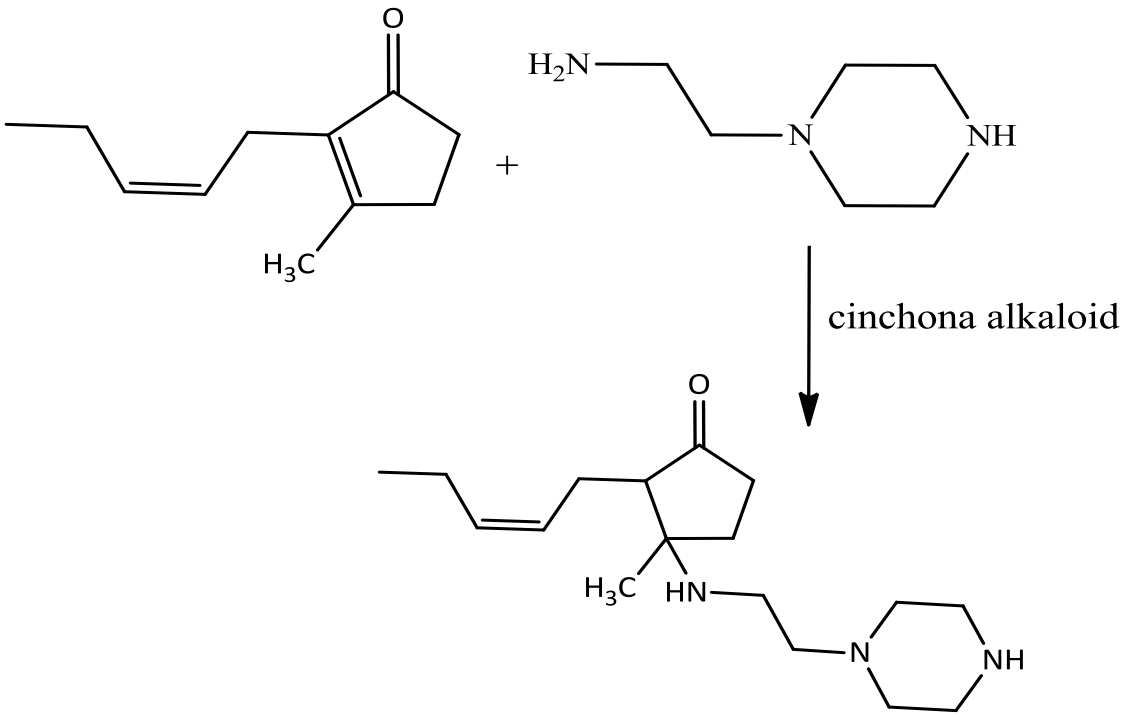

N6

Figure 8

Mechanism of Michael Addition of amine N6

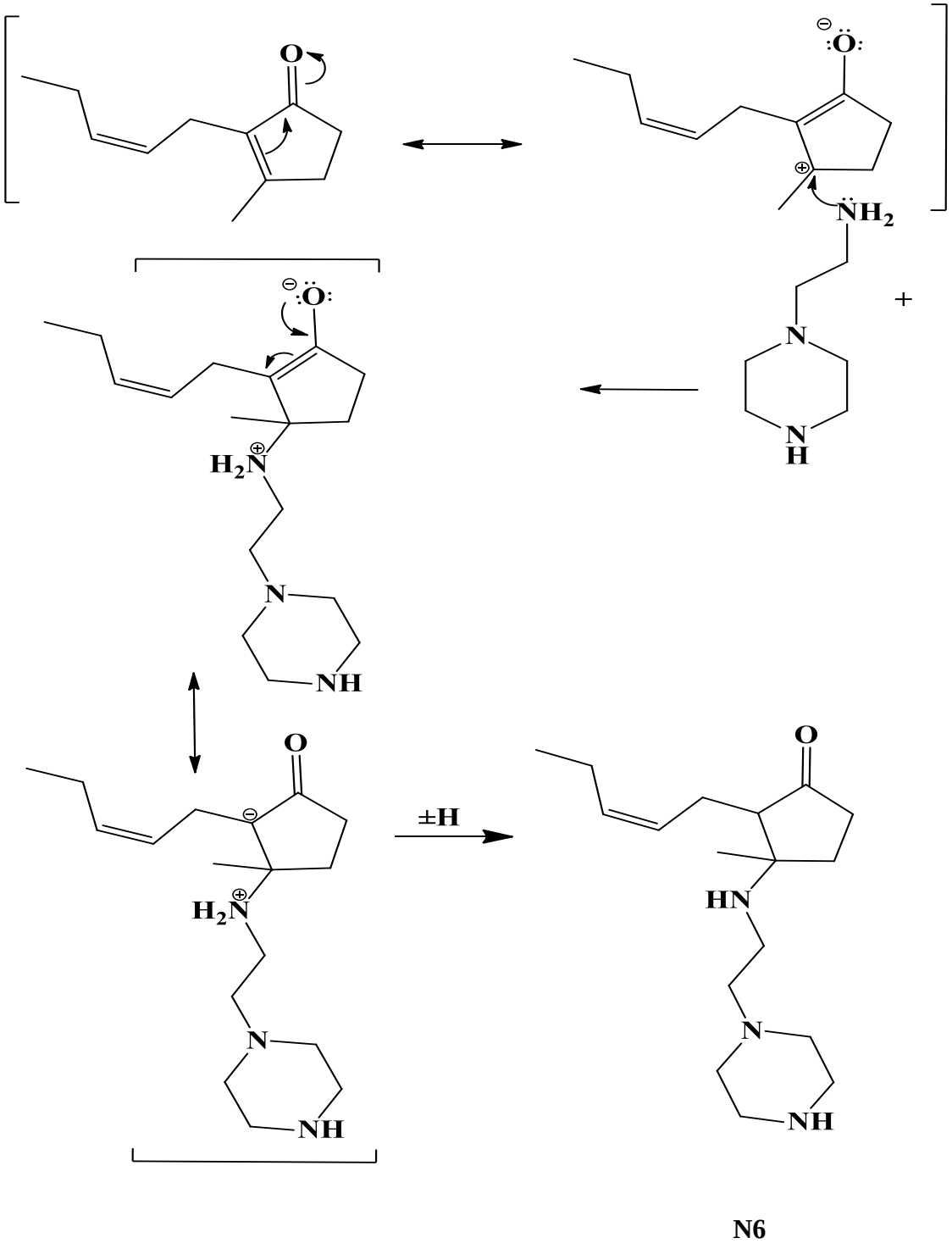

N6

Equation 6

Schiff base of cis-jasmone with 2-(piperazin-1-yl)ethanamine

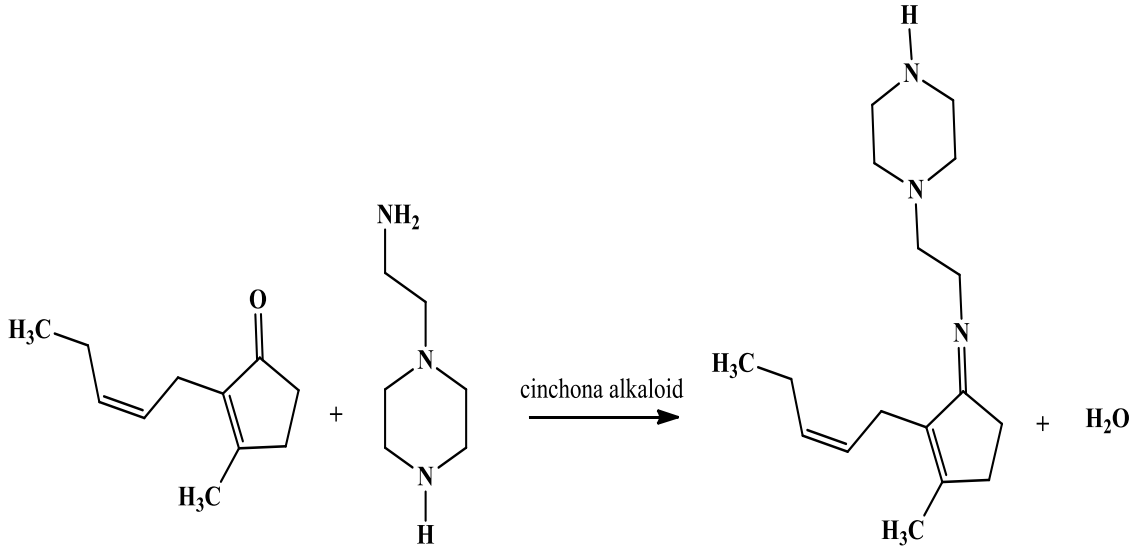

Equation 7

Amine of cis-jasmone with secondary nitrogen atom of 2-(piperazin-1-yl)ethanamine

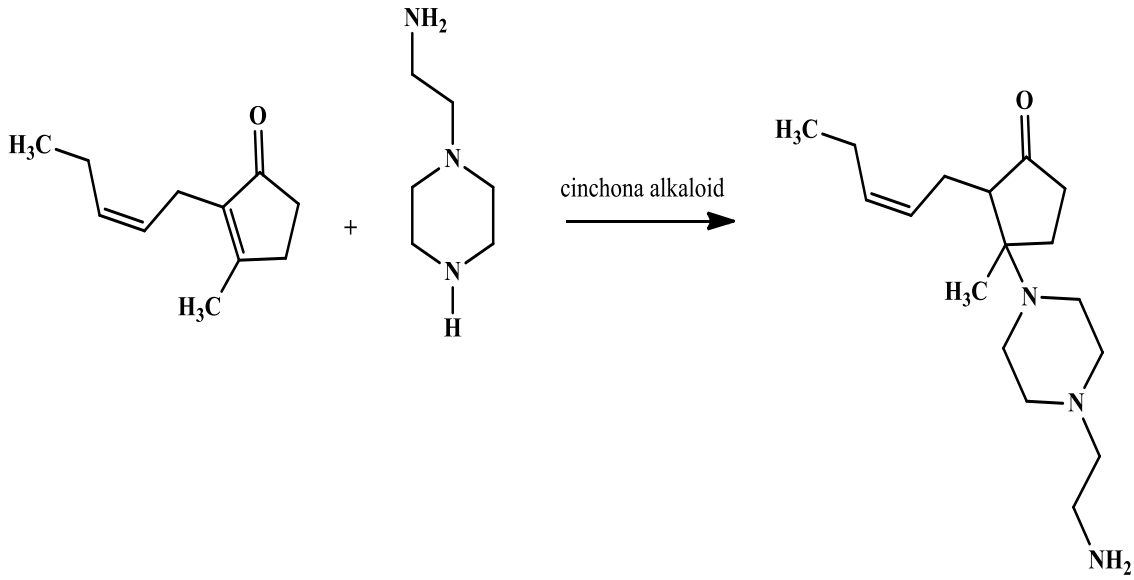

cis-Jasmone 1 eq. was reacted with phenylhydrazine 1 eq. to produce **N8** with a yield of 34.45%. The equation of synthesis is shown in Scheme 8. The low yield may be attributed to the possibility of the formation Schiff base according to Equation 8 or the attack of the secondary nitrogen atom of phenyl hydrazine as in Equation 9. Spectroscopic analysis identified the structure of **N8**. FT-IR and ^{13}C-NMR spectra are presented in Appendix B, Figures B10, and B30.

Scheme 8

Synthesis of N8

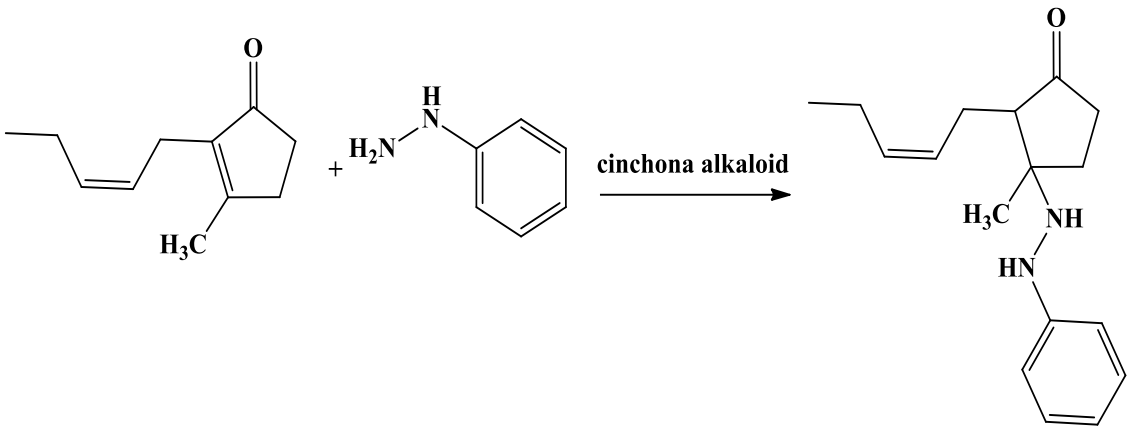

N8

Equation 8

Schiff base of cis-jasmone with phenyl hydrazine

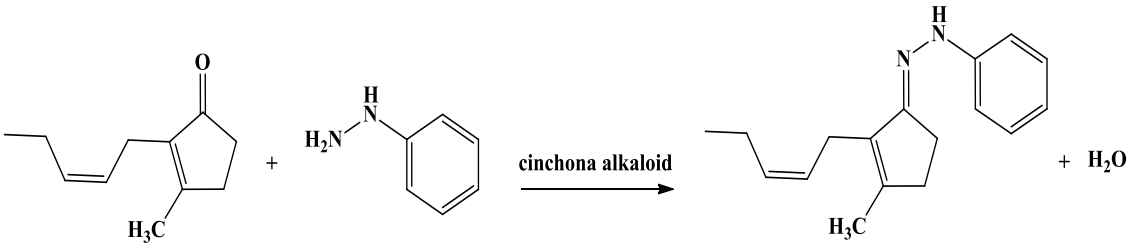

Equation 9

Amine of cis-jasmone with secondary nitrogen atom of phenyl hydrazine

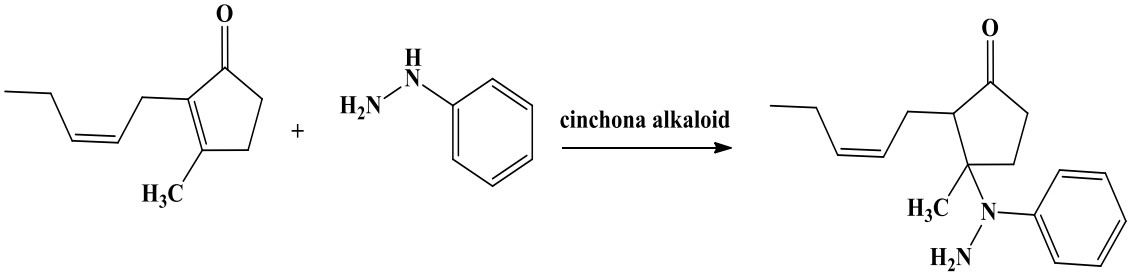

3.1.4 Thymol derivatives

Thymol esters (**J16, J10,** and **J11**) were prepared by condensation of the required acid with thymol after converting the required acid to acid chloride, as followed in Scheme 9**. J16** was produced by condensation of 3-thiophene carbonyl chloride 1 eq. with 1.2 eq. and 1.5 eq. TEA with a yield 72.80%, **J10** was synthesized by condensing of 1.2 eq. 5-bromo-2 thiophene carbonyl chloride with 1eq. thymol and 1.52 eq. TEA to yield 86.05%.

J11 was formed by condensing 1.33 eq. of 4-bromo-2 thiophene carbonyl chloride with 1 eq. thymol and 2 eq. TEA to give 89.52% yield. The structures of new compounds were identified by FT-IR, ^{1}H-NMR, and ^{13}C-NMR. The spectra of each compound are shown in Appendix B; for **J16** B11, B31, and B32, for **J10** B12, B33, and B34, for **J11** B13, B35, and B36 to indicate FT-IR, ^{1}H-NMR and ^{13}C-NMR analysis respectively for each compound.

Scheme 9

Synthesis of thymol esters

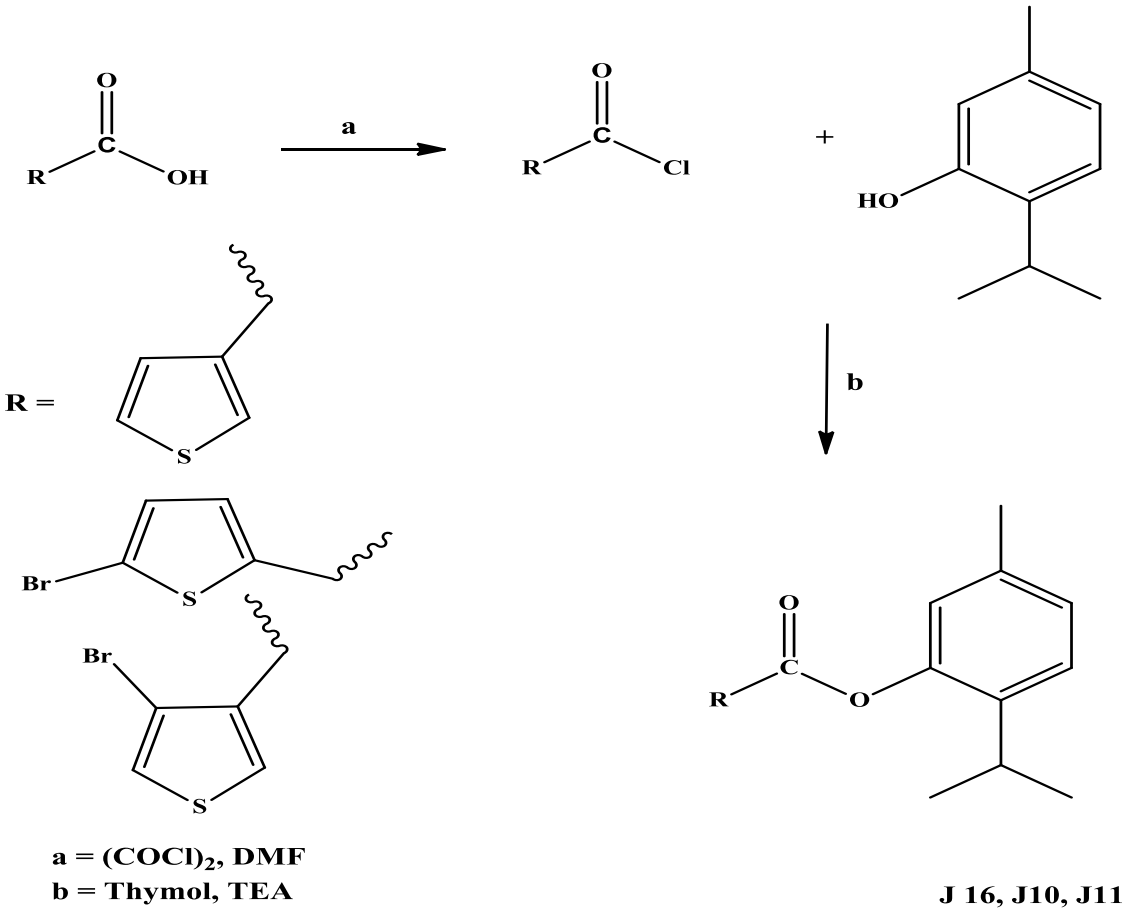

J12 was prepared by Fischer Esterification by reflux of furan-3-carboxylic acid 1 eq. with 10 eq. of thymol in acidic condition Scheme 10 to yield 38.43%. Spectroscopic analysis identified the structure of **J12**. The spectra in Figures B14, B37, and B38 in Appendix B show the FT-IR, ^{1}H-NMR, and ^{13}C-NMR respectively.

Scheme 10

Synthesis of J12

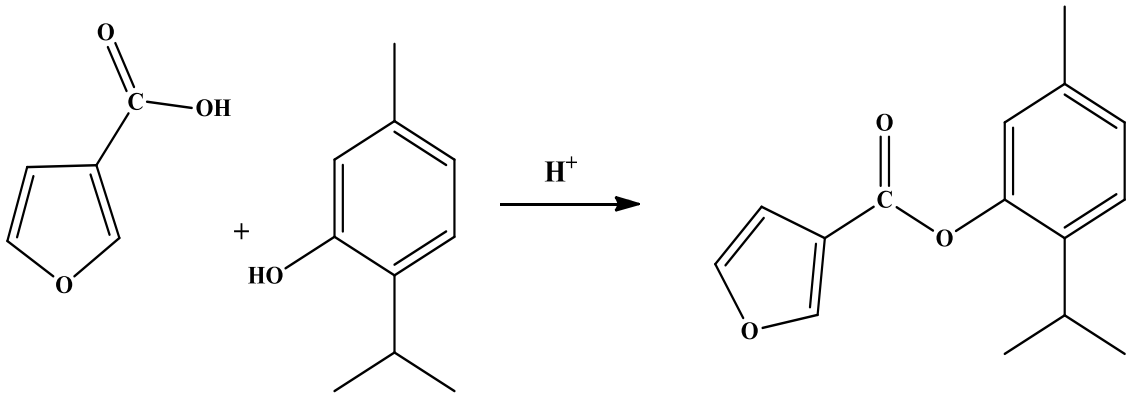

J12

3.2 Biological Activities

3.2.1 Anticancer activity

The ester of citronellol with thiophene-3-carboxylic acid (**J3**) was tested against six cell lines: colorectal carcinoma cell line (CaCo-2), hepatocellular carcinoma (Hep-3B and Hep-G2), cervical adenocarcinoma (HeLa), breast carcinoma (MCF-7), and normal cell line LX-2. The inhibition% of CaCo-2, Hep-3B, Hep-G2, HeLa and MCF-7 cell lines was measured as (72.49 - -3.94%), (84.91 - -2.16%), (71.98 - 0.30%), (82.96 - 2.83%), (91.85 - 1.08%) respectively within the studied concentration range. Cell inhibition was increased when the concentration of citronellol ester **J3** increased. However, it was detected that **J3** prompted propagation instead of inhibition at a lower concentration (50 μg/ml) as the percentage inhibition results were negative in CaCo-2 and Hep-3B cell lines Table A5 Appendix A. Citronellol was tested against the same cell lines and also observed negative result of inhibition percentage in cell lines of CaCo-2 at 50 μg/ml. The new ester compound **J3** was slightly more effective than citronellol on the MCF-7 cell line at 91.85%, while citronellol was 90.69% at the same 500 μg/ml concentration. The new ester compound **J3** and citronellol were also tested against normal cell line LX-2 and their inhibition% range was (67.79% - 0.88%) and (61.05 - 7.99%) respectively at the same concentration range (500 - 50 μg/ml), this indicates that **J3** has a higher effect on normal cells at higher concentration but lower effect at lower concentration Figure B39 Appendix B in comparison with citronellol. The results show that CaCo-2, Hep-3B, Hep-G2, HeLa, and MCF-7 cell lines are all sensitive to anticancer assays of the new citronellol ester **J3**

but less potent than citronellol as indicated by IC_{50} of both compounds in Table 2. It is worth indicating the **J3** is less toxic on normal cells LX-2 than citronellol with IC_{50} 330.57 μg/ml in comparison to IC_{50} of citronellol 275.31μg/ml Table 2**.** The ester of Citronellol with thiophene-2-carboxylic acid **J15** was tested against CaCo-2, Hep-G2, HeLa, MCF-7 and B16-F1 (skin cancer) cell lines at the range of concentration of 1000-50 μg/ml. The range of inhibition% was (96.24 - 0.81%), (96.90 - 4.37%), (96.96 - 5.95%), (95.44 - 6.96), and (97.59 - -0.90%) respectively. However, it was detected that **J15** prompted the growth instead of inhibition at a lower concentration (50μg/ml) as percentage inhibition results were negative in cell lines of B16-F1 Table A6 Appendix A. It was also observed that at higher concentrations the inhibition % against cancer cell lines increased. The new ester of citronellol **J15** had higher inhibition activity at a concentration 500 of μg/ml than citronellol against CaCo-2, Hep-G2, HeLa and MCF-7, respectively 94.91% > 91.34%, 96.49 > 84.64%, 88.66 > 86.09% and 94.68% > 90.69%. It was observed that **J15** is most potent against the Hep-G2 cell line in terms of IC_{50} 208.5 μg/ml than citronellol 208.5 μg/ml < 252.69 μg/ml and other citronellol esters **J3** 208.5 μg/ml < 440.24 μg/ml and **J13** 208.5 μg/ml < 574.85 μg/ml Table 2 and Figure B40 Appendix B. Also, **J15** was less potent (377.61 μg/ml) against normal cell lines LX-2 than citronellol 377.64 > 275.31 μg/ml. This can be interpreted that the new ester **J15** was less toxic on normal cells than citronellol. The result of this study showed that citronellol ester with 2TCA **J15** could be considered a new potential chemopreventive against liver cancer Hep-G2 with more preservation to normal cells. The new ester of citonellol with 4-Bromo-3-thiophene carboxylic acid (**J13**) was tested against CaCo-2, Hep-G2, HeLa, MCF-7 and B16-F1 (skin cancer) cell lines at the range of concentration of 1000-50 μg/ml and their range of inhibition% was (85.04 - -0.34), (87.78 - 0.74%), (67.00 - 1.02), (89.40 - 2.87%) and (91.81 - 0.00%) respectively. However, it was noticed that **J13** prompted cell growth instead of inhibition at a lower concentration (50 μg/ml) as inhibition percentage results were negative in cell lines of CaCo-2 Table A7 Appendix A. The results showed that **J13** was less potent in terms of IC_{50} against all cell lines and more potent against normal cell line (LX-2) 159.15 μg/ml Table 2. This means that **J13** is more toxic to normal cells. The study revealed that functionalization of citronellol with 2TCA provided inhibition against the Hep-G2 cancer cell line and proliferation of normal cells aligned with 3TCA functionality, but functionalization of citronellol with 4B3TCA was less potent as an anticancer agent and more toxic to the normal cells.

Table 2

IC_{50} of citronellol and new esters

	IC_{50} (μg/ml)			
Assay	Citronellol ± SD	J3 ± SD	J15 ± SD	J13 ± SD
CaCo-2	84.22 ± 0.141	393.12 ± 0.007	226.43 ± 0.304	483.86 ± 0.057
Hep3B	185.21 ± 0.148	384.94 ± 0.007	-	-
HepG2	252.6 ± 0.219	440.24 ± 0.170	208.5 ± 0.354	574.85 ± 0.537
HeLa	119.66 ± 0.516	349.90 ± 0.074	154.84 ± 0.007	412.56 ± 0.085
MCF-7	175.14 ± 0.099	344.35 ± 0.249	200.37 ± 0.262	459.42 ± 0.028
B16-F1	-	-	163.40 ± 0.007	258.17 ± 0.001
LX-2	275.31 ± 0.219	330.57 ± 0.267	377.64 ± 0.005	159.15 ± 0.106

p-CA ester with citronellol (**J2**) was tested against CaCo-2, Hep-3B, Hep-G2, HeLa, and MCF-7 at a concentration range of 500-50 μg/ml with inhibition% of (67.52 - -1.91%), (92.25 - -0.86%), (92.26 - 5.26%), (95.23 - 0.69%) and (95.41 - -1.40%) respectively. However, it was noticed that **J2** prompted cell growth instead of inhibition at a lower concentration (50 μg/ml) as percentage inhibition results were negative in cell lines of CaCo-2, Hep-3B and MCF-7; Table A8 Appendix A. The inhibition of **J2** against cancer cell lines is elevated at higher concentrations. The new ester **J2** shows higher inhibition% against Hep-3B, Hep-G2, HeLa, and MCF-7 than citronellol at 500 μg/ml (92.25 > 90.27%), (92.26 > 84.64%), (95.23 >86.09%), (95.41 > 90.69%) respectively but in the term of potency the new ester **J2** is less potent than citronelloll in all cancer cell lines except for the normal cell line LX-2 Table 3; both **J2,** and citronellol show the same inhibition% at 500 μg/ml (61%), but **J2** shows lower inhibition% than citronellol 300 μg/ml (39.63 < 52.69%) Figure B41 Appendix B. In addition, **J2** is less potent than citronellol with IC_{50} 380.52 > 275.31 μg/ml Table 3, this indicates that **J2** is less toxic to the normal cell than citronellol. The new ester of *p*-CA and thymol **J14** was tested against CaCo-2, Hep-G2, HeLa, MCF-7, and B16F1 at the range of concentration 1000-50 μg/ml and the inhibition% was (85.04 - -0.34%), (87.78 - 0.74%), (67.00 - 1.02%), (89.40 - 2.87), and (91.81 - 16.09%) respectively. However, it was noticed that **J14** prompted cell growth instead of inhibition at a lower concentration (50 μg/ml) as percentage inhibition results were negative in a cell line of CaCo-2; Table A9 Appendix A. **J14** shows the anti-

cancer effect against all cell lines. The higher inhibition of cancer cell lines goes at a higher concentration. The new ester **J14** is the most potent anticancer agent among the compounds; citronellol, thymol, *p*-CA, and **J2.** The potency in terms of IC_{50} shows that **J14** has the lowest IC_{50} in all cell lines and compounds Table 3. The potency of **J14** against normal cell line LX-2 in terms of IC_{50} is higher than citronellol and thymol, lower than *p*-CA, and nearly equal to **J2;** 379.08 > 275.31, > 217.97, < 1283.62, and ≈ 380.52 μg/ml respectively Table 3. The study result revealed that the *p*-CA ester with thymol **J14** could be considered a new potential chemopreventive agent against CaCo-2, Hep-G2, HeLa, and MCF-7 cell lines while preserving the normal cells. The result was coordinated with the suggestion that both phenol and carboxylate parts may make promising interactions with human epithelial cells so that they can more easily cross cancer cells. It has been proven that both *ortho*- and *para*-phenolic compounds tend to have a superior inhibitory activity than the *meta*-analogs, but the potency also depends on the residual structural characteristics of the compounds, in addition non-conjugated analogs of *p*-coumaric acid were already tested, presenting very low inhibitory activity [121, 122].

Table 3

IC_{50} of p-CA esters

	IC_{50} (μg/ml)				
Assay	Citronellol± SD	Thymol± SD	*p*-CA± SD	J2± SD	J14± SD
CaCo-2	84.22 ± 0.141	199.71 ± 1.018	1029.41 ± 0.290	250.99 ± 0.071	63.36 ± 0.311
Hep-3B	185.21 ± 0.148	185.52 ± 0.007	447.46 ± 0.325	276.87 ± 0.205	-
Hep-G2	252.69 ± 0.219	187.3 ± 0.035	2466.68 ± 0.223	279.79 ± 0.142	66.5 ± 0.905
HeLa	119.66 ± 0.516	201.26 ± 0.007	685.03 ± 0.024	226.61 ± 0.276	47.38 ± 0.266
MCF-7	175.14 ± 0.099	179.92 ± 0.057	498.34 ± 0.085	230.45 ± 0.028	66.46 ± 0.382
B16-F1	-	-	-	-	38.06 ± 0.028
LX-2	275.31 ± 0.219	217.97 ± 0.007	1283.62 ± 0.270	380.52 ± 0.341	379.08 ± 0.018

The amide compound of *p*-CA and 1-(2-aminoethyl)piperazine **J19** was tested against Hep-3B, HeLa, MCF-7 and B16-F1 at concentration range of 1000 - 62.5 μg/ml with inhibition % range of (37.24 - -0.85%), (12.44 - -64.23%), (48.87 - -11.2%), and (51.08 - -12.02%) respectively. It was detected that the greater the concentration the greater the inhibition% of cancer cell lines. However, it was observed that **J19** prompted cell growth

instead of inhibition at a concentration of 62.5 μg/ml as negative results of percentage inhibition were obtained in cell lines of Hep-3B and MCF-7, at 500 μg/ml - 62.5 μg/ml in HeLa cell line and at 250 μg/ml - 62.5 μg/ml in B16-F1 cell line Table A10 Appendix A. The new ester **J19** is much less potent than *p*-CA and 1-(2-aminoethyl)piperazine in the term of IC_{50} Table A11 Appendix A**.** The study revealed that *p*-CA amide **J19** is not effective as an anticancer agent and is more toxic against normal cells.

The anhydride of *p*-CA **N2** was tested against Hep-3B, HeLa, MCF-7, and B16-F1 using a concentration range of 1000-62.5 μg/ml with inhibition % of (96.36 - -0.53%), (98.17 - -68.78%), (100.03 - -3.29%), (99.25 - -52.69%) respectively. However, it was observed that **N2** prompted cell growth rather than inhibition at a concentration of 62.5 μg/ml as percentage inhibition results were negative in cell lines of Hep-3B, at 125 μg/ml-62.5 μg/ml in HeLa and MCF-7 cell lines, and 250 - 62.5 μg/ml in B16-F1 cell line Table A12 Appendix A. The anhydride **N2** was more potent in terms of IC_{50} than *p*-CA and the anhydride **N4** against Hep-3B (409.97 < 447.46, < 690.26 μg/ml, respectively), and MCF-7 cell lines (315.3 < 498.34, < 434.43 μg/ml respectively) Table A14 Appendix A. The anhydride **N2** was also more potent in terms of IC_{50} against skin cancer cells B16-F1 than **N4** (366.18 < 443.28 μg/ml), but unfortunately, **N2** is less preserving at normal cell lines LX-2 than *p*-CA, and **N4** (380.81 < 1283.62, < 429.18 μg/ml respectively). The anhydride **N4** was tested against Hep-3B, HeLa, MCF-7, and B16-F1 at a concentration range of 1000 - 62.5 μg/ml, and the inhibition% was (53.64 - -2.56%), (98.96 - 1.94%), (63.69 - -4.17%), and 100.54 - - 6.47%) respectively. However, it was detected that **N4** prompted cell growth rather than inhibition at a concentration 62.5 μg/ml as percentage inhibition results were negative in cell lines of Hep-3B, at 250 μg/ml in HeLa, at 250 - 62.5 μg/ml in MCF-7 cell lines, and at 125 - 62.5 μg/ml in B16-F1 cell lines Table A13 Appendix A. The inhibition percentage of **N4** increases with increasing concentration. In a comparison of the inhibition% of **N4** and **N2** at higher concentrations (1000 μg/ml), **N4** nearly has identical inhibition% against HeLa (98.96% ≈ 98.17%), and B16-F1 (100.54% ≈ 99.25%) with **N2,** and lesser inhibition% against Hep-3B (53.65 < 96.36%), and MCF-7 (63.69% < 100.04% than **N2** Figure B42 Appendix B**. N4** showed higher inhibition% at concentration 500 μg/ml against HeLa cell line than **N2** and *p*-CA (70.98 > 44.30, > 40.44% respectively), lower inhibition% against Hep-3B than **N2,** and *p*-CA (45.39 < 66.21, < 59.14% respectively), lower inhibition% than **N2** and higher activity than *p*-CA against MCF-7 (61.05% < 88.21%, > 50.20% respectively) cell line Figure B43 Appendix

B. The newly *p*-CA anhydride **N4** showed higher efficacy than *p*-CA and **N2** against HeLa cell lines in terms of IC_{50} (405.95 < 685.03, < 553.09 μg/ml respectively). **N4,** Also showed higher efficacy than *p*-CA but lower than **N2** against MCF-7 in terms of IC_{50} (434.43 < 498.34, > 315.3 μg/ml respectively) but more preserving at normal cell line than **N2** and less than *p*-CA (429.18 > 380.81, < 1283.62 μg/ml respectively). This indicates that **N4** is less toxic against normal cell lines than **N2** but more toxic than *p*-CA Table A14 Appendix A.

The *cis*-jasmone amine and 2-(piperazin-1-yl)ethanamine **N6** was tested against Hep-3B, HeLa, MCF-7, B16-F1 at concentration range of (1000 - 62.50 μg/ml). The inhibition% was in the range of (97.29 - -4.05%), (97.73 - 57.94%), (100.77 - 27.01%) and (83.91 - -31.84%) respectively. However, it was detected that **N6** prompted cell growth rather inhibition at a concentration of 125 - 62.5 μg/ml as percentage inhibition results were negative in cell lines of Hep-3B and B16-F1, Table A15 Appendix A. The greater the concentration of **N6,** the greater the inhibition % is obtained. The new amine compound **N6** is more potent than *cis*-jasmone in terms of IC_{50} in cell lines of HeLa (59.42 < 66.64 μg/ml) and B16-F1 (283.61 < 391.57 μg/ml), but less potent than *cis*-jasmone in cell lines of Hep-3B (334.45 > 74.84 μg/ml) and MCF-7 (78.47 > 69.03 μg/ml) Table A17 Appendix A. The cytotoxicity of **N6** on normal cell line (LX-2) is lower than *cis*-jasmone as indicated in IC_{50} (362.32 > 92.64 μg/ml) Table A17 Appendix A. The second *cis*-jasmone amine **N8** was obtained by reacting *cis*-jasmone with phenylhydrazine. **N8** was tested against Hep-G2, Hep-3B, HeLa, MCF-7, and B16-F1 cell lines in a concentration range of 500 - 62.5 μg/ml and the inhibition % was in range of (87.84 - -16.40%), (83.52 - 7.78%), (85.99 - -17.06%), (74.78 - -3.26%) and (85.16 - -21.64%). However, it was detected that **N8** prompted cell growth rather than inhibition at a concentration of 125 - 62.5 μg/ml as percentage inhibition results were negative in cell lines of Hep-G2, at 62.5 μg/ml in HeLa, MCF-7 and B16-F1 cell lines, Table A16 Appendix A. The new amine **N8** is more potent than *cis*-jasmone against the B16-F1 cell line in terms of IC_{50} (182.74 < 391.57 μg/ml) on the other side **N8** is less effective than *cis*-jasmone against Hep-G2 (195.97 > 70.43 μg/ml), Hep-3B (322.16 > 74.84%), HeLa (176.25 > 66.64%), and MCF-7 (169.61 > 69.03%) cell lines. The toxicity of **N8** is lower than *cis*-jasmone as the potency in terms of IC_{50} is higher than *cis*-jasmone (202.02 > 92.64 μg/ml) Table A17 Appendix A. **N8** is more active in the term of IC_{50} against Hep-3B and B16-F1 than **N6** (322.16 < 334.45 μg/ml) and (182.74 < 283.61 μg/ml) respectively Table A17 Appendix

A**.** On the other side, **N6** is more active in the term of IC_{50} against cell lines of HeLa (59.45 < 176.25 μg/ml), MCF-7 (78.47 < 169.61 μg/ml), and less toxic on normal cell LX-2 than **N8** (202.02 < 362.32 μg/ml) Table A17 Appendix A. Both **N6** and **N8** are less active than *cis*-jasmone against Hep-3B (334.45, 322.16 > 74.84 and MCF-7 (78.47, 169.61 > 69.03 μg/ml) Table A17 Appendix A, but both of them are more active than *cis*-jasmone against B16-F1 (283.61, 182.74 < 391.57 μg/ml) Table A17 Appendix A. Both new *cis*-jasmone amines are less toxic on normal cell line LX-2 than *cis*-jasmone (362.32, 202.02 > 92.64 μg/ml) Table A17 Appendix A. The study showed that the new *cis*-jasmone amines display the best characteristics of anticancer agents since they are active on cancer cells but not on normal cells. The depletion of ATP through mitochondrial disturbance, or induction of cell apoptosis by reactive oxygen species (ROS) production is the potential mechanisms of anticancer action of jasmone derivatives [123].

The ester of thymol **J16** which was produced by condensing thymol with thiophene-3-carboxylic acid was tested against CaCo-2, Hep-G2, HeLa, MCF-7, and B16F1 cell lines at a concentration range 1000 – 50 μg/ml and the inhibition% was (95.98 - 8.29%), (96.12 - 23.23%), (95.37 - 37.88%), (96.12 - 17.49%) and (97.59 - 69.90%) respectively. The inhibition% increases with increasing the concentration of **J16** Table A18 Appendix A**.** The potency of **J16** is higher than thymol against cancer cell lines in terms of IC_{50}μg/ml; CaCo-2 (76.61 < 199.71), Hep-G2 (64.97 < 187.30), HeLa (60.45 < 201.25), MCF-7 (67.54 < 179.92) in addition **J16** is less toxic on normal cell (LX-2) than thymol (372.86 > 217.97) Table 4 and Figure B44 Appendix B. The ester of thymol **J10** which was produced by condensing thymol with 5B2TCA was tested against CaCo-2, Hep-G2, HeLa, MCF-7, and B16-F1 at range concentrations of 1000 – 50 μg/ml and the inhibition% was (83.33 - -0.51 μg/ml), (76.59 - 12.81 μg/ml), (70.11 - 6.50 μg/ml), (87.90 - 8.08 μg/ml) and (91.3 - 1.23 μg/ml) respectively. However, it was detected that **J10** prompted cell growth rather than inhibition at a concentration 50 μg/ml as percentage inhibition results were negative in cell lines of CaCo-2, Table A19 Appendix A. The greater the concentration of **J10** the greater the inhibition% is. In terms of IC_{50} the potency of **J10** is less potent than thymol Table 4 in CaCo-2 (690.30 > 199.71 μg/ml), Hep-G2 634.10 > 187.30 μg/ml), HeLa (681.78 > 201.25 μg/ml), and MCF-7 (609.10 > 179.92 μg/ml) cell lines Figure B45 Appendix B. The ester of thymol **J11** which was produced by condensation of thymol with 4B3TCA was tested against CaCo-2, Hep-G2, Hep-3B, HeLa, MCF-7, and B16-F1 at range concentrations of 1000 - 50 μg/ml and the

inhibition% was (100 - 1.81%), (97.23 - 5.70%), (94.78 - 0.80%), (99.60 - 10.57%), (99.92 - 6.06%) and (11.98 - -3.19%) Table A20, Appendix A. However, it was detected that **J11** prompted cell growth rather than inhibition at a concentration 50 μg/ml as percentage inhibition results were negative in cell lines of B16-F1, Table A20 Appendix A. The inhibition% is increased by increasing the concentration of **J11**. In terms of IC_{50} **J11** was more potent than thymol in cancer cell lines of Hep-G2 (178.65 < 187.30 μg/ml) and HeLa (171.08 < 201.25 μg/ml), and less potent than thymol in cell lines of CaCo-2 (224.98 > 199.71 μg/ml), Hep-3B (191.06 > 185.51 μg/ml) and MCF-7 (183.62 > 179.92 μg/ml) Table 4, and Figure B46 Appendix B. **J11** has lower toxicity on normal cell line (LX-2) in term of IC_{50} 984.53 > 217.97 μg/ml. The ester **J12** was produced by condensation of thymol with F3CA. **J12** was tested against CaCo-2, Hep-G2, HeLa, MCF-7 and B16-F1 at concentration range of 1000-50 μg/ml and the inhibition% was (96.45 - 6.41%), (96.68 - 16.14%), (96.25 - 15.44%), (96.92 - 12.91%) and 98.67 - 4.26%) Table A21 Appendixes A. In term of IC_{50} μg/ml for **J12** which is more potent than thymol against cancer cell lines; CaCo-2 (193.28 < 199.71), Hep-G2 (186.22 < 187.30), HeLa (140.55 < 201.25) and MCF-7 (175.36 < 179.92), in addition, **J12** has less toxicity on normal cell line (LX-2) 372.30 > 217.97) Table 4 and Figure B47 Appendix B. The four esters of thymol **J16**, **J10**, **J11,** and **J12** were tested against skin cancer B16-F1, **J16** was the most potent and **J11** was less potent in terms of IC_{50} μg/ml and the order of potency was **J16** > **J12** > **J10** > **J11** (32.60 < 82.45 < 276.26 < 3577.50 μg/ml) respectively. The toxicity of the four esters against normal cell LX-2 in terms of IC_{50} μg/ml in order of less toxicity to more toxic was **J11** > **J16**, **J12** > **J10** (984.53 > 372.86, 372.30 > 360.43 μg/ml) Figure B48 Appendix B and Table 4. The study showed that the new thymol esters display the best characteristics of anticancer agents since they influence cancer cells but not normal cells. The study showed that the new ester **J16** was the most potent potential anticancer agent among all new esters including the parent compound thymol. This study revealed that esterification of thymol with heterocyclic compounds such as 3TCA and F3CA may increase the potency of anticancer properties of thymol. Studies have shown that thymol can cause cellular impairment, such as apoptosis, lipid degeneration, nucleolar segregation and mitochondrial damage in cancer cells. Thymol can prompt oxidative stress-linked mitochondrial abnormality or impairment and other intrinsic and extrinsic apoptotic cell loss on cancer cells. It is also obvious to apply an antiproliferative effect in cancer cells. On the other hand, cytoprotective and antioxidant effects along with

the antiapoptotic, antigenotoxic, and anti-inflammatory/ immunomodulatory effects in normal cells could be the important mechanisms of thymol's anticancer action in diverse test systems [124].

Table 4

IC_{50} µg/ml of Thymol, J16, J10, J11 and J12

	IC_{50} (µg/ml)				
Assay	Thymol ± SD	J16± SD	J10± SD	J11± SD	J12± SD
CaCo-2	199.71 ± 1.018	76.61 ± 0.163	690.30 ± 0.158	224.98 ± 0.014	193.28 ± 0.198
Hep-G2	187.30 ± 0.035	64.97 ± 0.757	634.10 ± 0.035	178.65 ± 0.247	186.22 ± 0.156
Hep-3B	185.51 ± 0.007	-	-	191.06 ± 0.042	-
HeLa	201.25 ± 0.007	60.45 ± 0.042	681.78 ± 0.085	171.08 ± 0.007	140.55 ± 0.318
MCF-7	179.92 ± 0.057	67.54 ± 0.332	609.10 ± 0.069	183.62 ± 0.269	175.36 ± 0.007
B16-F1	-	32.6 ± 0.283	276.26 ± 0.042	3577.50 ± 0.356	82.45 ± 0.389
LX-2	217.97 ± 0.007	372.86 ± 0.102	360.43 ± 0.304	984.53 ± 0.335	372.30 ± 0.213

3.2.2 Antimicrobial activity

The broth microdilution method in sterile 96-well microplates was used to investigate the antimicrobial activity of new compounds and the minimum inhibition concentration (MIC) was considered the lowest concentration of the sample, which inhibited bacterial growth. The esters of citronellol **J3** (citronellol with 3TCA), **J15** (citronellol with 2TCA), and **J13** (citronellol with 4B2TCA**)**, were resistant to all microorganism strains except for antifungal microorganism (*Candida albicans*) as **J3** and **J15** inhibited the growth of *Candida albicans*. **J3** showed higher antifungal activity against *Candida albicans* than **J15** at MIC of 0.75 mg/ml and 1.50 mg/ml respectively. It was observed that citronellol was resistant to all microbial stains as shown in Table 5. The study revealed that functionalizing citronellol with 3TCA and 2TCA appeared more efficient in inhibitory properties to fungal strain *Candida albicans* compared with parent compound and its functionality with 4B2TCA.

Table 5

MICmg/ml of J3, J15, J13 and citronellol

Item	Type	J3	J15	J13	Citronellol
MRSA	gram-positive	R	R	R	R
Staphylococcus aureus	gram-positive	R	R	R	R
Klebsiella pneumoniae	gram-negative	R	R	R	R
Escherichia coli	gram-negative	R	R	R	R
Proteus vulgaris	gram-negative	R	R	R	R
Pseudomonas aeruginosa	gram-negative	R	R	R	R
Candida albicans	yeast	0.75	1.50	R	R

The esters of *p*-CA **J2** which is a combination of *p*-CA, and citronellol show resistance to all microorganisms despite *p*-CA having antimicrobial activity against MRSA, *Staphylococcus aureus* and *Klebsiella pneumoniae* at MIC 3.00 mg/ml Table 6 but the ester **J14** which is a combination of *p*-CA and thymol has antimicrobial activity much better than *p*-CA and thymol against all microbial stains except for *Pseudomonas aeruginosa* all of **J14**, *p*-CA, and thymol are resistance to it Table 6. Esters having aromatic groups improved the antibacterial potential activity as demonstrated by high antibacterial activity of compounds. The antibacterial efficiency of **J14** having aromatic substituents agrees with the results of a previous study [50].

Table 6

MIC (mg/ml) of J2, J14, Citronellol, p-CA and Thymol

Item	Type	J2	J14	*p*-CA	citronellol	thymol
MRSA	gram-positive	R	0.02	3.00	R	3.00
Staphylococcus aureus	gram-positive	R	0.02	3.00	R	1.50
Klebsiella pneumoniae	gram-negative	R	0.75	3.00	R	1.50
Escherichia coli	gram-negative	R	1.50	R	R	1.50
Proteus vulgaris	gram-negative	R	0.75	R	R	1.50
Pseudomonas aeruginosa	gram-negative	R	R	R	R	R
Candida albicans	yeast	R	0.01	R	R	0.19

The amide of *p*-CA **J19**, which is a combination of *p*-CA and 2-(piperazin-1-yl)ethanamine has antimicrobial against all the microbial strains at one MIC 3.00 mg/ml which is overcome the *p*-CA in *Escherichia coli*, *Proteus vulgaris*, *Pseudomonas aeruginosa* and *Candida albicans* that *p*-CA is resistance to them and equally affect MSA, *Staphylococcus aureus* and *Klebsiella pneumoniae* as *p*-CA at MIC 3.00 mg/ml Table 7. The antibacterial efficiency of **J19** having bulky substituents agrees with the results of a previous study [50].

Table 7

MIC (mg/ml) of J19 and p-CA

Item	Type	J19	*p*-CA
MRSA	gram-positive	3.00	3.00
Staphylococcus aureus	gram-positive	3.00	3.00
Klebsiella pneumoniae	gram-negative	3.00	3.00
Escherichia coli	gram-negative	3.00	R
Proteus vulgaris	gram-negative	3.00	R
Pseudomonas aeruginosa	gram-negative	3.00	R
Candida albicans	yeast	3.00	R

The anhydride of *p*-CA **N2** and **N4**, which are a combination of *p*-CA and TsCl, are resistance to all microbial strains that were tested against Table 8. At the same time, *p*-CA is active against MRSA, *Staphylococcus aureus* and *Klebsiella pneumoniae* at MIC of 3.00 mg/ml and resistance against *Escherichia coli*, *Proteus vulgaris*, *Pseudomonas aeruginosa* and *Candida albicans*.

Table 8

MIC (mg/ml) of N2, N4 and p-CA

Item	Type	N2	N4	*p*-CA
MRSA	gram-positive	R	R	3.00
Staphylococcus aureus	gram-positive	R	R	3.00
Klebsiella pneumoniae	gram-negative	R	R	3.00
Escherichia coli	gram-negative	R	R	R
Proteus vulgaris	gram-negative	R	R	R
Pseudomonas aeruginosa	gram-negative	R	R	R
Candida albicans	yeast	R	R	R

The *cis*-jasmone amine **N6** which is a combination of *cis*-jasmone and 2-(piperazin-1-yl)ethanamine is active against all bacterial strains at MIC of 1.5 mg/ml and against fungal strain *Candida albicans* at MIC of 0.75 mg/ml. The *cis*-jasmone amine **N8** which is a combination of *cis*-jasmone and phenylhydrazine active against *Klebsiella pneumoniae, Proteus vulgaris Pseudomonas aeruginosa,* and *Candida albicans* at MIC of 0.1875 mg/ml, 0.1875 mg/ml, 0.9375 mg/ml and 0.023438 mg/ml respectively and resistance to MRSA, *Staphylococcus aureus,* and *Escherichia coli,* while *cis*-jasmone is active against all microbial strains but resistance against *Pseudomonas aeruginosa* Table 9. We should note that the starting concentration of *cis*-jasmone in the first well of 96 microplate was 50 mg/ml while for **N6** and **N8** was 3mg/ml. The *cis*-jasmone amine **N8** is more active against *Klebsiella pneumoniae, Proteus vulgaris*, *Pseudomonas aeruginosa,* and *Candida albicans* than **N6;** (0.19 < 1.50 mg/ml), (0.09 < 1.50) and (0.02 < 0.75 mg/ml) respectively Table 9, Figure B49 Appendix B. The new *cis*-jasmone amine **N6** is more active than *cis*-jamone against all microbial strains except against *proteus vulgaris* and yeast of *Candida albicans*, *cis*-jasmone is more active at 0.39 < 1.50 mg/ml and 0.10 < 0.75 mg/ml respectively Table 9. The study showed that the amination of *cis*-jasmone could improve the activity of the parent compound against MRSA, *Staphylococcus aureus, Klebsiella pneumoniae, Escherichia coli, Proteus vulgaris Pseudomonas aeruginosa* and *Candida albicans*.

Table 9

MIC (mg/ml) of N6, N8 and cis-jasmone

Item	Type	N6	N8	*cis*-jasmone
MRSA	gram-positive	1.50	R	50.00
Staphylococcus aureus	gram-positive	1.50	R	6.25
Klebsiella pneumoniae	gram-negative	1.50	0.19	6.25
Escherichia coli	gram-negative	1.50	R	25.00
Proteus vulgaris	gram-negative	1.50	0.19	0.39
Pseudomonas aeruginosa	gram-negative	1.50	0.09	R
Candida albicans	yeast	0.75	0.02	0.10

The ester of thymol **J16** which is a combination of thymol with 3TCA is active against all bacterial strains and fungal strains but resistant to *Pseudomonas aeruginosa* such as thymol and other thymol esters **J10**, **J11** and **J12**. Thymol and **J16** have the same activity against *Escherichia coli* at MIC of 1.50 mg/ml. **J16** shows more activity than thymol against MRSA, *Staphylococcus aureus, Klebsiella pneumoniae, Proteus vulgaris* and *Candida albicans* at MIC of 0.05 < 3.00, 0.05 < 1.50, 0.75 < 1.5, 0.38 < 1.50 and 0.05 < 0.19 mg/ml respectively. Studies conducted on thymol esters having electron-donor groups resulted in a significant increase in activity, such as thymyl 4-methoxibenzoate [125].

The ester of **J10** which is a combination of thymol and 5B2TCA shows antimicrobial activity against all bacterial and fungal strains. **J10** is more active than thymol against MRSA at MIC of 1.50 mg/ml < 3.00 mg/ml; **J10** has the same activity as thymol against *Staphylococcus aureus* at MIC of 1.50 mg/ml and less activity than thymol against *Klebsiella pneumoniae*, *Escherichia coli*, *Proteus vulgaris*, and *Candida albicans* at MIC of 3.00 > 1.50 mg/ml and > 0.19 mg/ml respectively. The ester of thymol **J11** which is a combination of thymol and 4B3TCA shows resistance to all microbial strains. The ester **J12** which is a combination of thymol and F3CA shows antimicrobial activity against all strains. **J12** shows higher activity than thymol against all other microbial strains; MRSA, *Staphylococcus aureus, Klebsiella pneumoniae*, *Escherichia coli*, *Proteus vulgaris*, and *Candida albicans* at MIC of 0.75 < 3.00 mg/ml, 0.38 < 1.50 mg/ml, 0.75 < 1.50 mg/ml,

0.38 < 1.5 mg/ml and 0.10 < 0.1875 mg/ml respectively Table 10 and Figure B50 Appendix B.

The most regularly stated mechanism of antibacterial action of thymol includes the interference with bacterial membrane causing bacterial lysis and escape of intracellular contents leading to death. Other suggested mechanisms of antibacterial action comprise the reduction of efflux pumps, inhibition in the formation and disruption of preformed biofilms, inhibition of bacterial motility, and inhibition of membrane ATPases. Additionally, thymol has been established to act additively or synergistically with common antibiotics important in controlling the problem of bacteriastrength in food and disease [126].

Previous study showed that esters of thymol with furan and thiophene unit exhibited high potential antifungal activity [107].

Table 10

MIC (mg/ml) of J16, J10, J11, J12 and Thymol

Item	Type	J16	J10	J11	J12	Thymol
MRSA	gram-positive	0.05	1.50	R	0.75	3.00
Staphylococcus aureus	gram-positive	0.05	1.50	R	0.38	1.50
Klebsiella pneumoniae	gram-negative	0.75	3.00	R	0.38	1.50
Escherichia coli	gram-negative	1.50	3.00	R	0.75	1.50
Proteus vulgaris	gram-negative	0.38	3.00	R	0.38	1.50
Pseudomonas aeruginosa	gram-negative	R	R	R	R	R
Candida albicans	yeast	0.05	3.00	R	0.09	0.19

The higher potency of thymol esters **J14** and **J16** as antimicrobial and anticancer agents is related to the phenolic structure of these compounds; the lipophilic part of the compound; the benzene ring and the aliphatic parts incorporate into the lipid film of the cell membrane; increases the membrane surface deformation, on the other side the hydrophilic part of the compound reacts with the polar part of the membrane. This leads to disrupt the lipid film, by increasing fluidity and decreasing elasticity that may cause to enhance the permeability to hydrogen and potassium ions and this also disrupts the

function of protein of the internal membrane such as receptors and enzymes that leads to destabilize the cell and increase cell membrane pressure that causes cancer cell death through apoptosis [127, 128]. The importance of dual activity of thymol esters as antimicrobial and anticancer is necessary for cancer patients. Cancer patients who have undertaken chemotherapy treatments are more susceptible to microbial infections due to weakened immunity. Therefore, monotherapy with dual action as an anticancer and antimicrobial might be inexpensive and decrease drug taking frequency, side effects, and antimicrobial resistance [129].

3.3 Conclusions

Fourteen new compounds were prepared from four natural compounds; among them were esters, amides, anhydrides, and amines by condensation reaction and Michel addition. TLC and FT-IR spectroscopy were used to check the reaction in the course of the synthesis. FT-IR, ^{1}H-NMR, and ^{13}C-NMR spectroscopy were used to describe all of the compounds. The biological activity, such as anticancer and antimicrobial properties, of all the newly prepared compounds was studied and compared between them according to their groups. Most of the prepared compounds showed biological activity in varying proportions. The new citronellol ester **J15** was more potent than citronellol, **J3**, and **J13** against the liver cell cancer Hep-G2. The citronellol esters **J3** and **J15** were better at preserving normal cells than citronellol and **J13**. The ester **J15** was more potent than **J13** against skin cell cancer B16-F1. The citronellol esters **J3**, **J15**, **J13**, and citronellol were resistant to all microorganisms except **J3** and **J15**, which showed antifungal activity against *Candida albicans*. **J3** was more active than **J15**. The *p*-CA ester **J14** was the most potent anticancer agent than **J2**, *p*-CA, citronellol, and thymol against CaCo-2, Hep-G2, HeLa, and MCF-7 cancer cell lines and nearly had the same preserving normal cells as **J2**. **J2** and **J14** were better at preserving normal cells than citronellol and thymol but less than *p*-CA. The *p*-CA ester **J2** was resistant to all microorganisms, while **J14** showed distinctively higher activity against all microorganisms except *Pseudomonas aeruginosa*, which was resistant to it. The *p*-CA amide **J19** was less potent than *p*-CA against Hep-3B, HeLa, and MCF-7, and less preserving for normal cell lines. The *p*-CA amide **J19** showed the same antimicrobial activity as *p*-CA against MRSA, *Staphylococcus aureus*, and *Klebsiella pneumoniae*, but **J19** showed antimicrobial efficacy against *Escherichia coli*, *Proteus vulgaris*, *Pseudomonas aeruginosa*, and *Candida albicans*, while *p*-CA

showed resistance to them. The *p*-CA anhydride **N2** was more potent than *p*-CA and **N4** against Hep-3B and MCF-7 cell lines. The *p*-CA anhydride **N4** was more potent than *p*-CA and **N2** against HeLa cell lines but less effective than **N2** against B16-F1 cell lines. It preserved more normal cell lines than **N2** but less than *p*-CA. The *p*-CA anhydride **N2** and **N4** showed resistance to all microorganisms, while *p*-CA showed antibacterial activity against MRSA, *Staphylococcus aureus,* and *Klebsiella pneumoniae*. The *cis*-jasmone amine **N6** was more potent than *cis*-jasmone against HeLa and B16-F1 cell lines, and the *cis*-jasmone amine **N8** was more potent than *cis*-jasmone against B16-F1. The two *cis*-jasmone amines, **N6** and **N8**, were better at preserving normal cell lines than *cis*-jasmone. The *cis*-jasmone amine **N6** showed antimicrobial activity against all tested microorganisms and higher activity than *cis*-jasmine, except for *Candida albicans* **N6** was less active than *cis*-jasmone, while the amine **N8** showed more distinctive antimicrobial activity against *Klebsiella pneumoniae*, *Proteus vulgaris*, *Pseudomonas aeruginosa,* and *Candida albicans* than **N6** but showed resistance against MRSA, *Staphylococcus aureus*, and *Escherichia Coli*. The thymol esters **J16** and **J12** were more potent than thymol, **J10**, and **J11** against CaCo-2, Hep-G2, HeLa, and MCF-7, but **J16** was more potent than **J12**. The thymol ester **J11** was more potent than thymol against Hep-G2 and HeLa. The thymol ester **J16** was the most potent against B16-F1 among the other thymol **J12** and **J10** esters. All new esters of thymol were better at preserving normal cell lines than thymol. All thymol esters, including thymol were resistant to *Pseudomonas aeruginosa*. The thymol ester **J16** showed distinctively higher activity against all microorganisms than thymol and other thymol esters but showed the same activity as thymol against *Escherichia coli*, and was less active than **J12** against *Klebsiella pneumonia*, *Escherichia coli*, and had the same activity as **J12** against *Proteus vulgaris*, the thymol ester **J10** showed higher activity than thymol against MRSA, the same activity as thymol against *Staphylococcus aureus* but less activity than thymol and other thymol esters against other microorganism. The ester **J11** showed resistance to all microorganisms, and the ester **J12** showed antimicrobial activity against all microorganisms. **J12** showed better antimicrobial activity than thymol and **J10** but was less active than **J16** except against *Klebsiella pneumonia,* and *Escherichia coli* **J12** was more active than **J16**. To understand the mechanism of the effect of these compounds on different biological cells, it would be good to conduct complementary studies in the future.

List of Abbreviations

Abbreviations	Meaning
WHO	World Health Organization
GLOBOCAN	Global Cancer Statistics
p-CA	*p*-Coumaric acid
CRC	Colorectal cancer
HL60	Human cancer leukemia cells
CIB	Citronellyl isobutyrate
CDB	Citronellyl 2,2-dimethyl butyrate
DLD	Colorectal adenocarcinoma cell lines
ROS	Reactive oxygen species
MFC-7	Breast carcinoma
DME Medium	Dulbecco's Modified Eagle Medium
FBS	Fetal bovine serum
PBS	Phosphoric acid buffer
OD	Optical density
SH-SY5Y	Human neuroblastoma cell line
Eq.	Equivalent
F3CA	Furan-3-caboxylic acid
2TCA	2-thiophene caboxylic acid
3TCA	3-thiophene caboxylic acid
4B3TCA	4-bromo-3-thiophene caboxylic acid
5B2TCA	5-bromo-2-thiophene caboxylic acid
DMF	Dimethylformamide
D.W	Distilled water
TsCl	4-Methylbenzene-1-sulfonyl chloride, Tosyl chloride
DCM	dichloromethane
d.b	Double bond

References

1. Bray, F., et al., *The ever-increasing importance of cancer as a leading cause of premature death worldwide.* Cancer, 2021.
2. WHO, *Global Health Estimates 2020: Deaths by Cause, Age, Sex, by Country and by Region, 2000-2019*. 2020.
3. Falah, B., J. Meshal, and W. Betawi, *Palestinian Health Sector Assessment: Macro-Analytical Study* 2020.
4. Dahanukar, S., R. Kulkarni, and N. Rege, *Pharmacology of medicinal plants and natural products.* Indian journal of pharmacology, 2000. **32**(4): p. S81-S118.
5. Russo, M., et al., *Exploring death receptor pathways as selective targets in cancer therapy.* Biochemical pharmacology, 2010. **80**(5): p. 674-682.
6. Qurishi, Y., et al., *Interaction of natural products with cell survival and signaling pathways in the biochemical elucidation of drug targets in cancer.* Future Oncology, 2011. **7**(8): p. 1007-1021.
7. Ridsdale, B., et al. *Mortality by cause of death and by socio-economic and demographic stratification 2010*. in *International Congress of Actuaries 2010*. 2010.
8. Mondal, S., et al., *Natural products: promising resources for cancer drug discovery. Anticancer Agents Med Chem, 12, 49-75*. 2012.
9. https://www.who.int/news-room/fact-sheets/detail/breast-cancer, *Breast cancer*. 2024.
10. https://www.who.int/news-room/fact-sheets/detail/colorectal-cancer, *Colorectal cancer*. 2024.
11. https://www.who.int/news-room/fact-sheets/detail/cervical-cancer, *cervical adenocarcinoma*. 2024.
12. Llovet, J.M., et al., *Immunotherapies for hepatocellular carcinoma.* Nature reviews Clinical oncology, 2022. **19**(3): p. 151-172.

13. Lu, Z., et al., *Mechanism of arctigenin-induced specific cytotoxicity against human hepatocellular carcinoma cell lines: Hep G2 and SMMC7721.* Plos one, 2015. **10**(5): p. e0125727.

14. https://www.who.int/news-room/fact-sheets/detail/ultraviolet-radiation, *Ultraviolet radiation*. 2022.

15. Craythorne, E. and F. Al-Niami, *Skin cancer.* Medicine, 2017. **45**(7): p. 431-434.

16. Ahmed, B., M.I. Qadir, and S. Ghafoor, *Malignant melanoma: skin cancer–diagnosis, prevention, and treatment.* Critical Reviews™ in Eukaryotic Gene Expression, 2020. **30**(4).

17. Cullen, J.K., et al., *Topical treatments for skin cancer.* Advanced drug delivery reviews, 2020. **153**: p. 54-64.

18. Jansen, M.H.E., et al., *Five-Year Results of a Randomized Controlled Trial Comparing Effectiveness of Photodynamic Therapy, Topical Imiquimod, and Topical 5-Fluorouracil in Patients with Superficial Basal Cell Carcinoma.* Journal of Investigative Dermatology, 2018. **138**(3): p. 527-533.

19. Pawełczyk, A., et al., *Linked drug-drug conjugates based on triterpene and phenol structures. Rational synthesis, molecular properties, toxicity and bioactivity prediction.* Arabian Journal of Chemistry, 2020. **13**(12): p. 8793-8806.

20. Torić, J., M. Barbarić, and J. Brala, *Hydroxytyrosol, Tyrosol and Derivatives and Their Potential Effects on Human Health.* Molecules (Basel, Switzerland), 2019. **24**(10): p. E2001-E2001.

21. Zang, H., et al., *Synthesis and biological activities of tyrosol phenolic acid ester derivatives.* Chemistry of Natural Compounds, 2019. **55**: p. 1043-1049.

22. Chen, T., et al., *Recent developments of small molecules with anti-inflammatory activities for the treatment of acute lung injury.* European Journal of Medicinal Chemistry, 2020. **207**: p. 112660.

23. Deng, S., et al., *Targeting autophagy using natural compounds for cancer prevention and therapy.* Cancer, 2019. **125**(8): p. 1228-1246.

24. Kasalović, M.P., et al., *Novel diphenyltin (IV) complexes with carboxylato N-functionalized 2-quinolone ligands: Synthesis, characterization and in vitro anticancer studies.* Journal of Inorganic Biochemistry, 2024. **250**: p. 112399.

25. Raut, J.S. and S.M. Karuppayil, *A status review on the medicinal properties of essential oils.* Industrial crops and products, 2014. **62**: p. 250-264.

26. Bayala, B., et al., *Anticancer activity of essential oils and their chemical components-a review.* American journal of cancer research, 2014. **4**(6): p. 591.

27. Stone, S., et al., *Evaluation of potential use of Cymbopogon sp. essential oils, (R)-citronellal and N-citronellylamine in cancer chemotherapy.* International Journal of Applied Research in Natural Products, 2013. **6**.

28. El-Far, M., et al., *Preclinical biochemical studies using a novel 5-aminolevulinic acid ester derivative with superior properties for photodynamic therapy of tumors.* International Journal of Medicine and Medical Sciences, 2009. **1**(7): p. 278-287.

29. Sharma, P.R., et al., *Anticancer activity of an essential oil from Cymbopogon flexuosus.* Chemico-biological interactions, 2009. **179**(2-3): p. 160-168.

30. *Handbook of essential oils: science, technology, and applications*, K.H.C. Bas¸er and G. Buchbauer, Editors. 2010.

31. Ganjewala, D. *Cymbopogon essential oils: chemical compositions and bioactivities*. 2009.

32. Pujiastuti, D.Y., L. Sulmartiwi, and A.S. Mubarak, *Increasing the value added of production citronella oil and carrageenan in Rungkut Barata Surabaya.* Kontribusia (Research Dissemination for Community Development), 2021. **4**(2): p. 399-403.

33. Kaur, S., et al., *Citronellol disrupts membrane integrity by inducing free radical generation.* Zeitschrift für Naturforschung C, 2011. **66**(5-6): p. 260-266.

34. Santos, M.R., et al., *Cardiovascular effects of monoterpenes: a review.* Revista Brasileira de Farmacognosia, 2011. **21**: p. 764-771.

35. Boukhris, M., et al., *Hypoglycemic and antioxidant effects of leaf essential oil of Pelargonium graveolens L'Hér. in alloxan induced diabetic rats.* Lipids in health and disease, 2012. **11**: p. 1-10.

36. Rajendran, J., P. Pachaiappan, and S. Subramaniyan, *Dose-dependent chemopreventive effects of citronellol in DMBA-induced breast cancer among rats.* Drug development research, 2019. **80**(6): p. 867-876.

37. Widiyarti, G., et al., *Molecular Docking of Citronellol, Geraniol and Ester Derivatives as Pim 1 Kinase Inhibitor of Leukemia Cancer.* Jurnal Kimia Valensi, 2019. **5**(2): p. 133-142.

38. Rajendran, J., P. Pachaiappan, and R. Thangarasu, *Citronellol, an acyclic monoterpene induces mitochondrial-mediated apoptosis through activation of proapoptotic factors in MCF-7 and MDA-MB-231 human mammary tumor cells.* Nutrition and Cancer, 2021. **73**(8): p. 1448-1458.

39. Widiyarti, G., S. Handayani, and M. Hanafi. *Synthesis and cytotoxic activity of citronellol esters*. in *AIP Conference Proceedings*. 2018. AIP Publishing LLC.

40. Widiyarti, G., et al., *Cytotoxic activity of cytronellyl caproate on Murine Leukemia (P388) Cells.* Int. J. App. Chem, 2016. **12**(3): p. 209-220.

41. Kong, C.S., et al., *Antiangiogenic effects of p-coumaric acid in human endothelial cells.* Phytotherapy Research, 2013. **27**(3): p. 317-323.

42. El-Seedi, H.R., et al., *Biosynthesis, natural sources, dietary intake, pharmacokinetic properties, and biological activities of hydroxycinnamic acids.* Journal of agricultural and food chemistry, 2012. **60**(44): p. 10877-10895.

43. Garrait, G., et al., *Gastrointestinal absorption and urinary excretion of trans-cinnamic and p-coumaric acids in rats.* Journal of agricultural and food chemistry, 2006. **54**(8): p. 2944-2950.

44. Kehan Pei, J.O., Junqing Huang,Shiyi Ou, *p-Coumaric acid and its conjugates: dietary sources, pharmacokinetic properties and biological activities.* Journal of the Science of Food and Agriculture, 2016. **96**(9): p. 2952-2962.

45. Tehami, W.a., et al., *New insights into the anticancer effects of p-coumaric acid: focus on colorectal cancer.* Dose-Response, 2023. **21**(1): p. 15593258221150704.

46. Serdar KARAKURT1, Gülsüm ABUŞOĞLU, and Z.C. ARITULUK, *Comparison of anticarcinogenic properties of Viburnum opulus and its active compound*

p-coumaric acid on human colorectal carcinoma. Turkish Journal of Biology, 2020. **44**: p. 252-263.

47. Gastaldello, G.H., et al., *Green Propolis Compounds (Baccarin and p-Coumaric Acid) Show Beneficial Effects in Mice for Melanoma Induced by B16f10.* Medicines, 2021. **8**(5): p. 20.

48. Bouzaiene, N.N., et al., *The effects of caffeic, coumaric and ferulic acids on proliferation, superoxide production, adhesion and migration of human tumor cells in vitro.* European journal of pharmacology, 2015. **766**: p. 99-105.

49. Menezes, J.C., et al., *Long chain alkyl esters of hydroxycinnamic acids as promising anticancer agents: Selective induction of apoptosis in cancer cells.* Journal of agricultural and food chemistry, 2017. **65**(33): p. 7228-7239.

50. Khatkar, A., et al., *Synthesis, antimicrobial evaluation and QSAR studies of p-coumaric acid derivatives.* Arabian Journal of Chemistry, 2017. **10**: p. S3804-S3815.

51. Buravlev, E.V., et al., *Synthesis and Antioxidant Ability of Novel Derivatives Based on para-Coumaric Acid Containing Isobornyl Groups.* Chemistry & biodiversity, 2019. **16**(10): p. e1900362.

52. Carmo-Martins, J.I., et al., *Esterification of p-coumaric acid improves the control over melanoma cell growth.* Biomedicines, 2023. **11**(1): p. 196.

53. Nonaka, H., et al., *Stereoselective synthesis of epi-jasmonic acid, tuberonic acid, and 12-oxo-PDA.* Organic & biomolecular chemistry, 2010. **8**(22): p. 5212-5223.

54. https://en.wikipedia.org/wiki/Jasmone. *Jasmone*. 2021; Available from: https://en.wikipedia.org/wiki/Jasmone.

55. https://www.chemeurope.com/en/encyclopedia/Jasmone.html, *Jasmone*, in *chemeurope.com*. 2021.

56. Dąbrowska, P. and W. Boland, *iso-OPDA: An Early Precursor of cis-Jasmone in Plants?* Chembiochem, 2007. **8**(18): p. 2281-2285.

57. Koch, T., K. Bandemer, and W. Boland, *Biosynthesis of cis-jasmone: a pathway for the inactivation and the disposal of the plant stress hormone jasmonic acid to the gas phase?* Helvetica Chimica Acta, 1997. **80**(3): p. 838-850.

58. Loughrin, J.H., et al., *Volatiles emitted by different cotton varieties damaged by feeding beet armyworm larvae.* Journal of Chemical Ecology, 1995. **21**(8): p. 1217-1227.

59. KOST, C. and M. Heil, *Herbivore-induced plant volatiles induce an indirect defence in neighbouring plants.* Journal of Ecology, 2006. **94**(3): p. 619-628.

60. Birkett, M.A., et al., *New roles for cis-jasmone as an insect semiochemical and in plant defense.* Proceedings of the National Academy of Sciences, 2000. **97**(16): p. 9329-9334.

61. Bruce, T.J., et al., *cis-Jasmone treatment induces resistance in wheat plants against the grain aphid, Sitobion avenae (Fabricius)(Homoptera: Aphididae).* Pest Management Science: formerly Pesticide Science, 2003. **59**(9): p. 1031-1036.

62. Pickett, J.A., et al., *cis-Jasmone as allelopathic agent in inducing plant defence.* Allelopathy Journal, 2007. **19**(1): p. 109-118.

63. Farmer, E.E. and C.A. Ryan, *Interplant communication: airborne methyl jasmonate induces synthesis of proteinase inhibitors in plant leaves.* Proceedings of the National Academy of Sciences, 1990. **87**(19): p. 7713-7716.

64. Fingrut, O. and E. Flescher, *Plant stress hormones suppress the proliferation and induce apoptosis in human cancer cells.* Leukemia, 2002. **16**(4): p. 608-616.

65. Rotem, R., et al., *Jasmonates: novel anticancer agents acting directly and selectively on human cancer cell mitochondria.* Cancer research, 2005. **65**(5): p. 1984-1993.

66. Samaila, D., et al. *Bioactive plant compounds inhibited the proliferation and induced apoptosis in human cancer cell lines, in vitro*. in *Transactions of the Integrated Bio-Medical Informatics & Enabling Technologies Symposiums*. 2004.

67. TONG, Q.s., et al., *Natural jasmonates of different structures suppress the growth of human neuroblastoma cell line SH-SY5Y and its mechanisms 1.* Acta Pharmacologica Sinica, 2008. **29**(7): p. 861-869.

68. Yeruva, L., et al., *Delayed cytotoxic effects of methyl jasmonate and cis-jasmone induced apoptosis in prostate cancer cells.* Cancer investigation, 2008. **26**(9): p. 890-899.

69. Xue, J., P.M. Davidson, and Q. Zhong, *Inhibition of Escherichia coli O157: H7 and Listeria monocytognes growth in milk and cantaloupe juice by thymol nanoemulsions prepared with gelatin and lecithin.* Food Control, 2017. **73**: p. 1499-1506.

70. Kazemi Oskuee, R., J. Behravan, and M. Ramezani, *Chemical composition, antimicrobial activity and antiviral activity of essential oil of Carum copticum from Iran.* Avicenna Journal of Phytomedicine, 2011. **1**(2): p. 83-90.

71. Pivetta, T.P., et al., *Development of nanoparticles from natural lipids for topical delivery of thymol: Investigation of its anti-inflammatory properties.* Colloids and Surfaces B: Biointerfaces, 2018. **164**: p. 281-290.

72. Salehi, B., et al., *Thymol, thyme, and other plant sources: Health and potential uses.* Phytotherapy Research, 2018. **32**(9): p. 1688-1706.

73. Prades-Sagarra, È., A. Yaromina, and L.J. Dubois, *Polyphenols as Potential Protectors against Radiation-Induced Adverse Effects in Patients with Thoracic Cancer.* Cancers, 2023. **15**(9): p. 2412.

74. Kamalia, A.Z. and W.A.S. Tunjung, *Efficacy of Different Solvents in the Extraction of Bioactive Compounds and Anticancer Activities of Thyme (Thymus vulgaris L.) Leaves and Twigs.* Indonesian Journal of Pharmacy: p. 419–430-419–430.

75. Elbe, H., et al., *Apoptotic effects of thymol, a novel monoterpene phenol, on different types of cancer.* Bratislavske lekarske listy, 2020. **121**(2): p. 122-128.

76. Kang, S.-H., et al., *Anticancer effect of thymol on AGS human gastric carcinoma cells.* Journal of microbiology and biotechnology, 2016. **26**(1): p. 28-37.

77. Sisto, F., et al., *Synthesis and Evaluation of Thymol-Based Synthetic Derivatives as Dual-Action Inhibitors against Different Strains of H. pylori and AGS Cell Line.* Molecules, 2021. **26**(7): p. 1829.

78. Cui, Z., X. Li, and Y. Nishida, *Synthesis and bioactivity of novel carvacrol and thymol derivatives containing 5-phenyl-2-furan.* Letters in Drug Design & Discovery, 2014. **11**(7): p. 877-885.

79. Zielińska-Błajet, M. and J. Feder-Kubis, *Monoterpenes and their derivatives—Recent development in biological and medical applications.* International Journal of Molecular Sciences, 2020. **21**(19): p. 7078.

80. Ashraf, Z., et al., *Kinetic and in silico studies of novel hydroxy-based thymol analogues as inhibitors of mushroom tyrosinase.* European journal of medicinal chemistry, 2015. **98**: p. 203-211.

81. Blažíčková, M., et al., *Newly synthesized thymol derivative and its effect on colorectal cancer cells.* Molecules, 2022. **27**(9): p. 2622.

82. Javan, A.J. and M.J. Javan, *Electronic structure of some thymol derivatives correlated with the radical scavenging activity: Theoretical study.* Food chemistry, 2014. **165**: p. 451-459.

83. Tang, Z., et al., *Discovery of novel Thymol-TPP antibiotics that eradicate MRSA persisters.* European Journal of Medicinal Chemistry, 2024. **270**: p. 116381.

84. Khwaza, V. and B.A. Aderibigbe, *Antifungal Activities of Natural Products and Their Hybrid Molecules.* Pharmaceutics, 2023. **15**(12): p. 2673.

85. Addo, J.K., et al., *Synthesis of 1, 2, 3-triazole-thymol derivatives as potential antimicrobial agents.* Heliyon, 2022. **8**(10).

86. Khan, Z., et al., *Current developments in esterification reaction: A review on process and parameters.* Journal of Industrial and Engineering Chemistry, 2021. **103**: p. 80-101.

87. Wade, L.G., *Organic chemistry*. 2013.

88. Vedantu, L.L.o. *The relative order of esterification of alcohols*. 2021 [cited 2021; Available from: https://www.vedantu.com/question-answer/the-relative-order-of-esterification-of-alcohols-class-12-chemistry-cbse-5f87e8468a0a932d9e3a176e.

89. Makuch, E., et al., *Enhancement of the antioxidant and skin permeation properties of eugenol by the esterification of eugenol to new derivatives.* AMB Express, 2020. **10**: p. 1-15.

90. Wu, Y., et al., *Enhancing the solubility and antimicrobial activity of cellulose through esterification modification using amino acid hydrochlorides.* International Journal of Biological Macromolecules, 2023. **226**: p. 793-802.

91. Brueckner, B., et al., *Delivery of 5-azacytidine to human cancer cells by elaidic acid esterification increases therapeutic drug efficacy.* Molecular cancer therapeutics, 2010. **9**(5): p. 1256-1264.

92. Arnold, L.A., et al., *Catalytic enantioselective synthesis of prostaglandin E1 methyl ester using a tandem 1, 4-addition-aldol reaction to a cyclopenten-3, 5-dione monoacetal.* Journal of the American Chemical Society, 2001. **123**(24): p. 5841-5842.

93. Mather, B.D., et al., *Michael addition reactions in macromolecular design for emerging technologies.* Progress in Polymer Science, 2006. **31**(5): p. 487-531.

94. Gimbert, C., et al., *Michael additions catalyzed by phosphines. An overlooked synthetic method.* Tetrahedron, 2005. **61**(36): p. 8598-8605.

95. Jackson, P.A., et al., *Covalent modifiers: a chemical perspective on the reactivity of α, β-unsaturated carbonyls with thiols via hetero-Michael addition reactions.* Journal of medicinal chemistry, 2017. **60**(3): p. 839-885.

96. Carvalho, M., R. Reis, and J.M. Oliveira, *Dendrimer nanoparticles for colorectal cancer applications.* Journal of materials chemistry B, 2020. **8**(6): p. 1128-1138.

97. Renault, K., et al., *Covalent modification of biomolecules through maleimide-based labeling strategies.* Bioconjugate Chemistry, 2018. **29**(8): p. 2497-2513.

98. An, J., et al., *ROS-augmented and tumor-microenvironment responsive biodegradable nanoplatform for enhancing chemo-sonodynamic therapy.* Biomaterials, 2020. **234**: p. 119761.

99. Rattanaburee, T., et al., *Trans-(−)-Kusunokinin: A potential anticancer lignan compound against HER2 in breast cancer cell lines?* Molecules, 2021. **26**(15): p. 4537.

100. Du, J.-Z., H.-J. Li, and J. Wang, *Tumor-acidity-cleavable maleic acid amide (TACMAA): a powerful tool for designing smart nanoparticles to overcome delivery barriers in cancer nanomedicine.* Accounts of chemical research, 2018. **51**(11): p. 2848-2856.

101. Lai, P.-S., et al., *Doxorubicin delivery by polyamidoamine dendrimer conjugation and photochemical internalization for cancer therapy.* Journal of Controlled Release, 2007. **122**(1): p. 39-46.

102. He, R., et al., *Peptide conjugates with small molecules designed to enhance efficacy and safety.* Molecules, 2019. **24**(10): p. 1855.

103. Raczuk, E., et al., *Different Schiff bases—structure, importance and classification.* Molecules, 2022. **27**(3): p. 787.

104. Tyagi, P., et al., *Design, spectral characterization, thermal, DFT studies and anticancer cell line activities of Co (II), Ni (II) and Cu (II) complexes of Schiff bases derived from 4-amino-5-(pyridin-4-yl)-4H-1, 2, 4-triazole-3-thiol.* Spectrochimica Acta Part A: Molecular and Biomolecular Spectroscopy, 2015. **145**: p. 155-164.

105. Hassan, A.S., et al., *Synthesis and in vitro antitumor evaluation of novel Schiff bases.* Medicinal Chemistry Research, 2018. **27**: p. 915-927.

106. Mahal, A., et al., *Schiff bases of tetrahydrocurcumin as potential anticancer agents.* ChemistrySelect, 2019. **4**(1): p. 366-369.

107. Wang, K., et al., *Synthesis and antifungal activity of carvacrol and thymol esters with heteroaromatic carboxylic acids.* Natural product research, 2019. **33**(13): p. 1924-1930.

108. Pal, S. and S.C. Pal, *Single-pot conversion of an acid to the corresponding 4-chlorobutyl ester.* Acta Chim. Slov, 2011. **58**: p. 596-599.

109. Ghadir Hanbali, S.J., Othman Hamed, Roland Bol, Bayan Khalaf, Asma Qdemat and Subhi Samhan *Enhanced Ibuprofen Adsorption and Desorption on Synthesized Functionalized Magnetic Multiwall Carbon Nanotubes from Aqueous Solution. Materials.* Materials, 2020. **13**(15): p. 3329.

110. Sanmartin, C., et al., *Symmetrical derivatives with nitrogenated functions as cytotoxic agents and apoptosis inducers.* Letters in Drug Design & Discovery, 2005. **2**(5): p. 341-354.

111. Sahoo, D., S. Sarkar, and S. Jana, *A simple synthesis of ketone from carboxylic acid using tosyl chloride as an activator.* Tetrahedron Letters, 2019. **60**(39): p. 151084.

112. Perdicchia, D. and K.A. Jørgensen, *Asymmetric aza-michael reactions catalyzed by cinchona alkaloids.* The Journal of organic chemistry, 2007. **72**(9): p. 3565-3568.

113. Lazarević, S., et al., *Synthesis, antimicrobial activity and in silico studies on thymol esters.* Acta Chimica Slovenica, 2017. **64**(3): p. 603-612.

114. Hawash, M., et al., *Synthesis and biological evaluation of benzodioxole derivatives as potential anticancer and antioxidant agents.* Heterocyclic Communications, 2020. **26**(1): p. 157-167.

115. Jaradat, N., M. Hawash, and G. Dass, *Phytochemical analysis, in-vitro anti-proliferative, anti-oxidant, anti-diabetic, and anti-obesity activities of Rumex rothschildianus Aarons. extracts.* BMC Complementary Medicine and Therapies, 2021. **21**(1): p. 1-11.

116. Tang, A.L., et al., *UM-SCC-104: A New human papillomavirus-16–positive cancer stem cell–containing head and neck squamous cell carcinoma cell line.* Head & neck, 2012. **34**(10): p. 1480-1491.

117. Arab-Bafrani, Z., et al., *Multiple MTS assay as the alternative method to determine survival fraction of the irradiated HT-29 colon cancer cells.* Journal of medical signals and sensors, 2016. **6**(2): p. 112.

118. Leber, A.L., *Clinical microbiology procedures handbook*. 2020: John Wiley & Sons.

119. Andrews, J., *BSAC standardized disc susceptibility testing method (version 5).* Journal of antimicrobial chemotherapy, 2006. **58**(3): p. 511-529.

120. Wayne, P., *Clinical and Laboratory Standards Institute (CLSI), Performance Standards for Antimicrobial Susceptibility Testing, CLSI supplement M100S.* Clinical and Laboratory Standards Institute., Wayne, PA, 2016.

121. Rosyda, M., N.S. Aminah, and A.N. Kristanti, *Various ester derivatives from esterification reaction of secondary metabolite compounds: a review.* MOJ Ecology & Environmental Sciences, 2020. **5**(3): p. 141-151.

122. Varela, M.T., et al., *Coumaric acid derivatives as tyrosinase inhibitors: Efficacy studies through in silico, in vitro and ex vivo approaches.* Bioorganic Chemistry, 2020. **103**: p. 104108.

123. Jarocka-Karpowicz, I. and A. Markowska, *Therapeutic potential of jasmonic acid and its derivatives.* International Journal of Molecular Sciences, 2021. **22**(16): p. 8437.

124. Islam, M.T., et al., *Anticancer activity of Thymol: A literature-based review and docking study with Emphasis on its anticancer mechanisms.* IUBMB life, 2019. **71**(1): p. 9-19.

125. Mesquita, B.M.d., et al., *Synthesis, larvicidal and acetylcholinesterase inhibitory activities of carvacrol/thymol and derivatives.* Quimica Nova, 2018. **41**(4): p. 412-416.

126. Kachur, K. and Z. Suntres, *The antibacterial properties of phenolic isomers, carvacrol and thymol.* Critical reviews in food science and nutrition, 2020. **60**(18): p. 3042-3053.

127. Perez, A.P., et al., *The anti MRSA biofilm activity of Thymus vulgaris essential oil in nanovesicles.* Phytomedicine, 2019. **57**: p. 339-351.

128. Ferreira, J.V.N., et al., *Mechanism of action of thymol on cell membranes investigated through lipid Langmuir monolayers at the air–water interface and molecular simulation.* Langmuir, 2016. **32**(13): p. 3234-3241.

129. Rostom, S.A., et al., *Synthesis of some pyrazolines and pyrimidines derived from polymethoxy chalcones as anticancer and antimicrobial agents.* Archiv der Pharmazie, 2011. **344**(9): p. 572-587.

Appendices

Appendix A

Tables

Table A.1

The newly prepared derivatives

<table>
<tr><td colspan="2"> 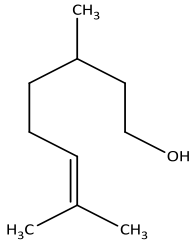
Citronellol
3,7-Dimethyloct-6-en--ol</td></tr>
<tr><td> 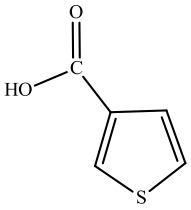
Thiophene-3-carboxylic acid</td><td> 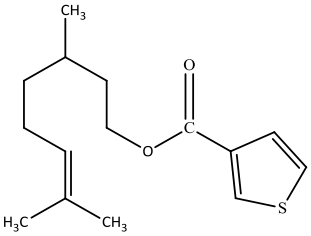
3,7-Dimethyloct-6-en-1-yl thiophene-3-carboxylate</td></tr>
<tr><td> 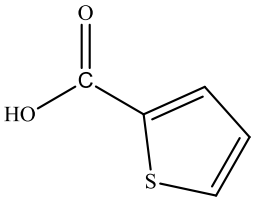
Thiophene-2-carboxylic acid</td><td> 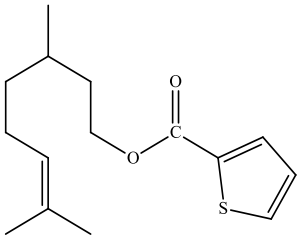
3,7-Dimethyloct-6-en-1-yl thiophene-2-carboxylate</td></tr>
<tr><td> 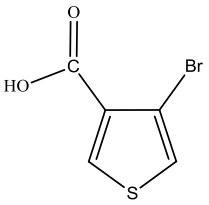
4-Bromothiophene-3-carboxylic acid</td><td> 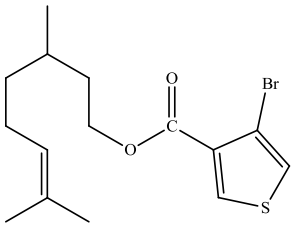
3,7-Dimethyloct-6-en-1-yl4-bromothiophene-3-carboxylate</td></tr>
</table>

<table>
<tr><td colspan="2"> 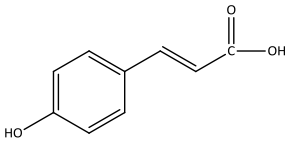
p-Coumaric acid (trans-4-Hydroxycinnamic acid)
(E)-3-(4-Hydroxyphenyl)acrylic acid</td></tr>
<tr><td> 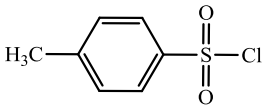
4-Methylbenzene-1-sulfonyl chloride</td><td> 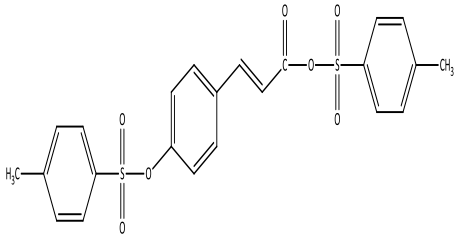
4-Methylbenzenesulfonic(E)-3-(4-(tosyloxy)phenyl)acrylic anhydride</td></tr>
<tr><td> 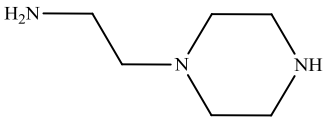
2-(Piperazin-1-yl)ethanamine</td><td> 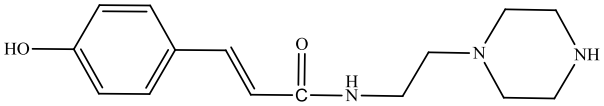
(E)-3-(4-Hydroxyphenyl)-N-(2-(piperazin-1-yl)ethyl)acrylamide</td></tr>
<tr><td> 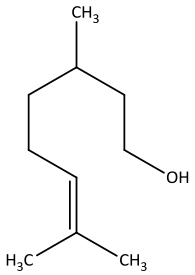
Citronellol
3,7-dimethyloct-6-en--ol</td><td> 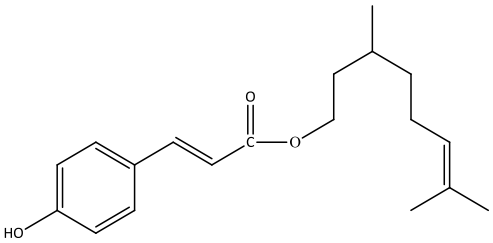
(E)-3,7-Dimethyloct-6-en-1-yl3-(4 hydroxyphenyl)acrylate</td></tr>
<tr><td> 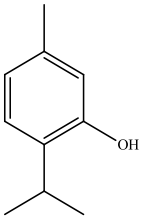
Thymol
2-isopropyl-5-methylphenol</td><td> 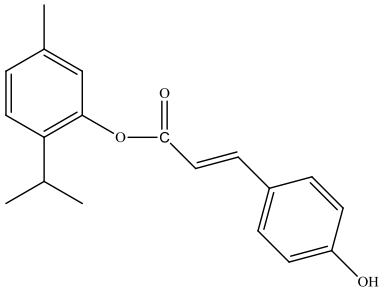
(E)-2-Isopropyl-5-methylphenyl3-(4-hydroxyphenyl)acrylate</td></tr>
</table>

<table>
<tr><td colspan="2"> 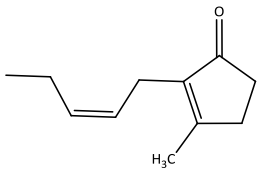
(Z)-3-Methyl-2-(pent-2-en-1-yl)cyclopent-2-enone
cis-Jasmone</td></tr>
<tr><td> 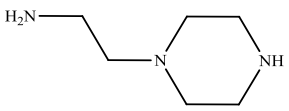
2-(Piperazin-1-yl)ethanamine</td><td> 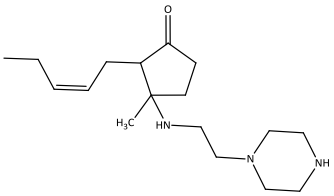
(Z)-3-Methyl-2-(pent-2-en-1-yl)-3-((2-(piperazin-1-yl)ethyl)amino)cyclopentanone</td></tr>
<tr><td> 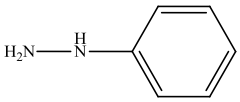
Phenylhydrazine</td><td> 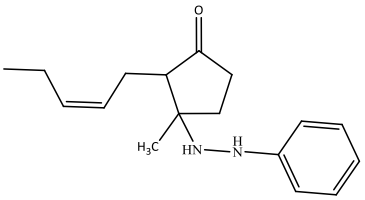
(Z)-3-Methyl-2-(pent-2-en-1-yl)-3-(2-phenylhydrazinyl)cyclopentanone</td></tr>
<tr><td colspan="2"> 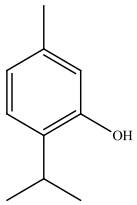
Thymol
2-Isopropyl-5-methylphenol</td></tr>
<tr><td> 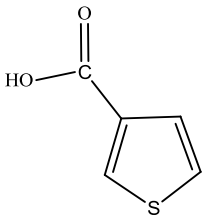
Thiophene-3-carboxylic acid</td><td> 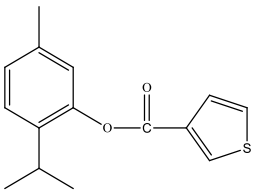
2-Isopropyl-5-methylphenylthiophene-3-carboxylate</td></tr>
<tr><td> 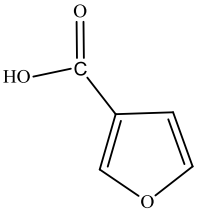
Furan-3-carboxylic acid</td><td> 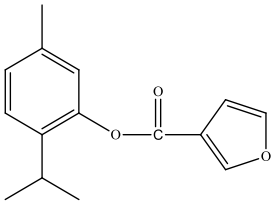
2-Isopropyl-5-methylphenyl furan-3-carboxylate</td></tr>
</table>

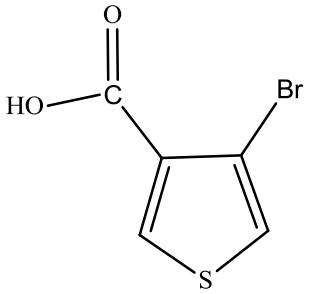 4-Bromothiophene-3-carboxylic acid	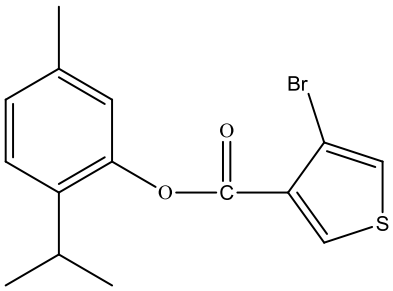 2-Isopropyl-5-methylphenyl 4-bromothiophene-3-carboxylate
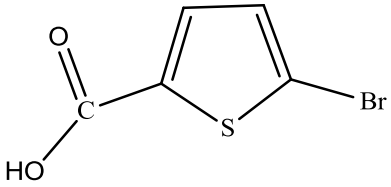 5-Bromothiophene-2-carboxylic acid	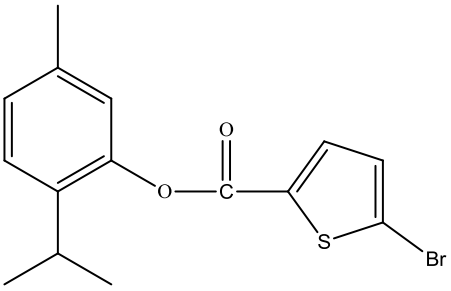 2-Isopropyl-5-methylphenyl 5-bromothiophene-2-carboxylate

Table A.2

The amounts used in the synthesis of citronellol esters

Sample	Starting acid	Oxalyl chloide	DMF	Citronellol	TEA	Total CH_2Cl_2 (ml)
J3 with 3TCA	0.154g 0.0012 moles 1.0909 eq.	1 ml 1.4785g 0.01165moles 10.5909 eq.	-	0.168g 0.0011 moles 1 eq.	0.154g 0.0015moles 1.3636 eq.	4
J15 with 2TCA	0.642g 0.0050 moles 1.6129 eq.	3 ml 4.4355g 0.03495 moles 11.27419 eq.	-	0.477g 0.0031 moles 1 eq.	0.461g 0.0046moles 1.48387 eq.	12
J13 with 4B3TCA	0.249g 0.0012moles 1.2eq.	155 µL 0.2292g 0.001805moles 1.805eq.	2 drop	0.160 g 0.0010 moles 1eq.	0.153g 0.0015 moles 1.5eq	24

Table A.3

The amounts used in the synthesis of thymol esters

Sample	Acid	Total CH_2Cl_2	Oxalyl chloride	DMF	Thymol	TEA
J16 with 3TCA	0.385 g 0.0030 mol 1 eq.	19 ml	0.73925 g 0.5 ml 0.005870 mol 1.94 eq.	4 drops	0.545 g 0.0036 mol 1.2 eq.	0.455 g 0.0045 mol 1.5 eq.
J10 with 5B2TCA	0.622 g 0.0030 mol 1.2 eq.	57 ml	0.5914 g 0.4 ml 0.004659 mol 1.86 eq.	2 drops	0.375 g 0.0025 mol 1 eq.	0.386 g 0.0038 mol 1.52 eq.
J11 with 4B3TCA	0.081 g 0.0004 mol 1.33 eq.	6 ml	0.73925 g 0.5 ml 0.005870 mol 19.56 eq.	2 drops	0.051 g 0.0003 mol 1 eq.	0.057 g 0.0006 mol 2 eq.

Table A.4

Citronellol esters with physical state, M.P, and yield%

Starting acid	Product esters (Structure No.)	Physical state	M.P	Yield%
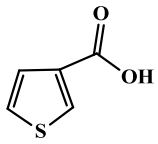	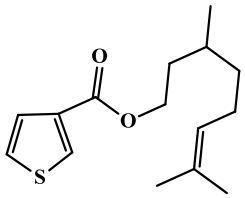 J3	liquid	-	71.66
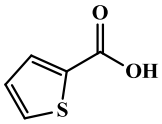	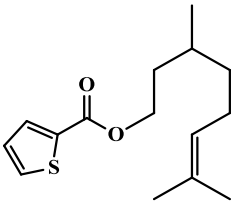 J15	liquid	-	83.13
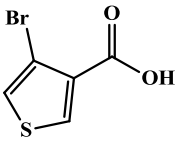	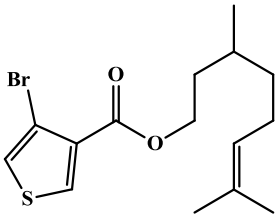 J13	Solid	115-117℃	56.92

Table A.5

Anticancer activity of J3

	Inhibition%					
Concentration μg/ml	CaCO-2	Hep-3B	HeLa	MCF-7	Hep-G2	LX-2
500	72.49	84.91	82.96	91.85	71.98	67.79
300	22.66	7.75	25.53	14.26	5.00	60.94
100	14.91	4.95	10.84	9.35	1.28	12.09
50	-3.94	-2.16	2.86	1.08	0.30	0.88
0	0	0.00	0.00	0.00	0.00	0.00

Table A.6

Anticancer activity of J15

	Inhibition%					
Concentration µg/ml	CaCO-2	B16F1	HeLa	MCF-7	Hep-G2	LX-2
1000	96.24	97.59	95.44	96.96	96.90	98.98
500	94.91	97.16	88.66	94.68	96.49	87.05
300	68.93	92.14	87.28	80.55	79.21	85.87
100	11.50	25.46	32.05	13.08	8.64	80.89
50	0.81	-0.90	6.96	5.95	4.73	54.38
0	0.00	0.00	0.00	0.00	0.00	0.00

Table A.7

Anticancer activity of J13

	Inhibition%					
Concentration µg/ml	CaCO-2	B16F1	HeLa	MCF-7	Hep-G2	LX-2
1000	85.04	91.81	67.00	89.40	87.78	97.40
500	51.92	74.73	60.71	55.61	42.58	96.38
300	8.85	56.98	25.30	12.56	15.21	78.12
100	5.13	16.09	3.99	5.14	2.29	59.98
50	-0.34	0.00	1.02	2.87	0.74	44.26
0	0.00	0.00	0.00	0.00	0.00	0.00

Table A.8

Anticancer activity of J2

	Inhibition%					
Concentration μg/ml	CaCO-2	Hep-3B	HeLa	MCF-7	Hep-G2	LX-2
500	67.52	92.25	95.23	95.41	92.26	61.31
300	58.45	55.63	73.52	69.97	51.37	39.63
100	13.63	0.41	1.00	5.07	11.80	30.50
50	-1.91	-0.86	0.69	-1.40	5.26	14.78
0	0.00	0.00	0.00	0.00	0.00	0.00

Table A.9

Anticancer activity of J14

	Inhibition%					
Concentration μg/ml	CaCO-2	B16F1	HeLa	MCF-7	Hep-G2	LX-2
1000	85.04	91.81	67.00	89.40	87.78	97.40
500	51.92	74.73	60.71	55.61	42.58	96.38
300	8.85	56.98	25.30	12.56	15.21	78.12
100	5.13	16.09	3.99	5.14	2.29	59.98
50	-0.34	0.00	1.02	2.87	0.74	44.26
0	0.00	0.00	0.00	0.00	0.00	0.00

Table A.10

Anticancer activity of J19

Inhibition%					
Concentration μg/ml	Hep-3B	HeLa	MCF-7	B16-F1	LX-2
1000	37.24	12.44	48.87	51.08	54.17
500	8.58	-61.10	46.74	2.07	25.62
250	2.52	-60.80	38.62	-12.52	9.22
125	4.31	-65.80	4.47	-13.18	7.44
62.5	-0.85	-64.23	-11.20	-12.02	2.37
0	0.00	0.00	0.00	0.00	0.00

Table A.11

IC_{50} of p-CA amide J19 and p-CA

	IC_{50} μg/ml	
Assay	*p*-CA ± SD	J19 ± SD
Hep-3B	447.46 ± 0.325	1450.08 ± 0.532
HeLa	685.03 ± 0.024	2321.07 ± 0.038
MCF-7	498.34 ± 0.085	824.09 ± 0.012
B16-F1	-	988.86 ± 0.042
LX-2	1283.62 ± 0.270	939.48 ± 0.014

Table A.12

Anticancer activity of N2

Inhibition%					
Concentration μg/ml	Hep-3B	HeLa	MCF-7	B16-F1	LX-2
1000	96.36	98.17	100.04	99.25	96.89
500	66.21	44.30	88.21	87.85	97.52
250	4.75	17.92	30.86	-4.31	81.44
125	2.67	-64.12	-1.90	-41.75	53.13
62.5	-0.53	-68.78	-3.29	-52.69	36.40
0.00	0.00	0.00	0.00	0.00	0.00

Table A.13

Anticancer activity of N4

Inhibition%					
Concentration μg/ml	MCF-7	B16-F1	HeLa	Hep-3B	LX-2
1000	63.69	100.54	98.96	53.65	91.00
500	61.05	58.50	70.98	45.39	79.72
250	-12.88	6.05	-4.77	20.65	58.07
125	-6.22	-1.58	8.35	2.86	53.29
62.5	-4.17	-6.47	1.94	-2.56	50.70
0	0.00	0.00	0.00	0.00	0.00

Table A.14

IC_{50} of p-CA, N2 and N4

	IC_{50} μg/ml		
Assay	*p*-CA ± SD	N2 ± SD	N4 ± SD
Hep-3B	447.46 ± 0.325	409.97 ± 0.014	690.26 ± 0.064
HeLa	685.03 ± 0.024	553.09 ± 0.064	405.95 ± 0.035
MCF-7	498.34 ± 0.085	315.3 ± 0.212	434.43 ± 0.304
B16-F1	-	366.18 ± 0.007	443.28 ± 0.035
LX-2	1283.62 ± 0.270	380.81 ± 0.136	429.18 ± 0.011

Table A.15

Anticancer activity of N6

Inhibition%					
Concentration μg/ml	MCF-7	B16-F1	HeLa	Hep-3B	LX-2
1000	100.77	83.91	97.73	97.29	97.09
500	100.11	71.31	98.70	95.97	98.42
250	99.23	43.12	99.93	16.23	98.89
125	99.49	-13.27	100.37	-3.92	78.28
62.5	27.01	-31.84	57.94	-4.05	48.56
0	0.00	0.00	0.00	0.00	0.00

Table A.16

Anticancer activity of N8

Inhibition%						
Concentration μg/ml	Hep-G2	Hep-3B	HeLa	MCF-7	B16-F1	LX-2
500	87.81	83.52	85.99	74.78	85.16	91.70
250	76.74	32.06	89.57	88.18	71.06	90.33
125	-9.63	10.20	6.26	17.09	18.91	83.36
62.5	-16.40	7.78	-17.06	-3.26	-21.64	52.97
0	0.00	0.00	0.00	0.00	0.00	0.00

Table A.17

IC_{50} of cis-jasmone and cis-jasmone amine N6, N8

IC_{50}μg/ml			
Assay	*cis*-Jasmone ±SD	N6 ± SD	N8 ± SD
CaCo-2	68.07 ± 0.969	-	-
Hep-G2	70.43 ± 0.304	-	195.97 ± 0.021
Hep-3B	74.84 ± 0.113	334.45 ± 0.318	322.16 ± 0.117
HeLa	66.64 ± 0.410	59.42 ± 0.148	176.25 ± 0.170
MCF-7	69.03 ± 0.849	78.47 ± 0.007	169.61 ± 0.283
B16-F1	391.57 ± 0.205	283.61 ± 0.276	182.74 ± 0.184
LX-2	92.64 ± 0.163	362.32 ± 0.225	202.02 ± 0.014

Table A.18

Anticancer activity of J16

Inhibition%						
Concentration μg/ml	CaCO-2	B16F1	HeLa	MCF-7	Hep-G2	LX-2
1000	95.98	97.59	95.37	96.12	96.49	99.27
500	94.91	88.45	87.67	90.10	95.31	88.02
300	94.62	88.03	87.35	88.56	95.01	86.21
100	66.92	80.12	80.49	81.01	87.63	85.70
50	8.29	69.90	37.88	17.49	23.23	73.26
0	0.00	0.00	0.00	0.00	0.00	0.00

Table A.19

Anticancer activity of J10

	Inhibition%					
Concentration µg/ml	CaCO-2	B16F1	HeLa	MCF-7	Hep-G2	LX-2
1000	83.33	91.34	70.11	87.90	76.59	86.26
500	24.57	65.88	37.00	35.61	39.55	77.84
300	6.84	53.10	10.25	14.76	17.91	57.72
100	3.85	18.03	10.11	9.51	13.77	35.90
50	-0.51	1.23	6.50	8.08	12.81	25.95
0	0.00	0.00	0.00	0.00	0.00	0.00

Table A.20

Anticancer activity of J11

	Inhibition%						
Concentration µg/ml	CaCo-2	Hep-G2	Hep-3B	HeLa	MCF-7	B16F1	LX-2
1000	100.00	97.23	94.78	99.60	99.92	11.98	54.67
500	95.05	92.70	91.84	91.88	92.39	9.36	18.94
300	72.95	88.76	88.94	83.88	87.14	8.63	2.40
100	4.09	19.36	9.89	27.30	17.53	1.88	-3.91
50	1.81	5.70	0.80	10.57	6.06	-3.19	-3.29
0	0.00	0.00	0.00	0.00	0.00	0.00	0.00

Table A.21

Anticancer activity of J12

	Inhibition%					
Concentration µg/ml	CaCO-2	B16F1	HeLa	MCF-7	Hep-G2	LX-2
1000	96.45	98.67	96.25	96.92	96.68	100.45
500	88.03	97.87	94.91	96.78	89.62	88.75
300	85.73	89.40	88.06	89.89	89.36	86.21
100	11.67	61.57	38.09	21.62	14.62	80.72
50	6.41	4.26	15.44	12.91	16.14	56.30
0	0.00	0.00	0.00	0.00	0.00	0.00

Appendix B

Spectroscopic analysis Spectra, anticancer and antimicrobial activities of new derivatives

Figure B.1

FT-IR for J3

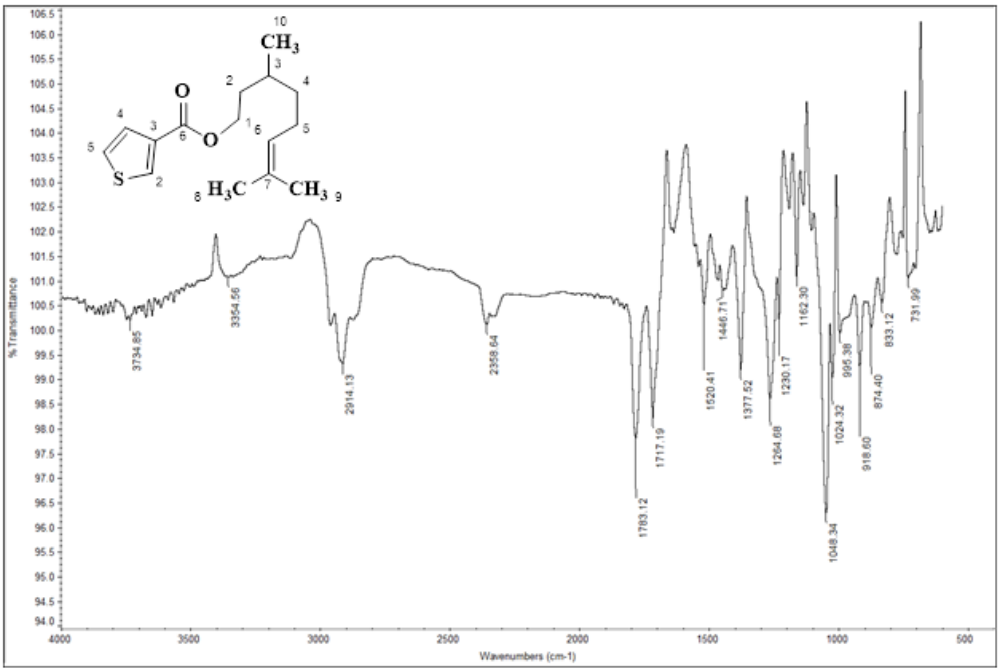

Figure B.2

F-IR for J15

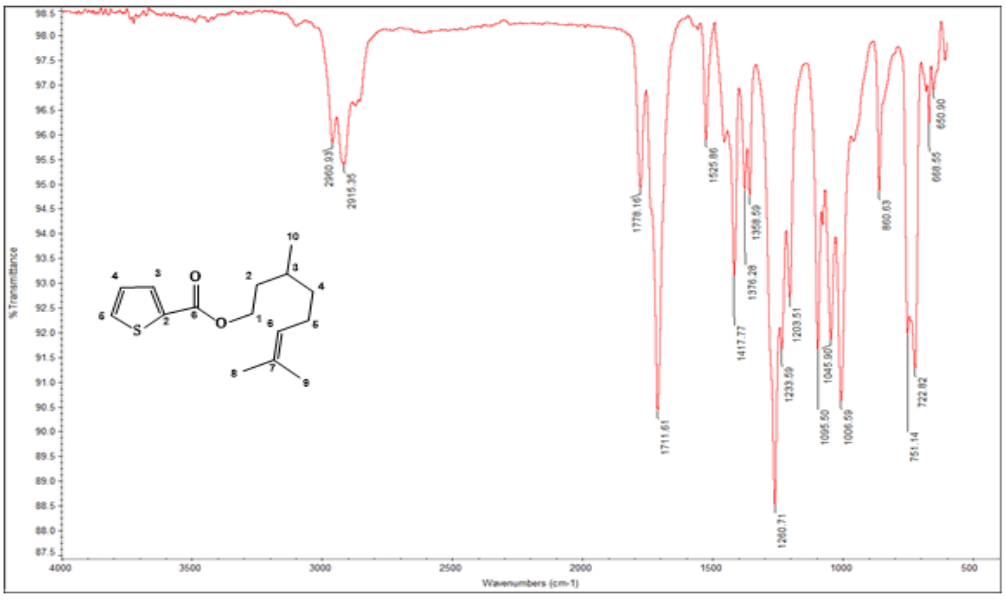

Figure B.3

FT-IR for J13

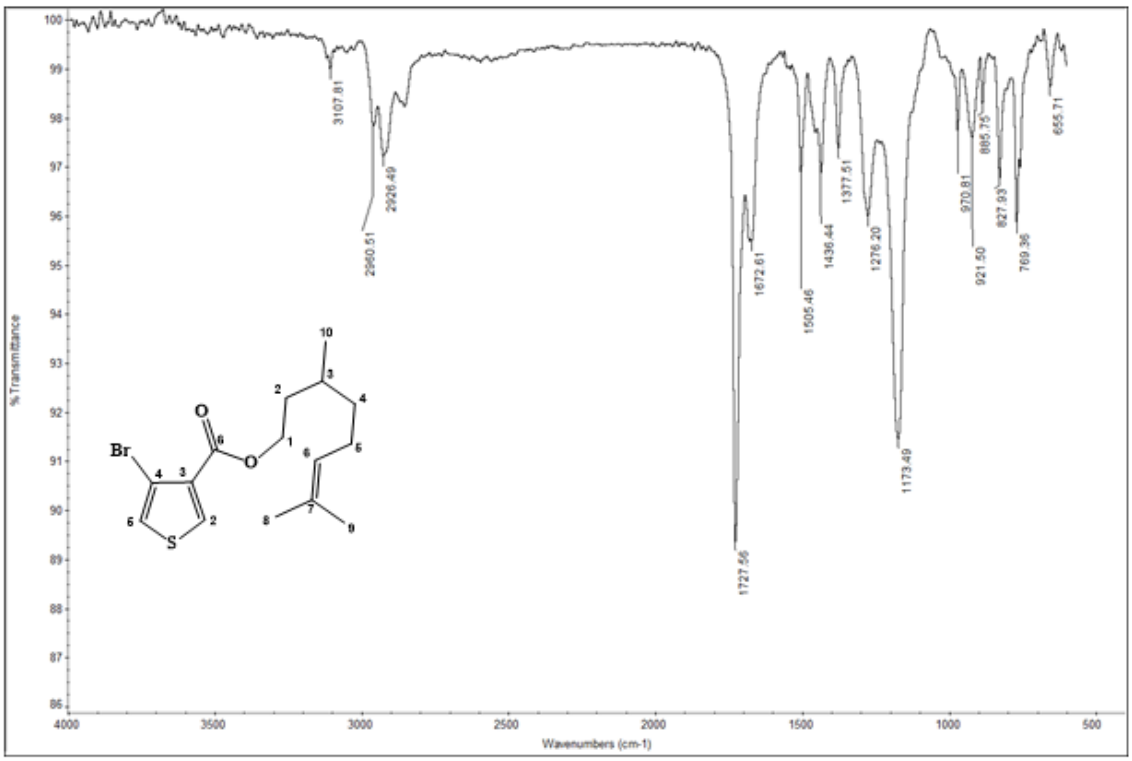

Figure B.4

FT-IR for J2

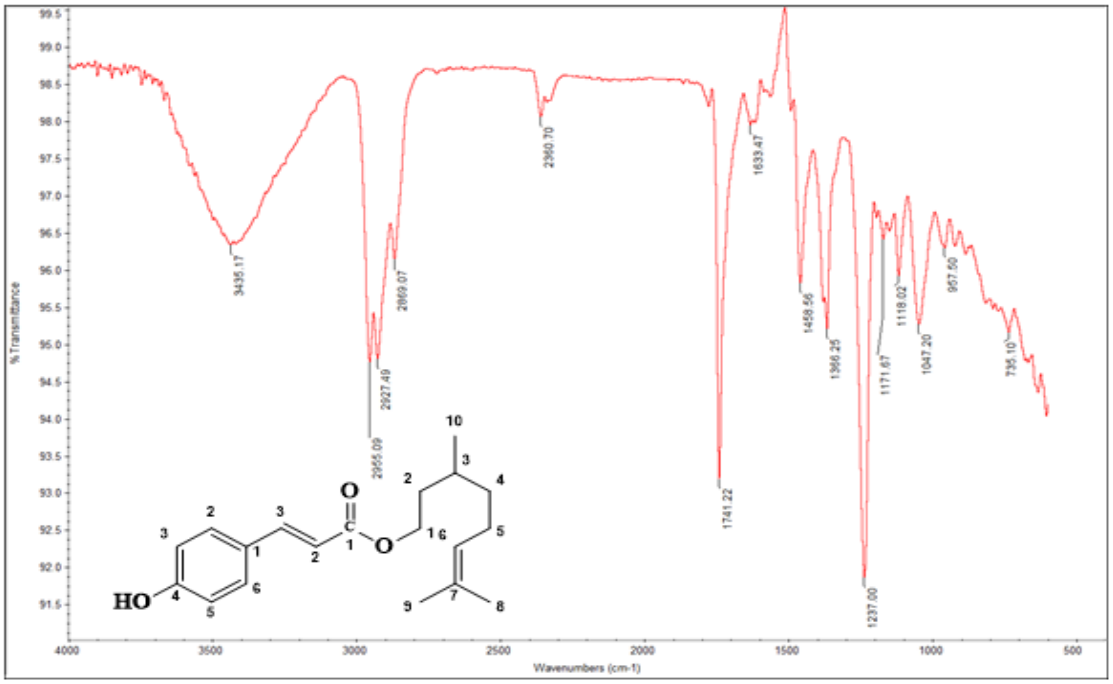

Figure B.5

FT-IR for J14

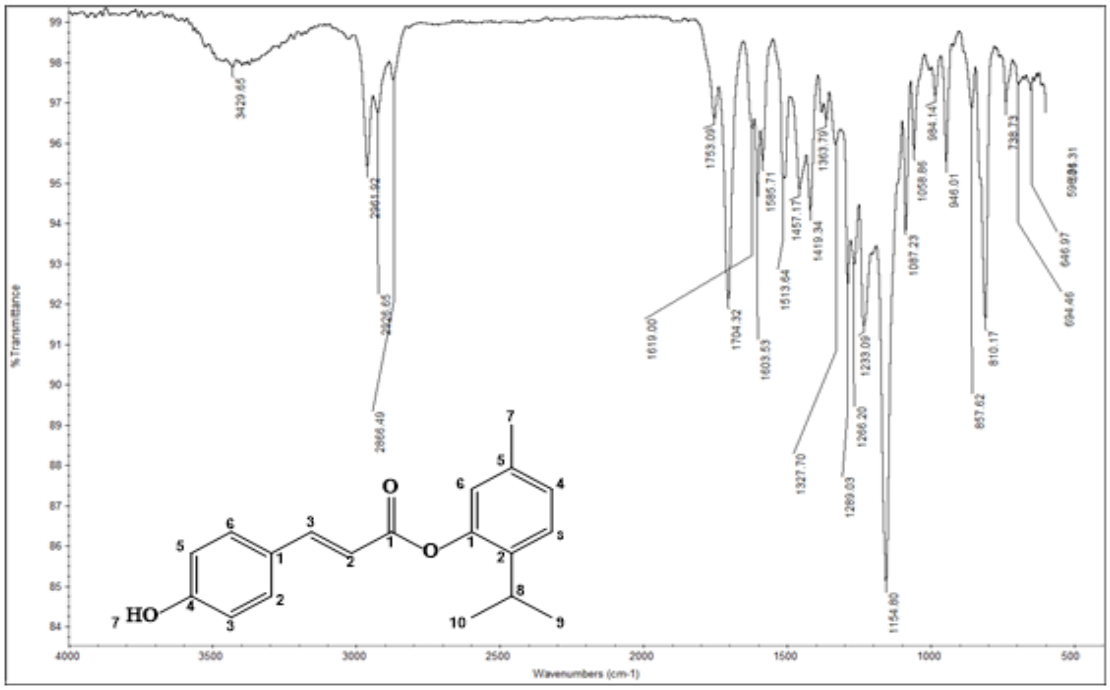

Figure B.6

FT-IR for J19

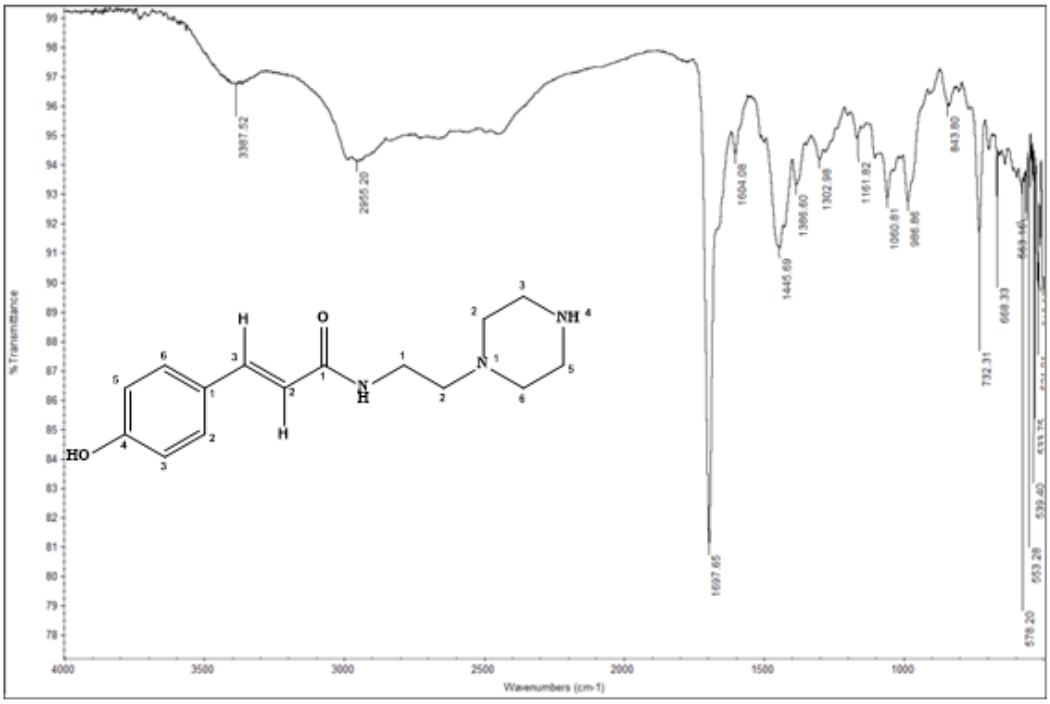

Figure B.7

FT-IR for N2

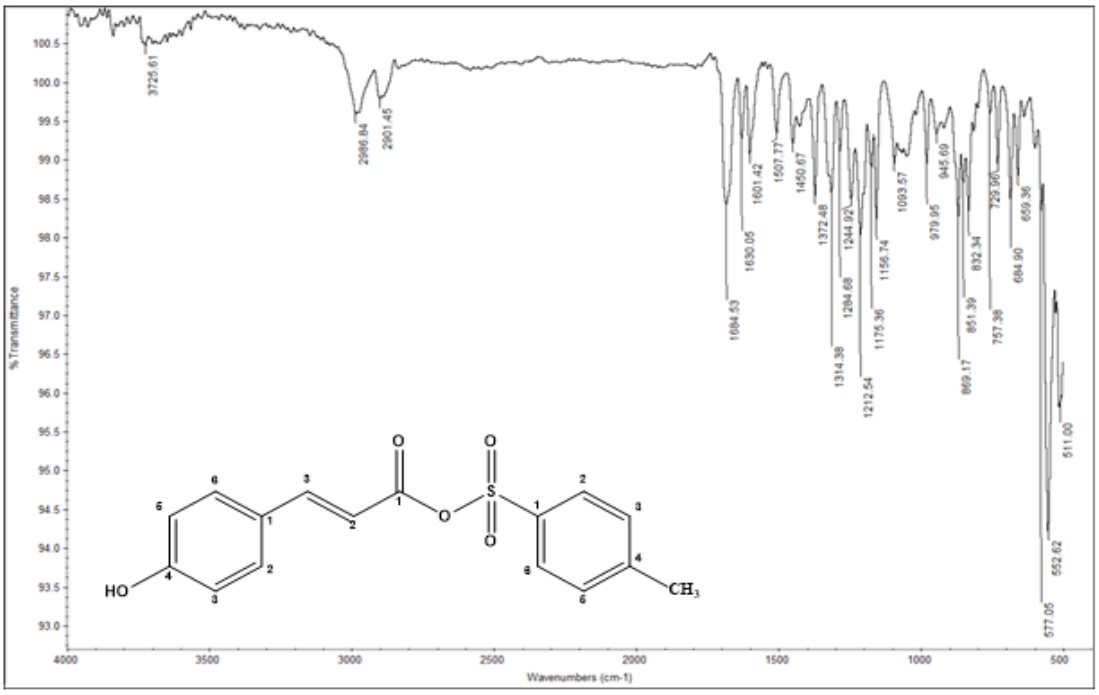

Figure B.8

FT-IR for N4

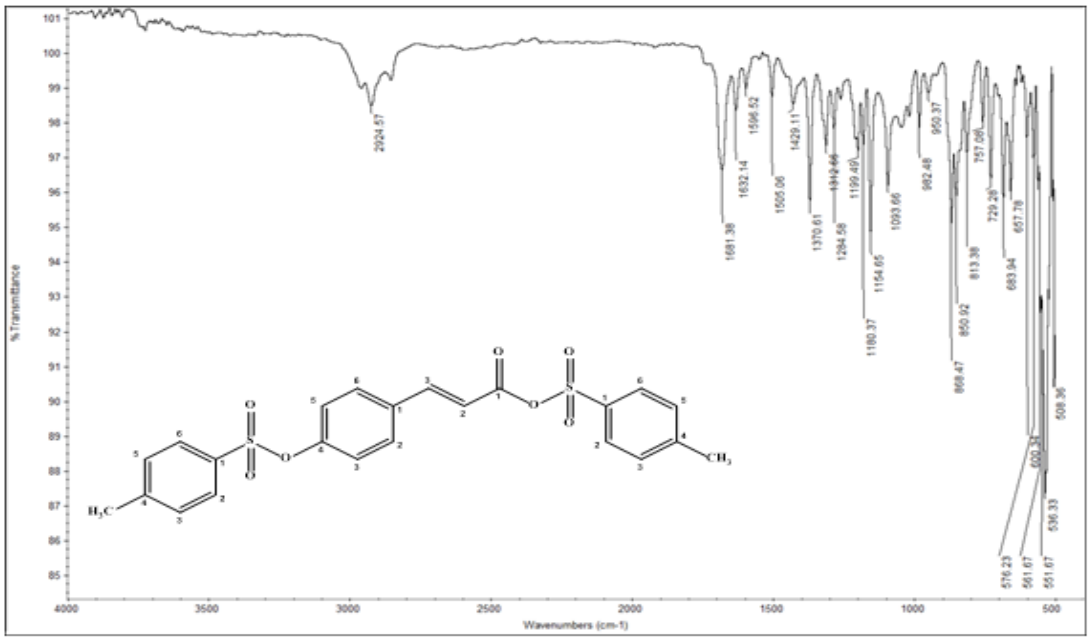

Figure B.9

FT-IR for N6

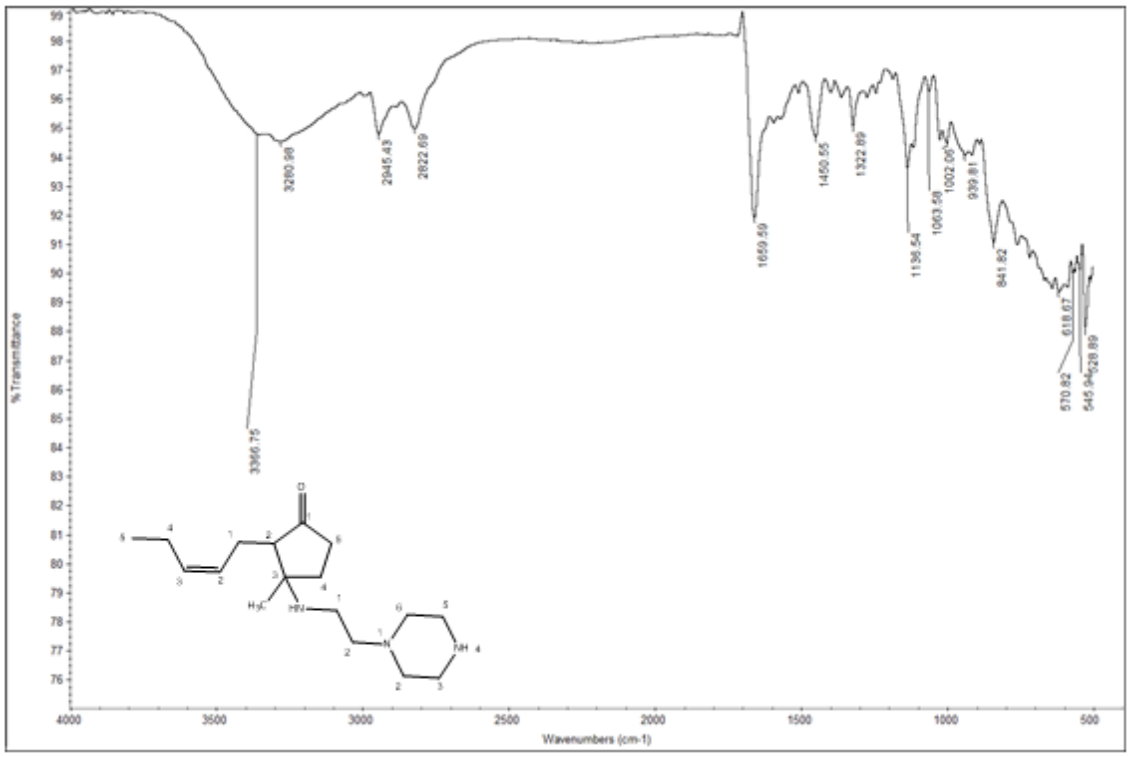

Figure B.10

FT-IR for N8

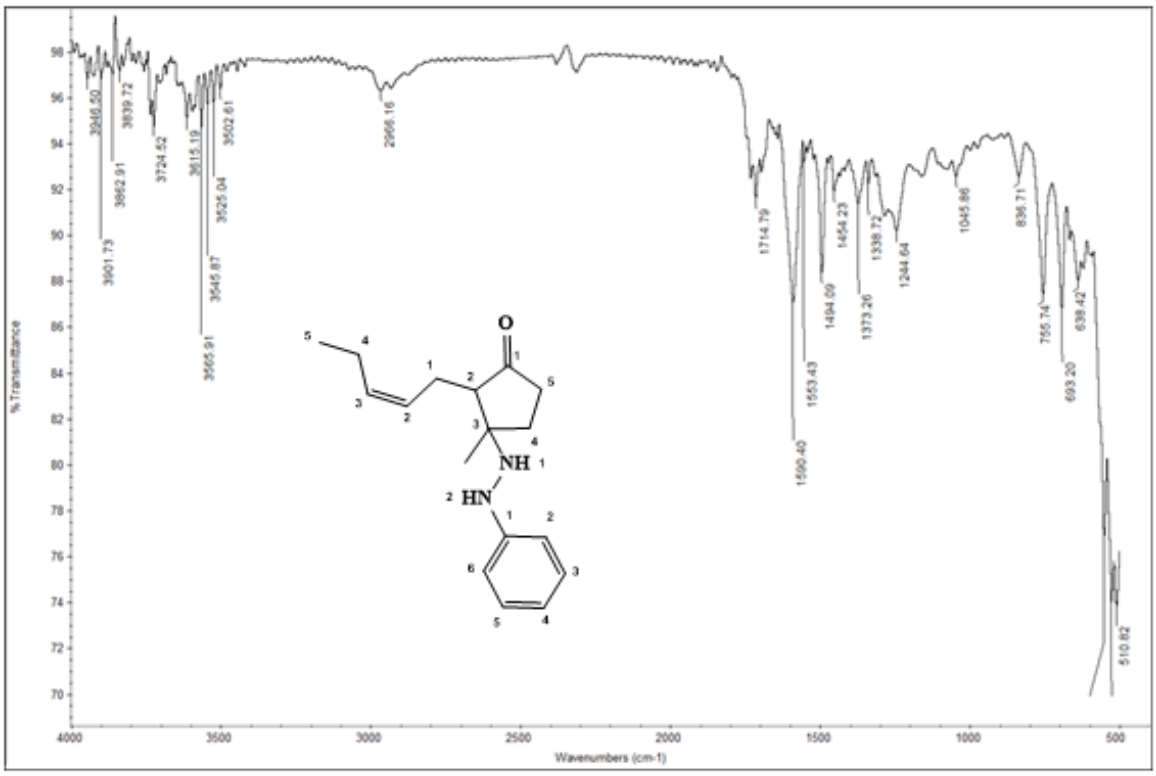

Figure B.11

FT-IR for J 16

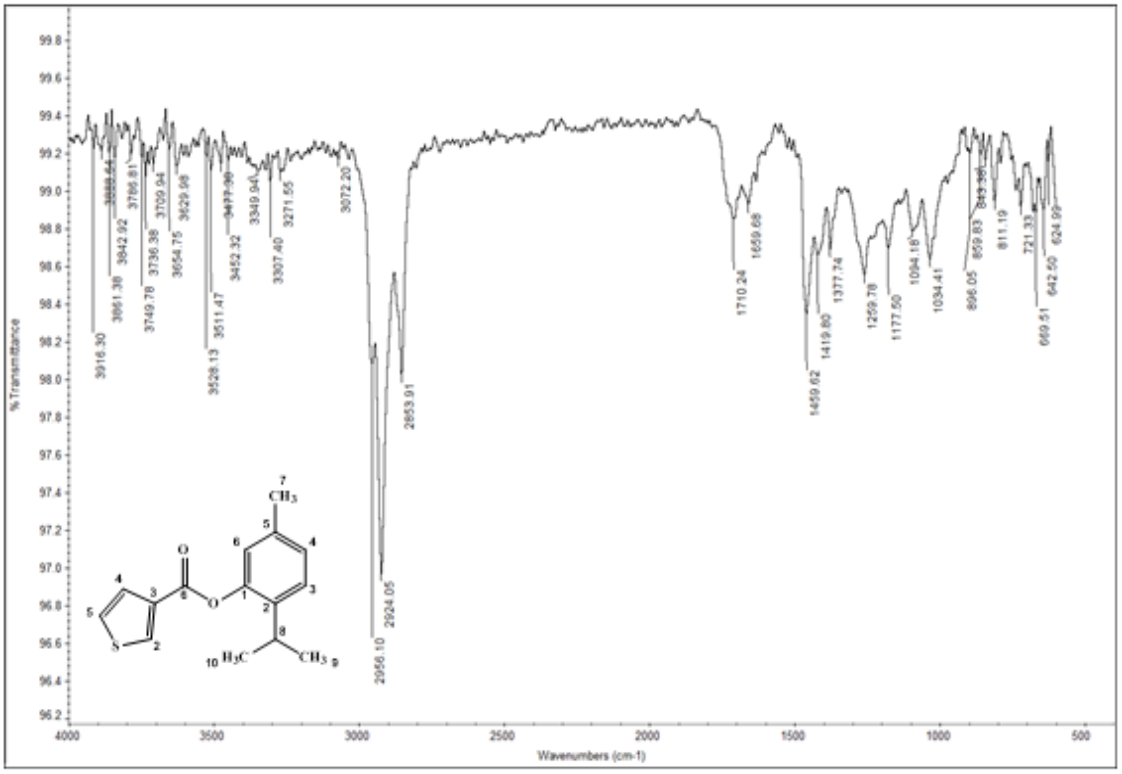

Figure B.12

FT-IR for J10

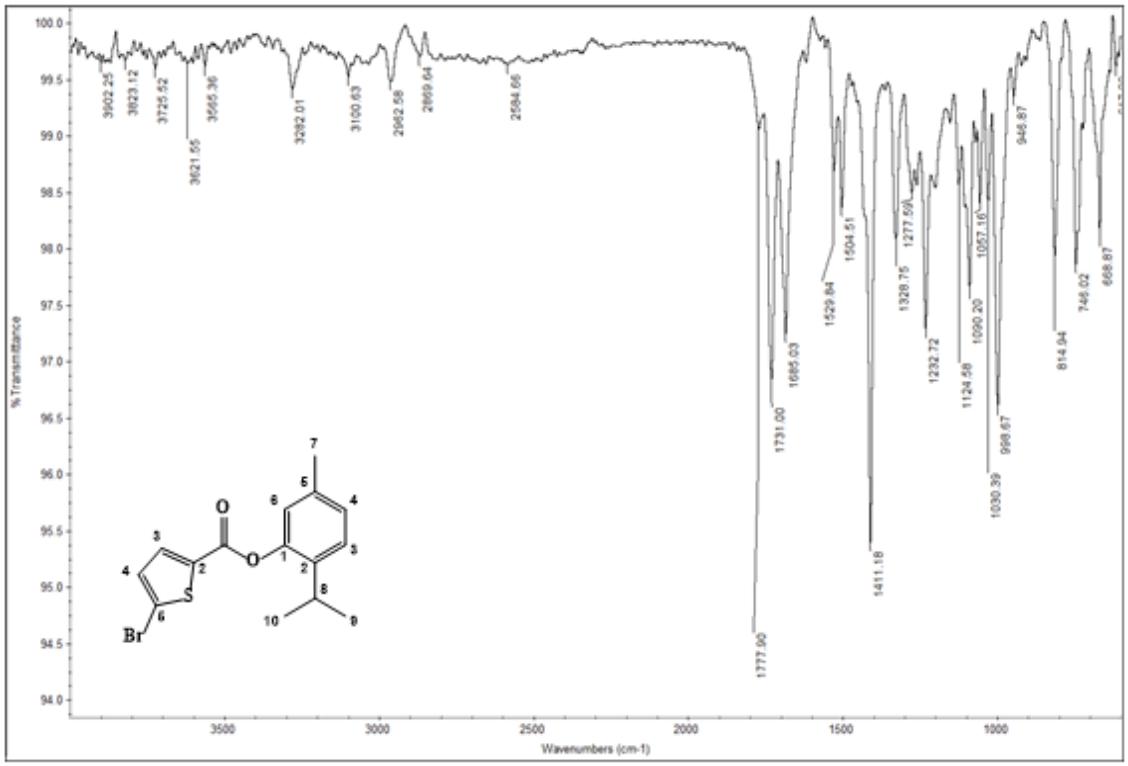

Figure B.13

FT-IR for J11

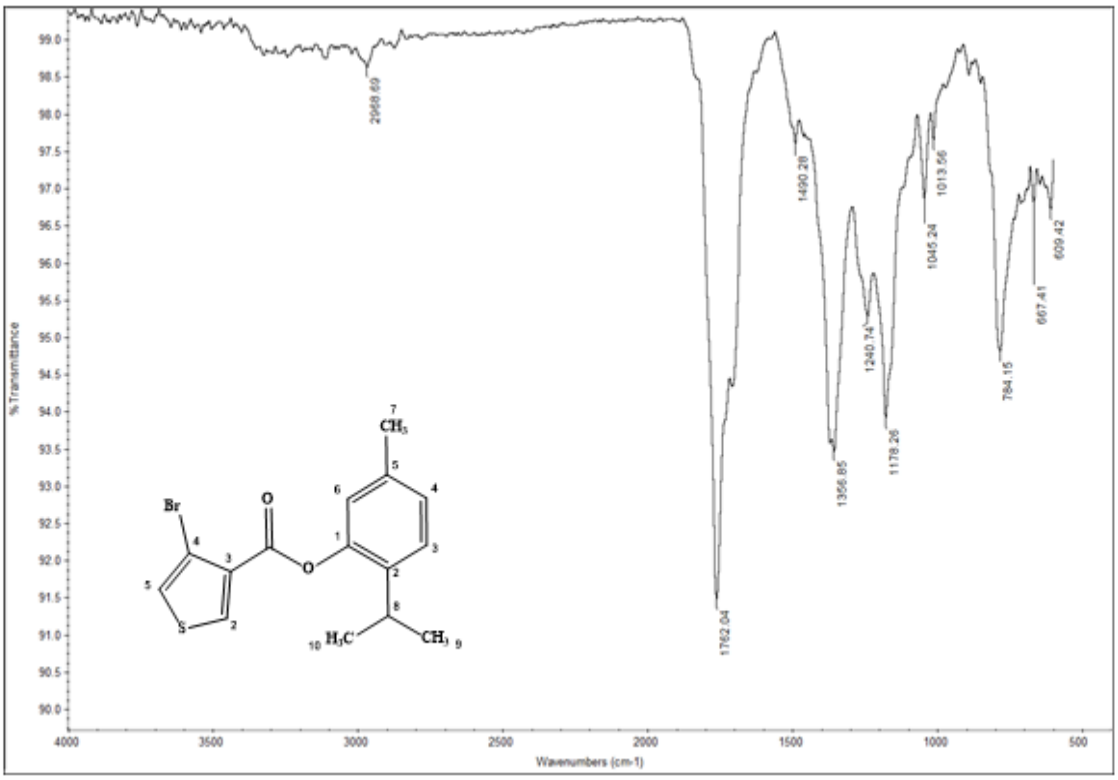

Figure B.14

FT-IR for J12

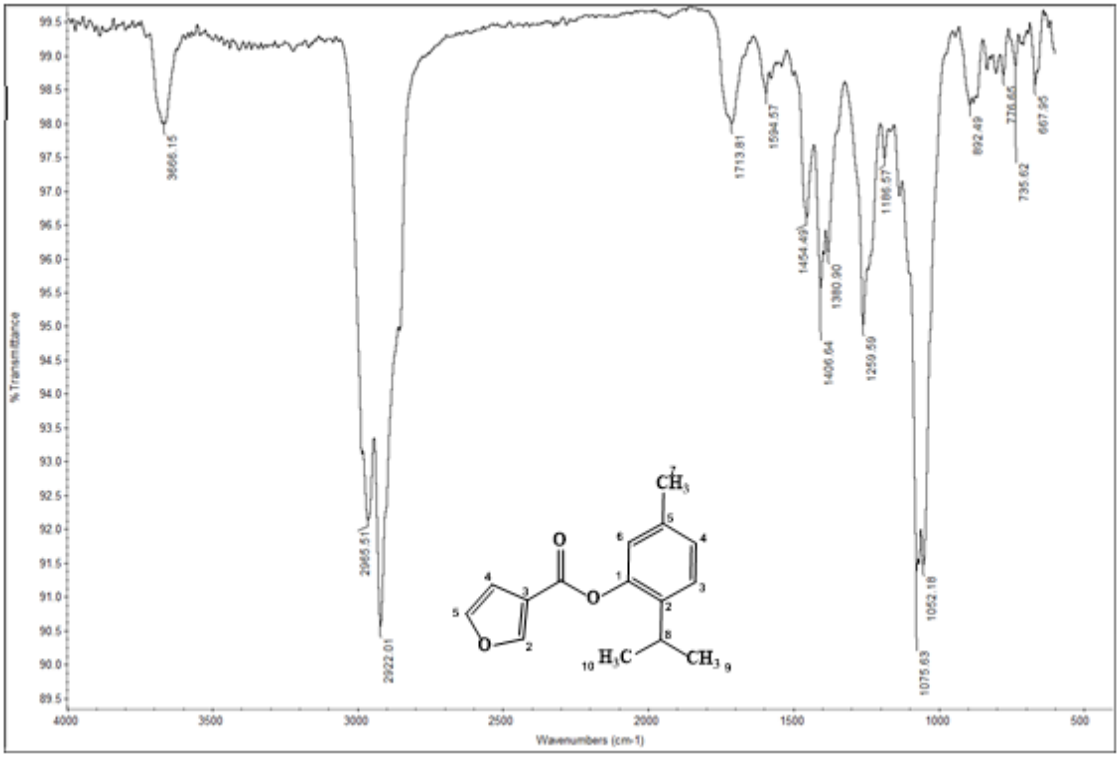

Figure B.15

[1]H-NMR for J3

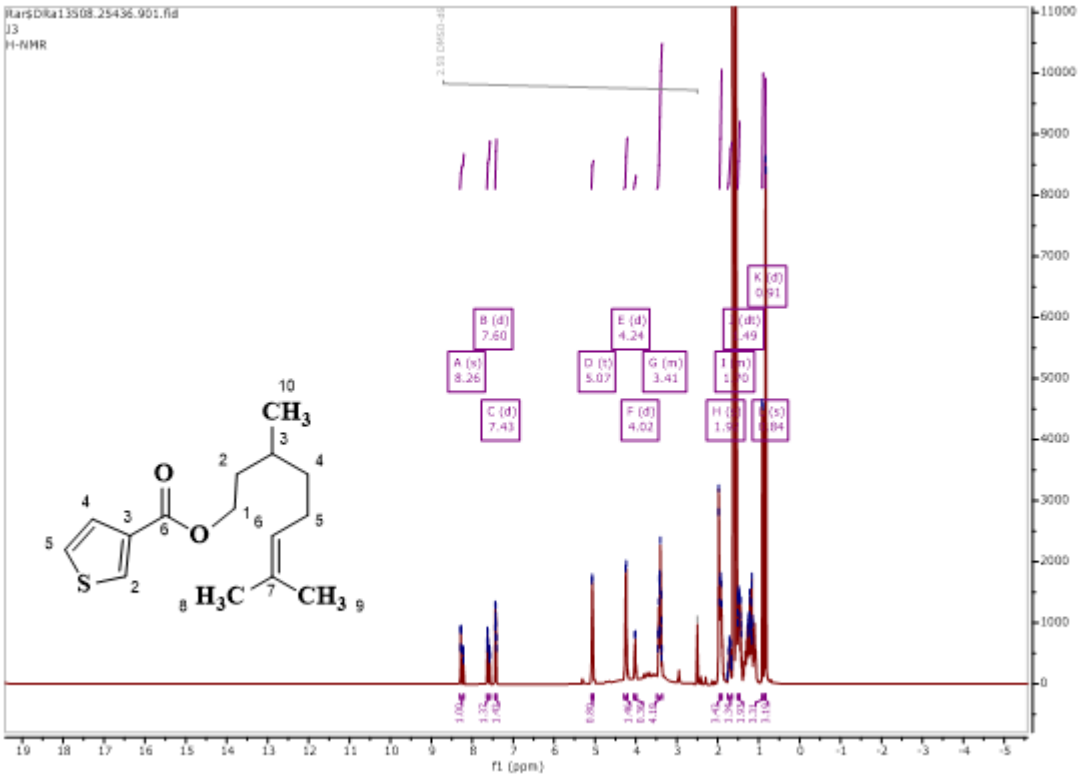

Figure B.16

[13]C-NMR for J3

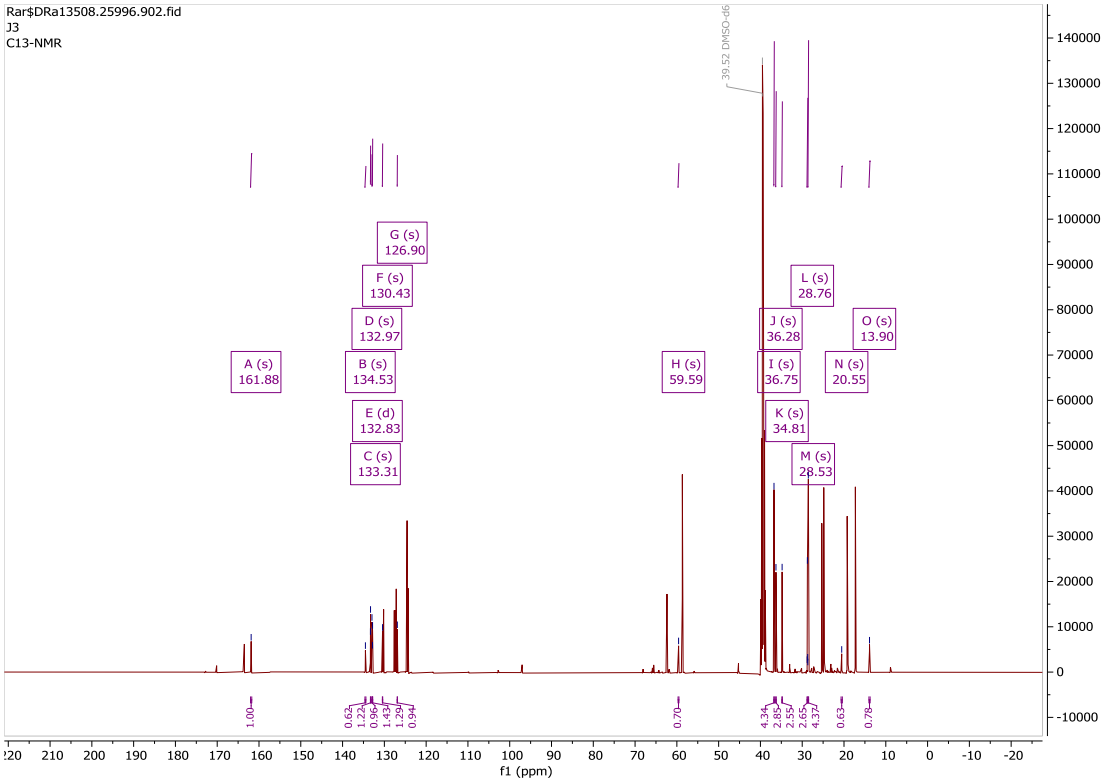

Figure B.17

[1]H-NMR for J15

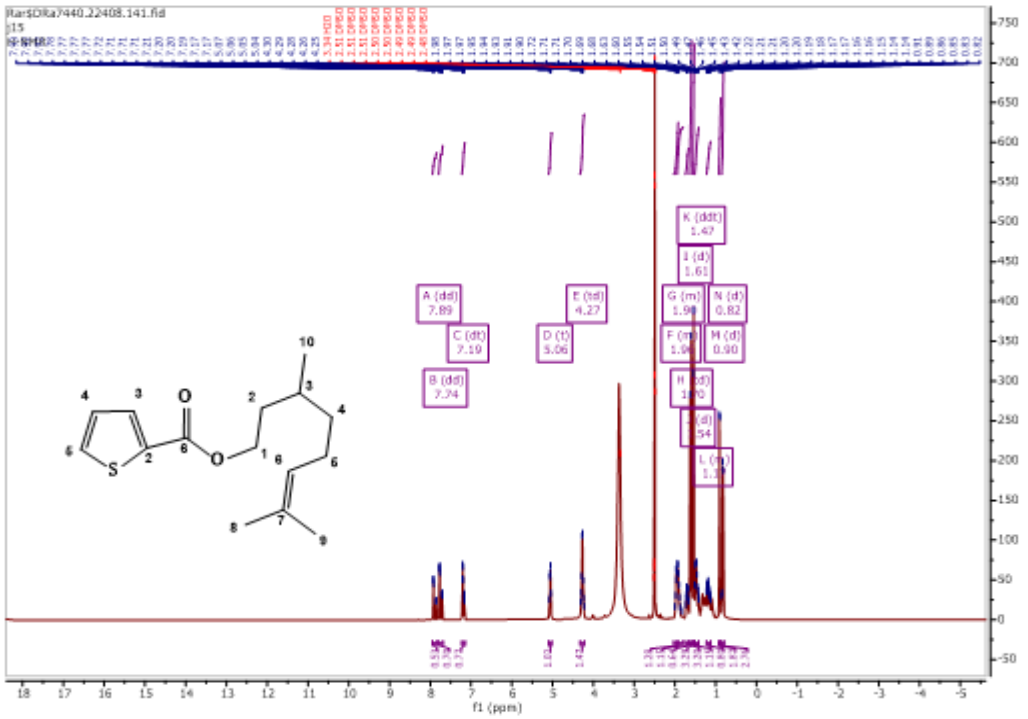

Figure B.18

[13]C-NMR for J15

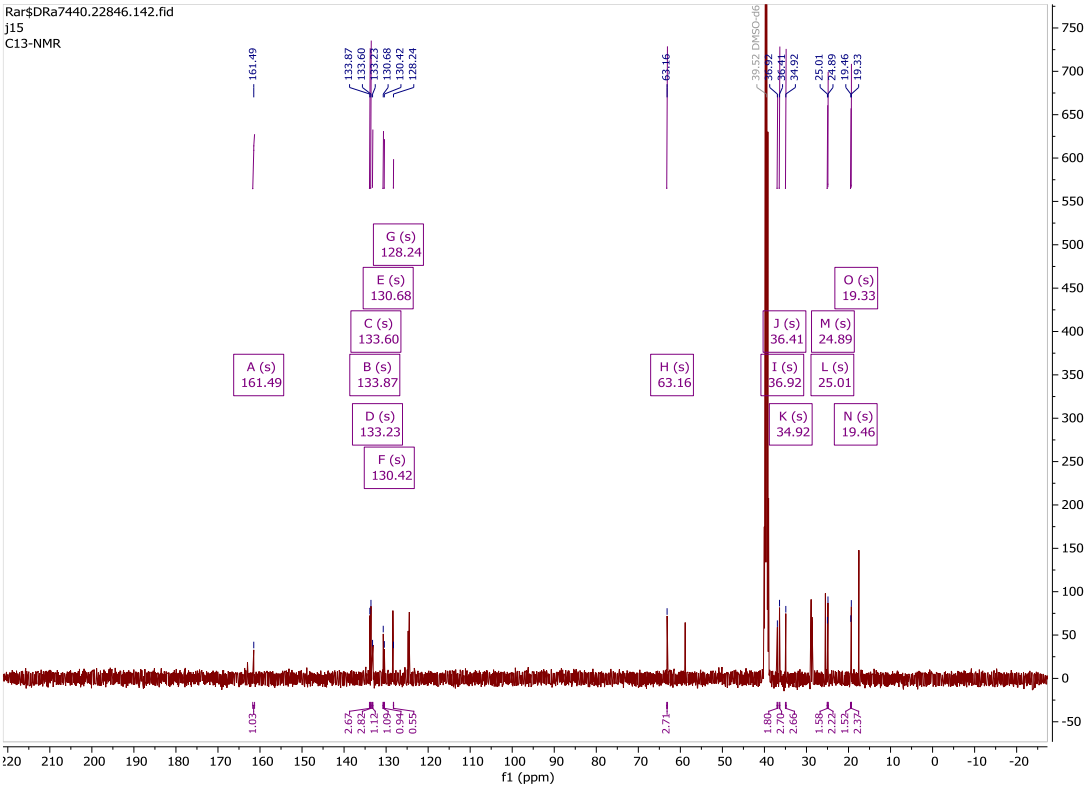

Figure B.19

^{1}H-NMR for J13

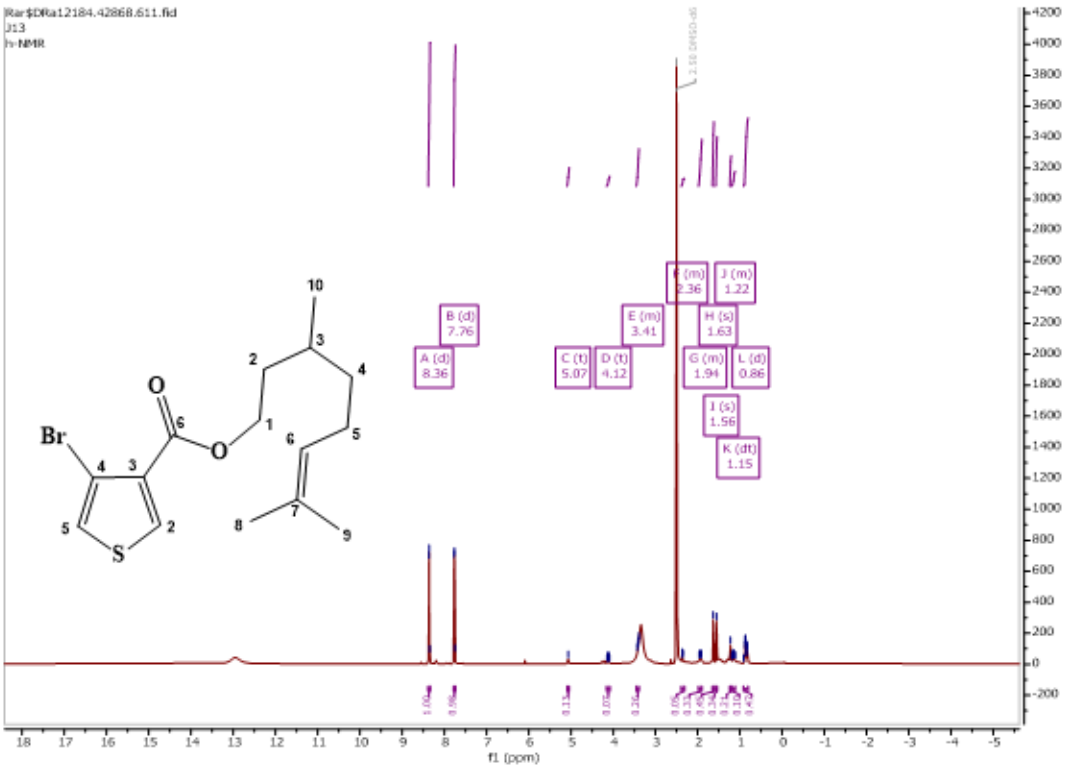

Figure B.20

^{13}C-NMR for J13

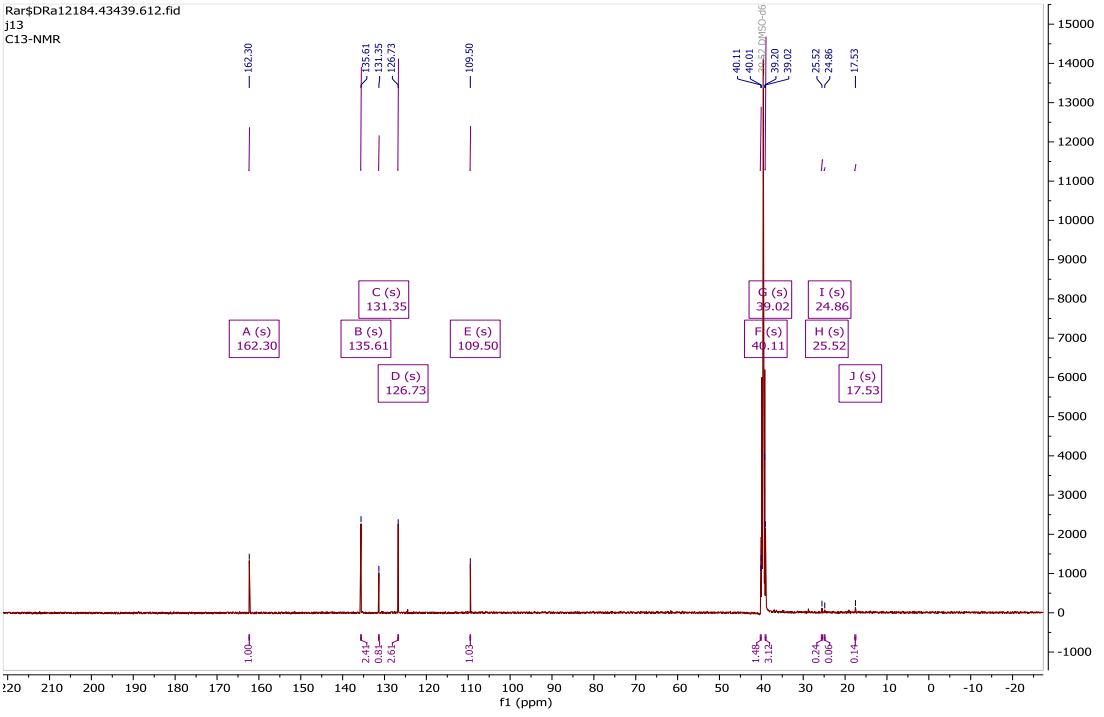

Figure B.21

^{13}C-NMR for J2

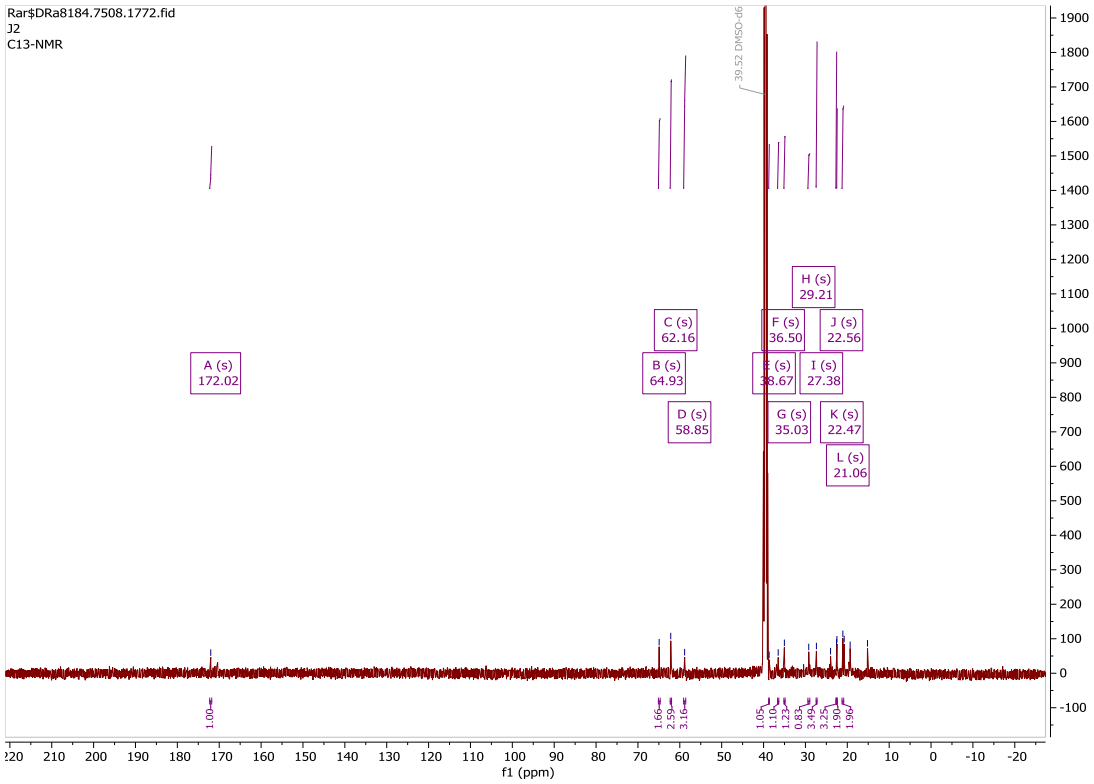

Figure B.22

^{13}C-NMR for J14

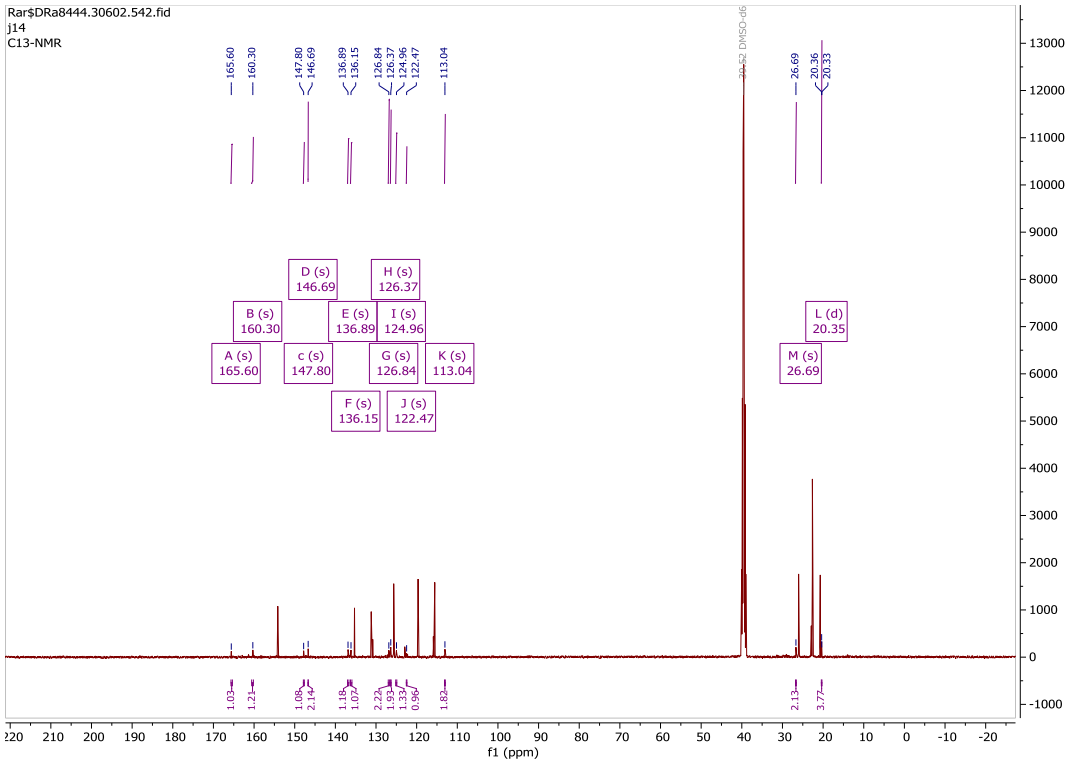

Figure B.23

[1]H-NMR for J19

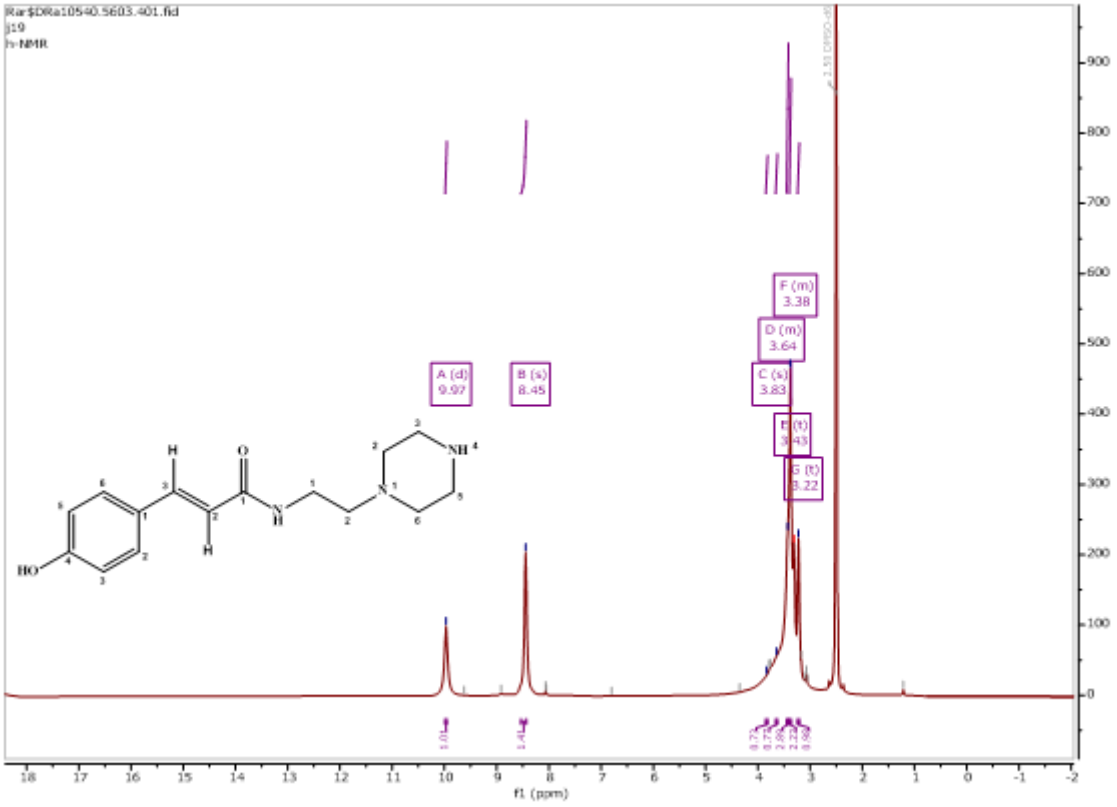

Figure B.24

[13]C-NMR for J19

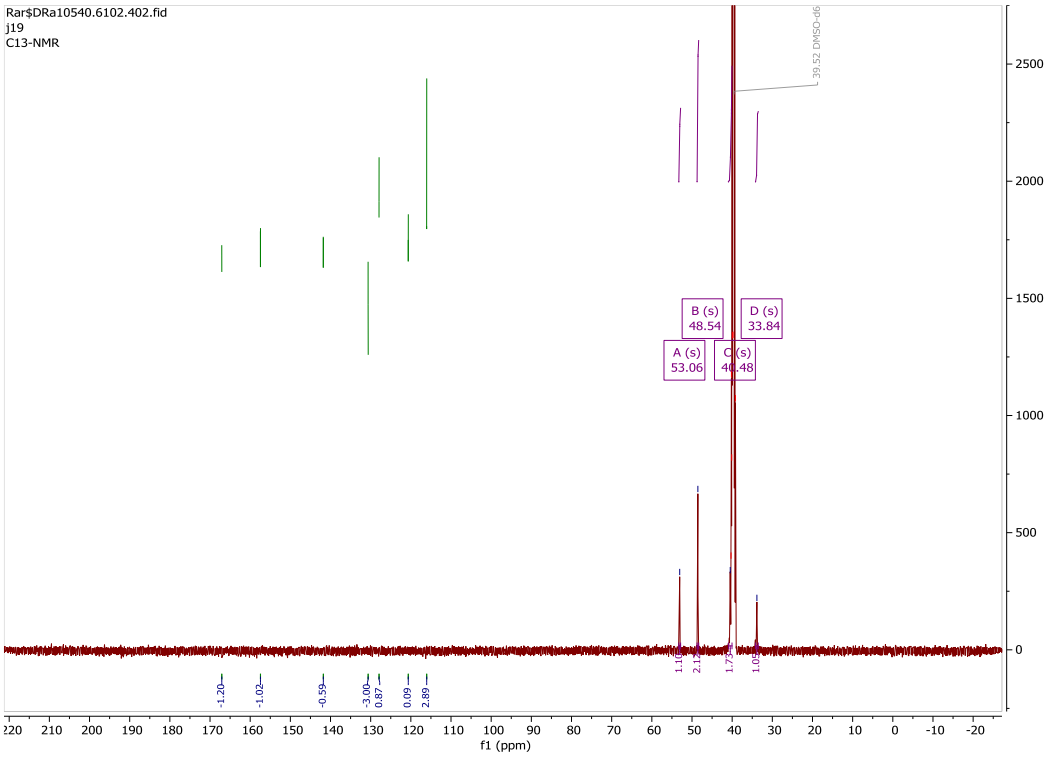

Figure B.25

[1]H-NMR for N2

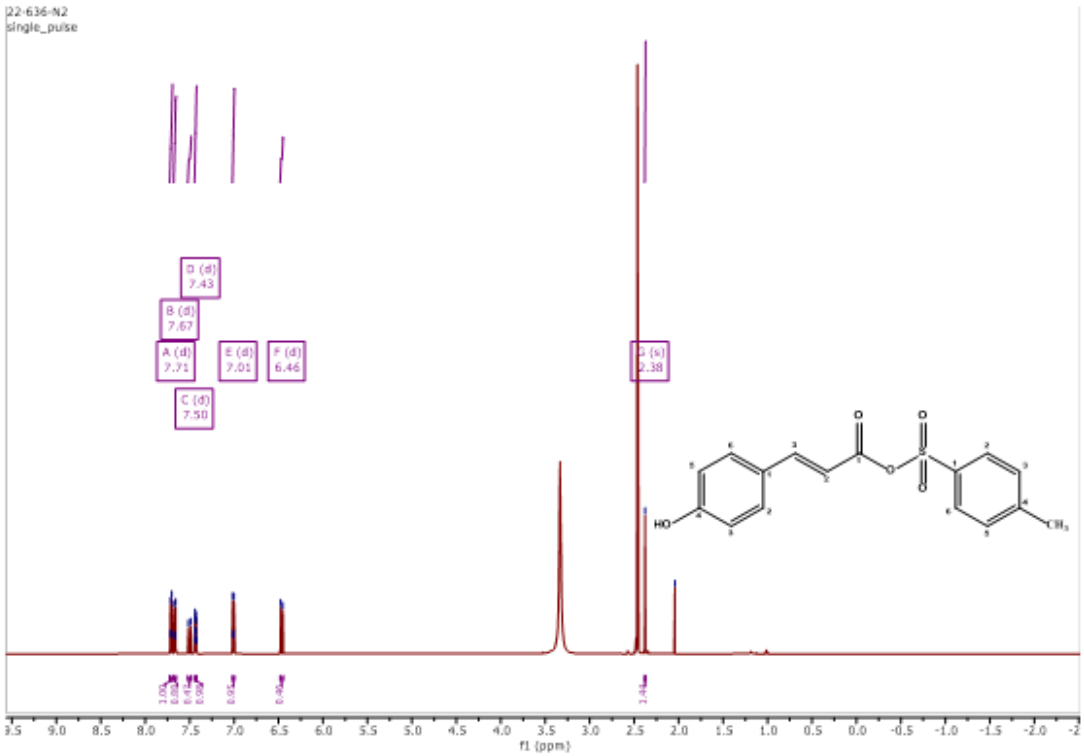

Figure B.26

[13]C-NMR for N2

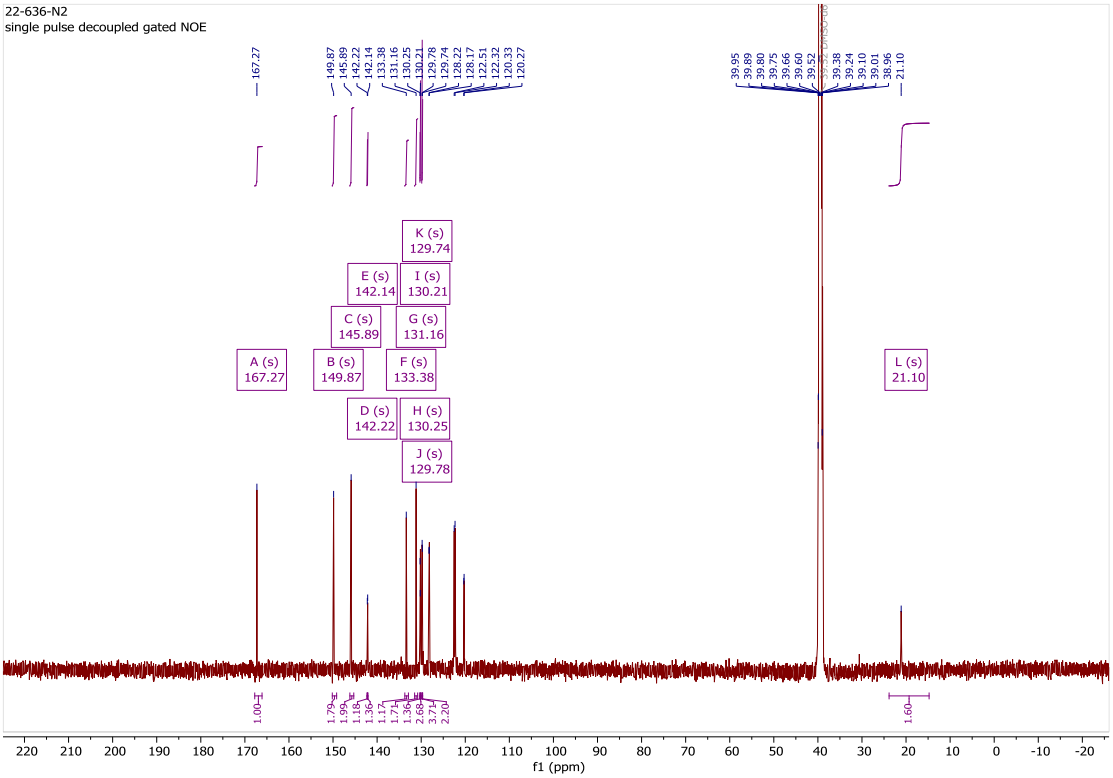

Figure B.27

[1]H-NMR for N4

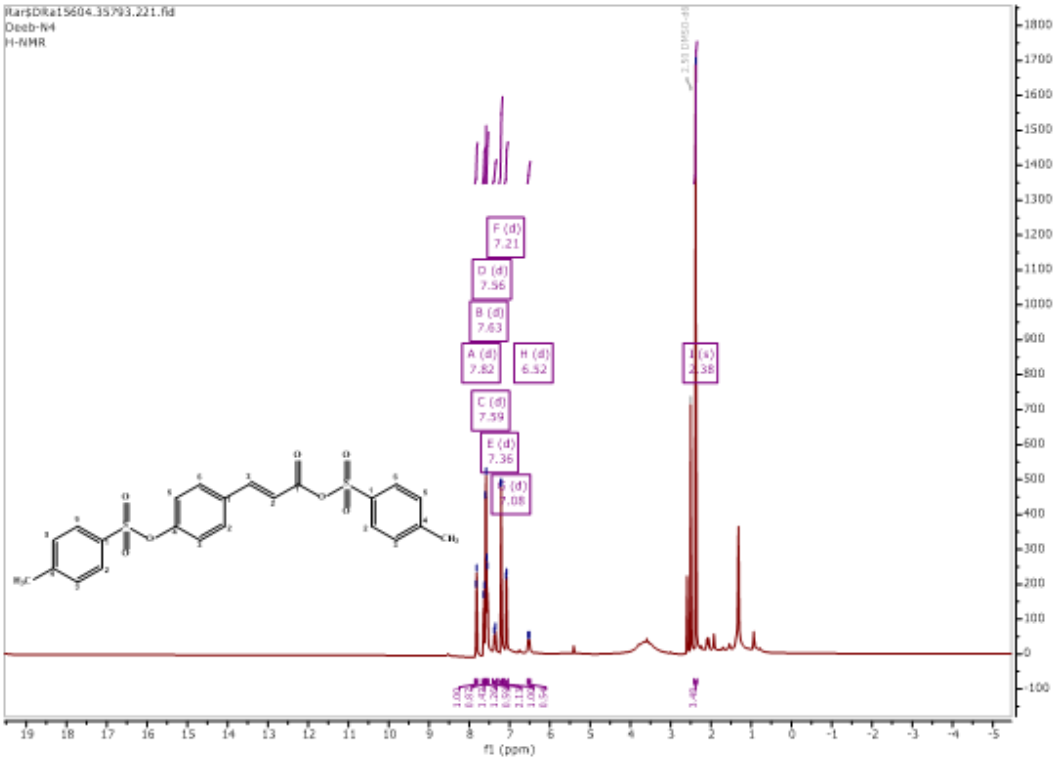

Figure B.28

[13]C-NMR for N4

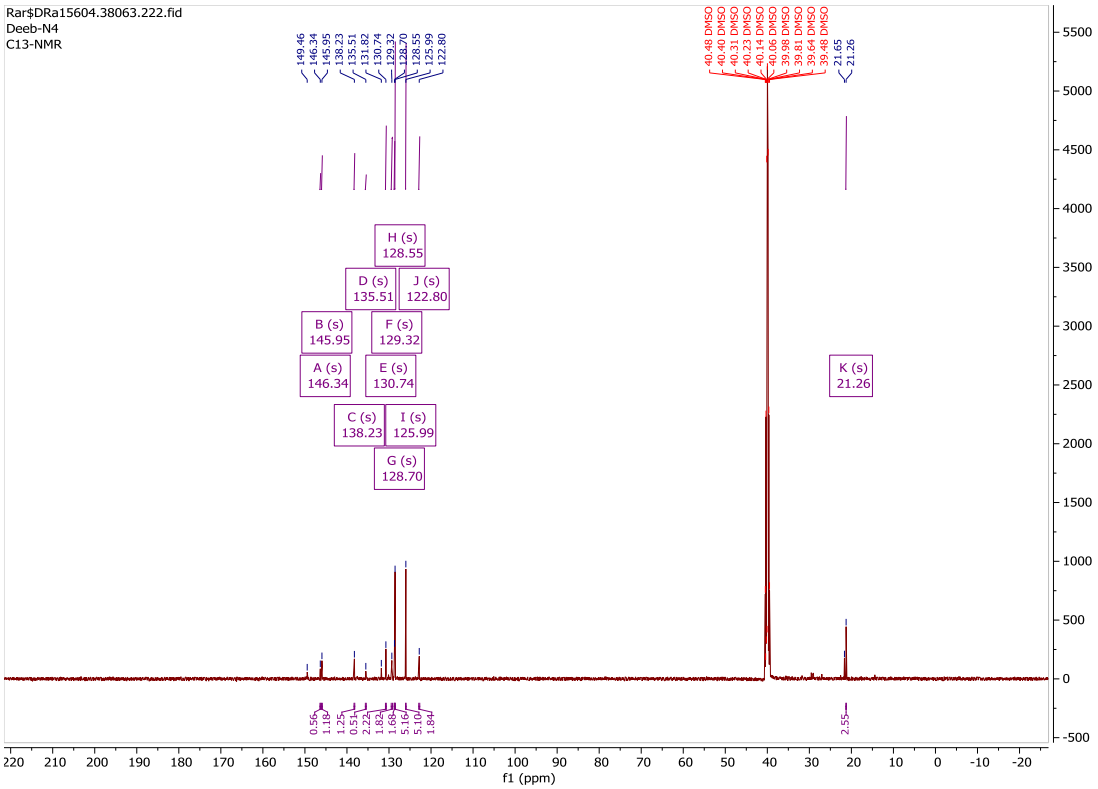

Figure B.29

^{13}C-NMR for N6

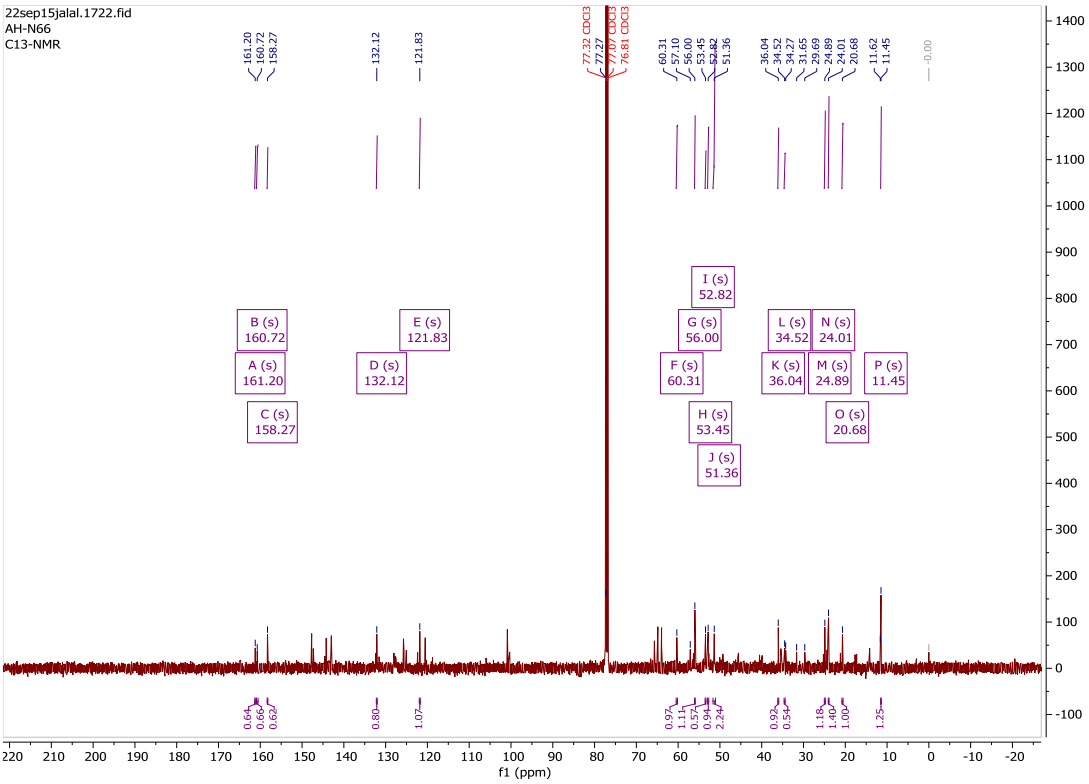

Figure B.30

^{13}C-NMR for N8

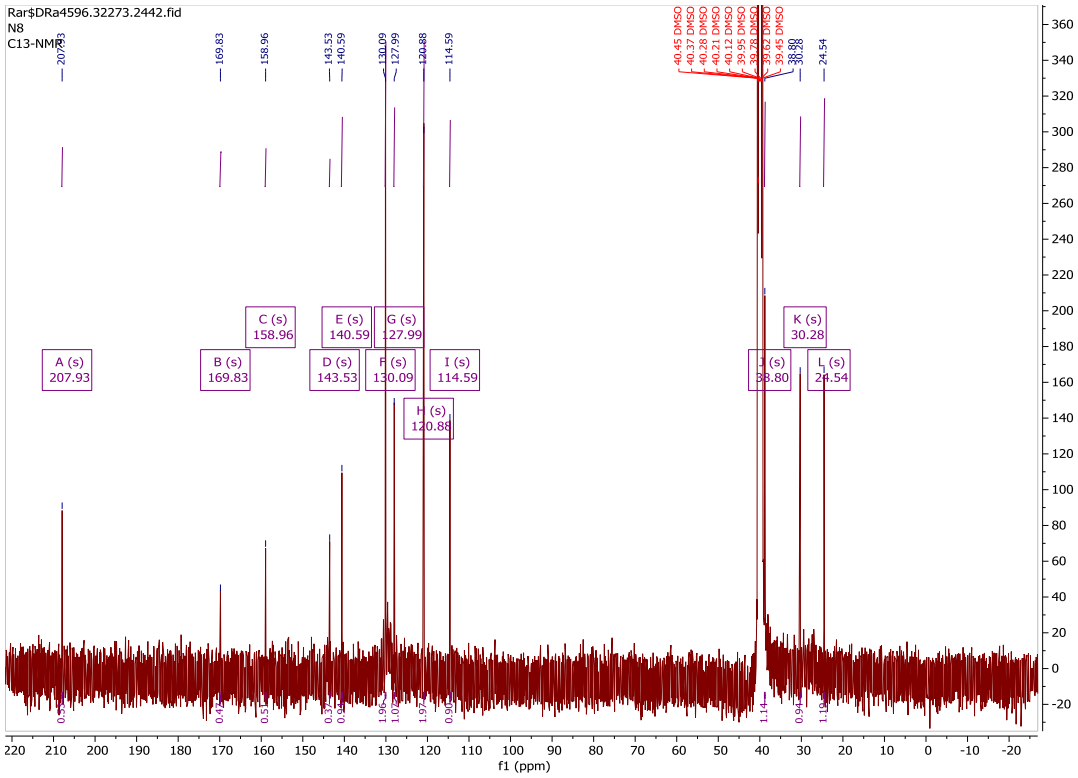

Figure B.31

[1]H-NMR for J16

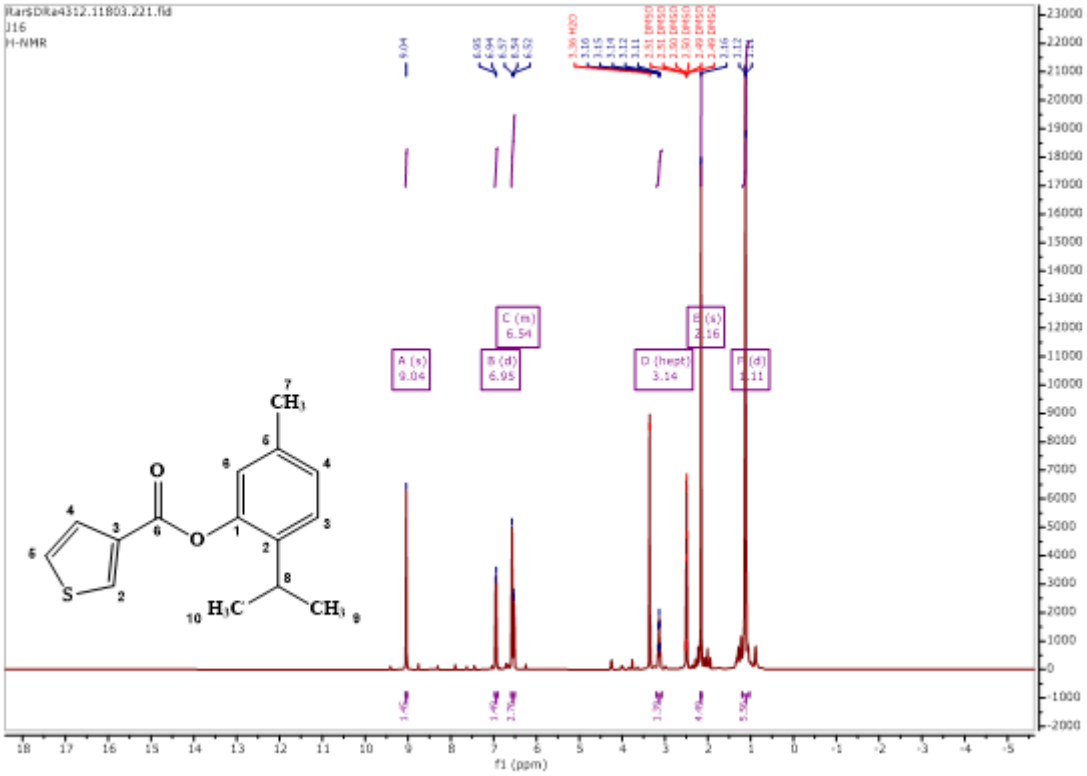

Figure B.32

[13]C-NMR for J16

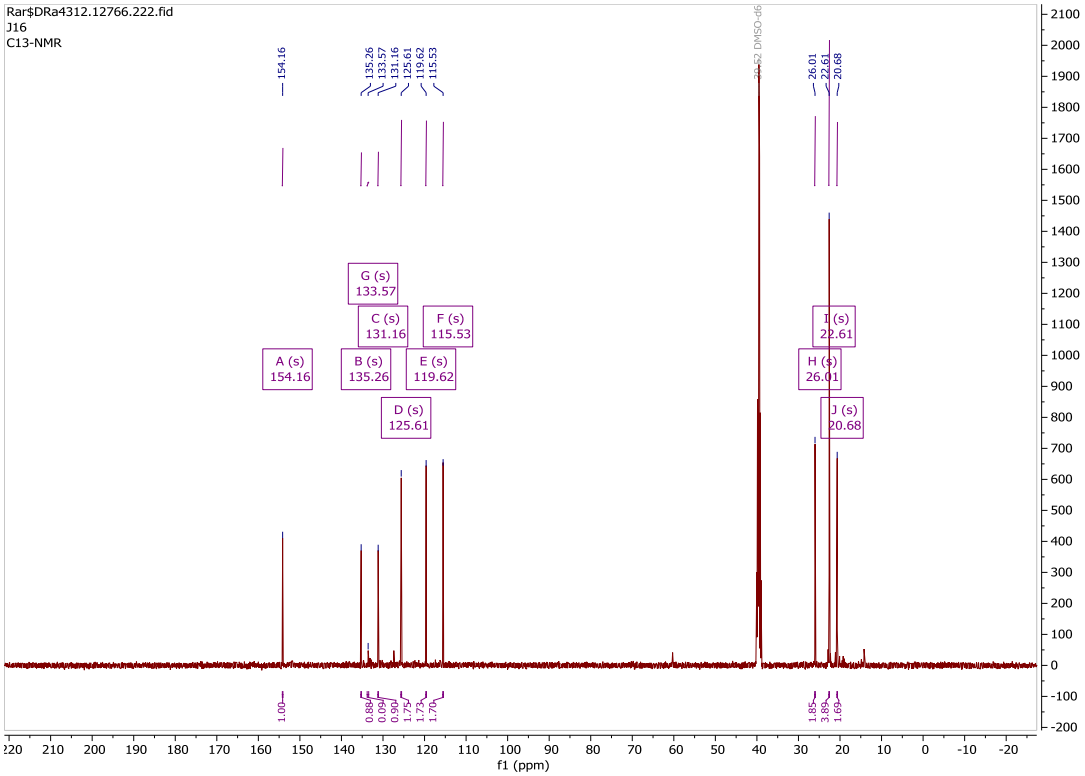

Figure B.33

[1]H-NMR for J10

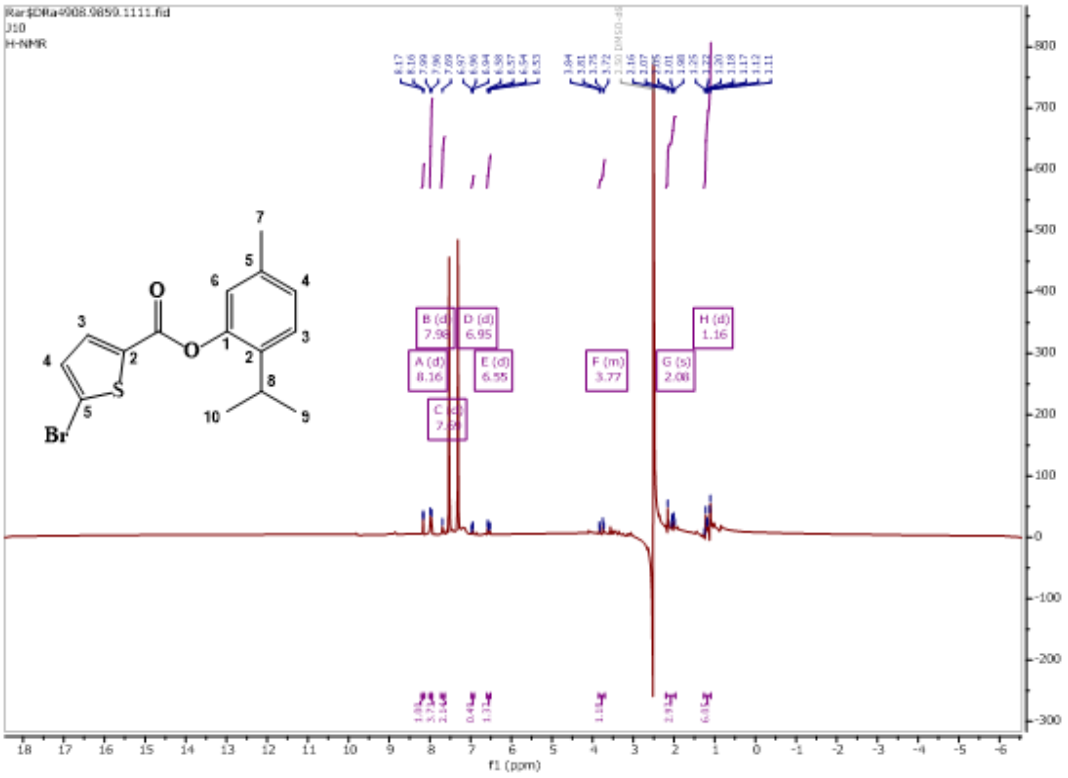

Figure B34

[13]C-NMR for J10

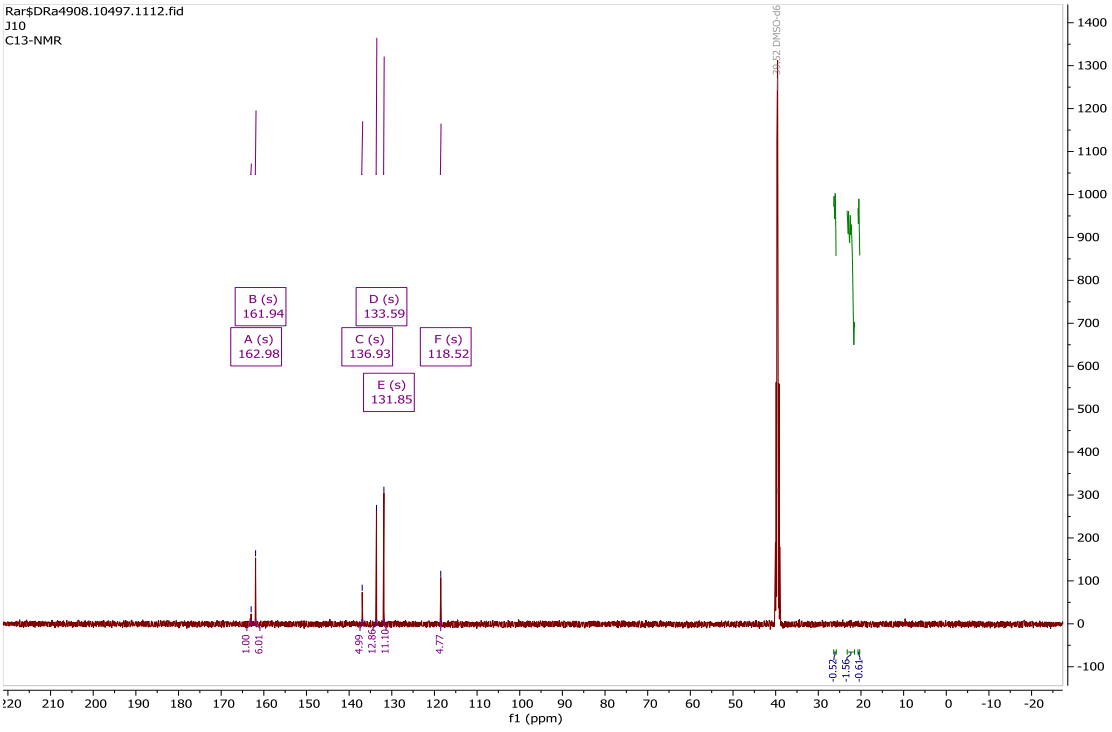

Figure B.35

[1]H-NMR for J11

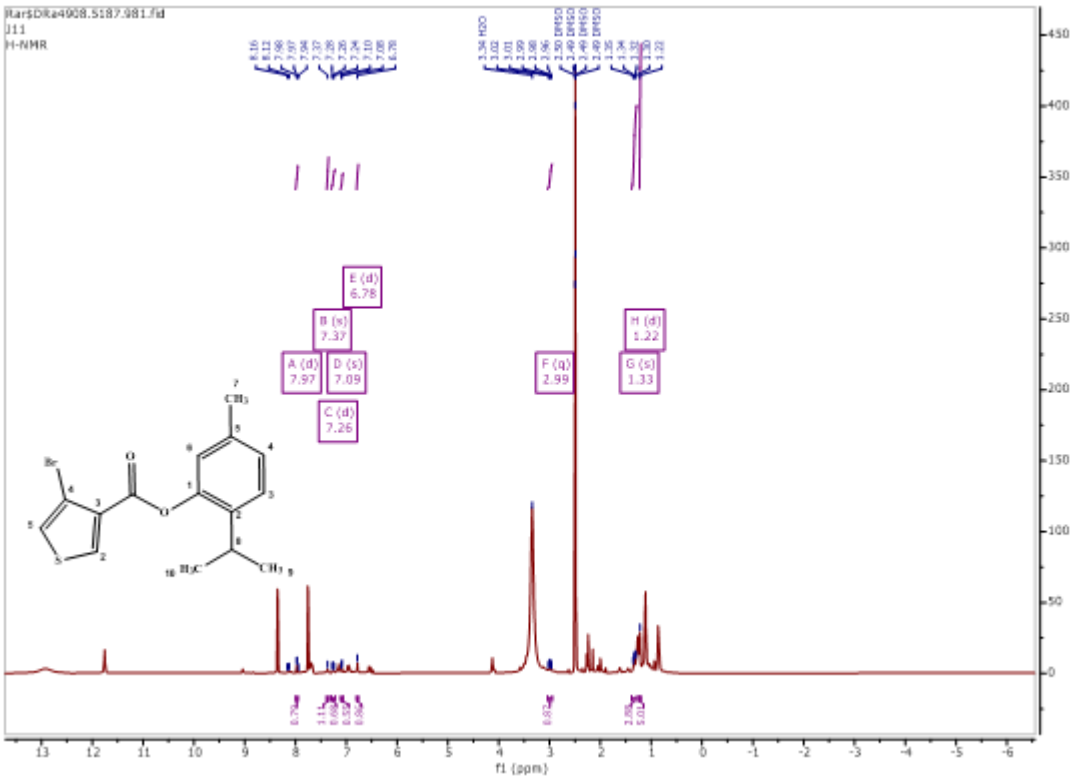

Figure B.36

[13]C-NMR for J11

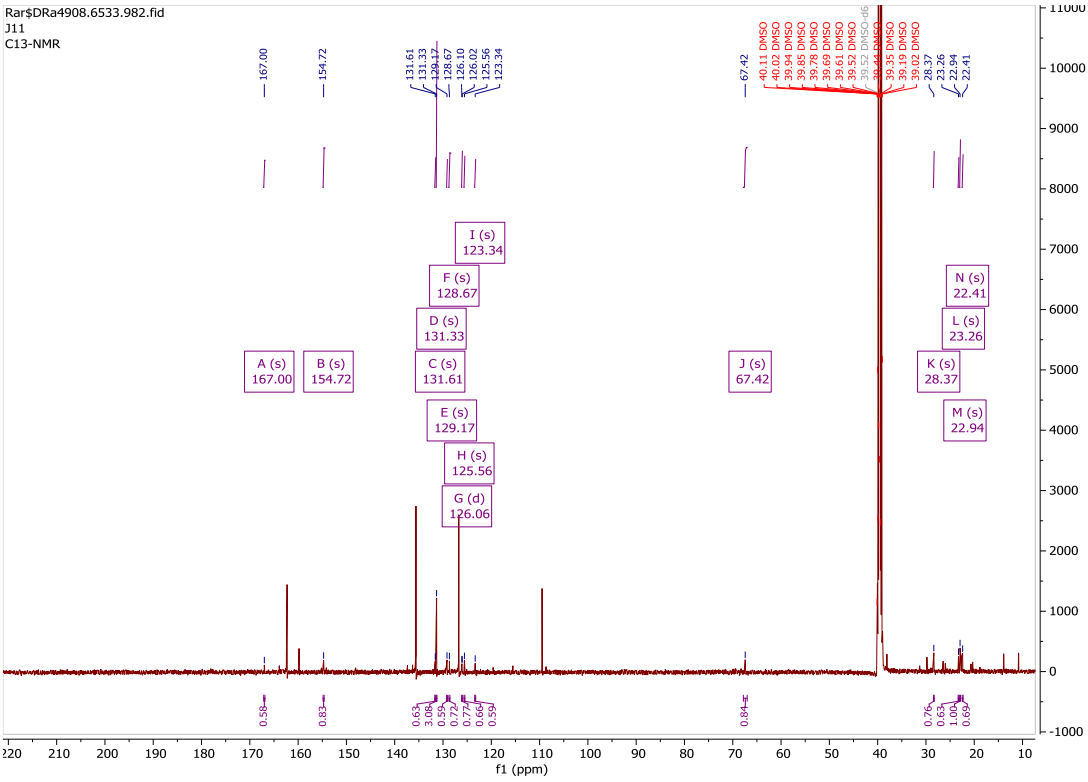

Figure B.37

[1]H-NMR for J12

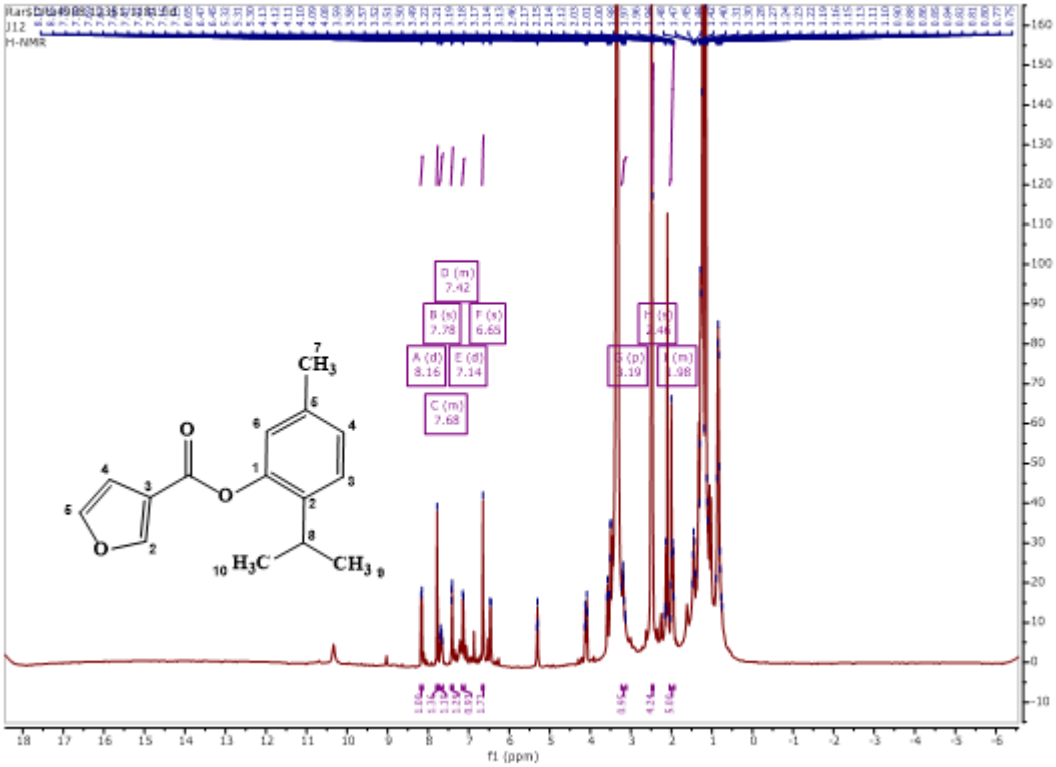

Figure B.38

[13]C-NMR for J12

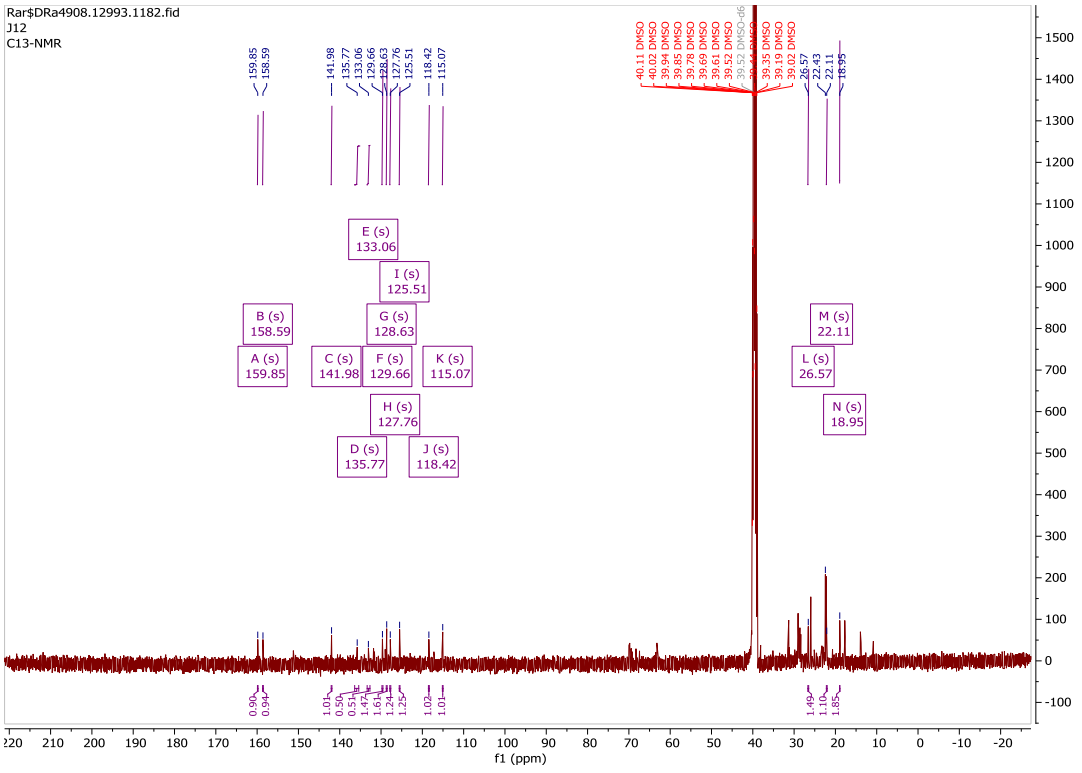

Figure B.39

LX-2 inhibition % for J3 and citronellol

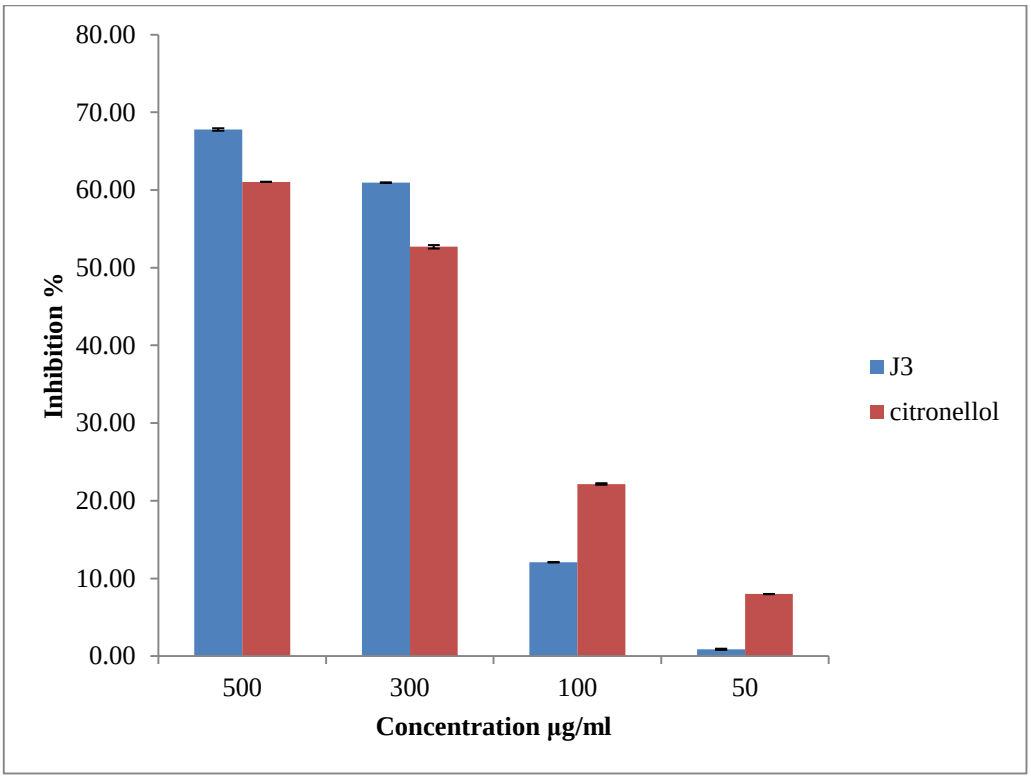

Figure B.40

IC_{50} of Hep-G2 of citronellol esters

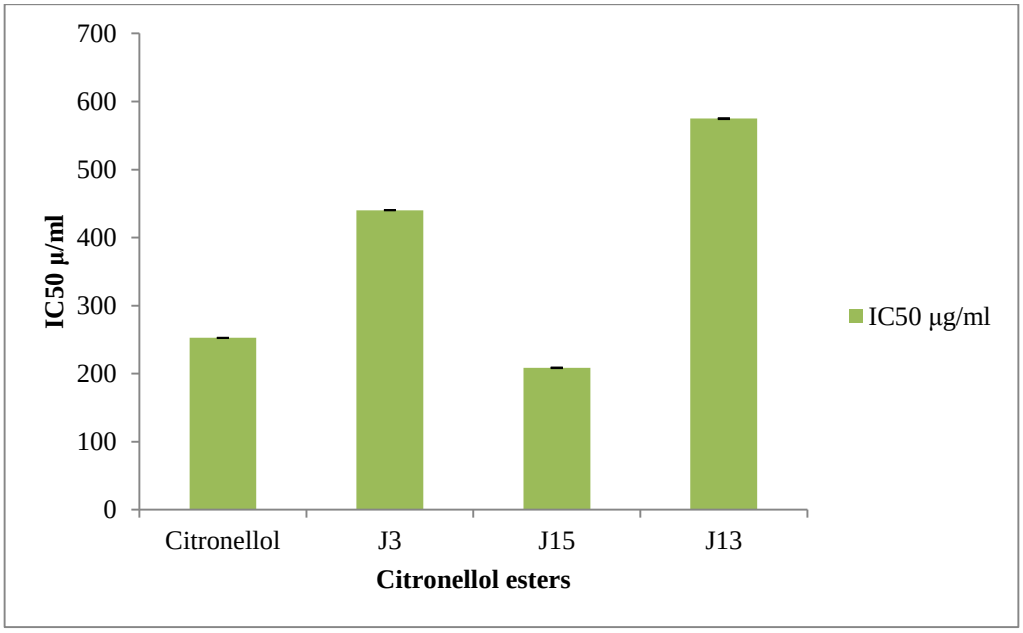

Figure B.41

Inhibition of LX-2 of J2 and Citronellol

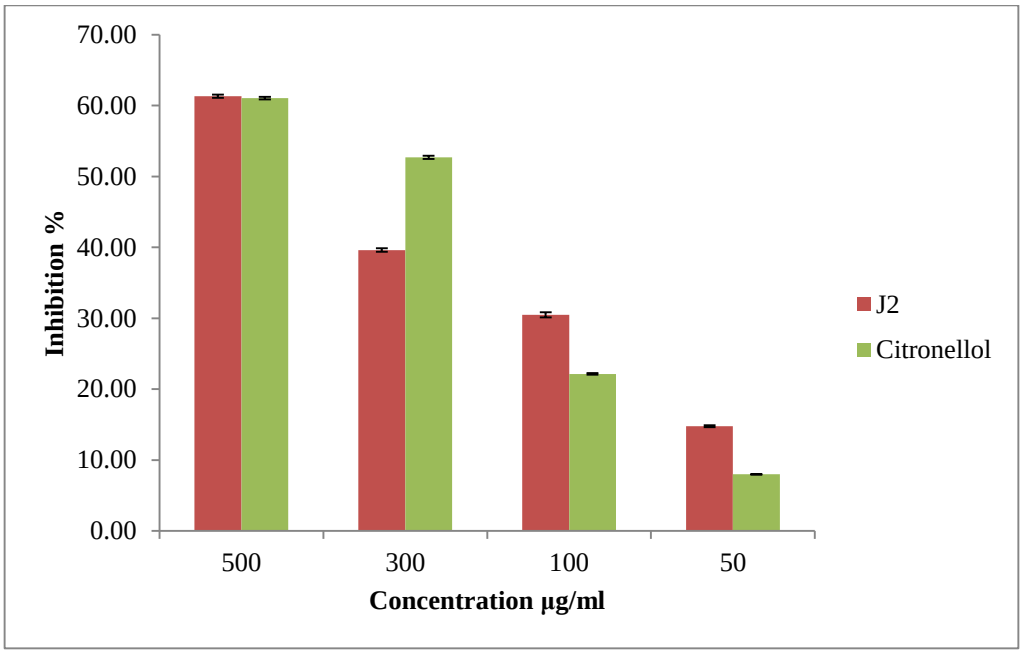

Figure B.42

Anticancer activity of N4 & N2 at 1000µg/ml

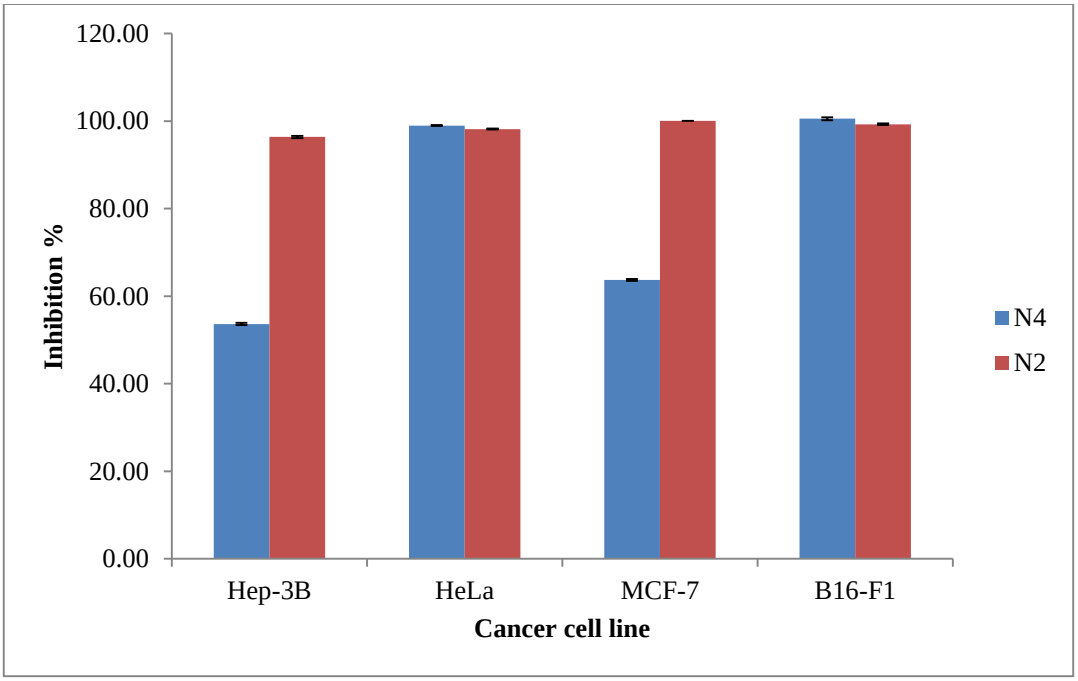

Figure B43

Anticancer activity of N4, N2 & p-CA at 500µg/ml

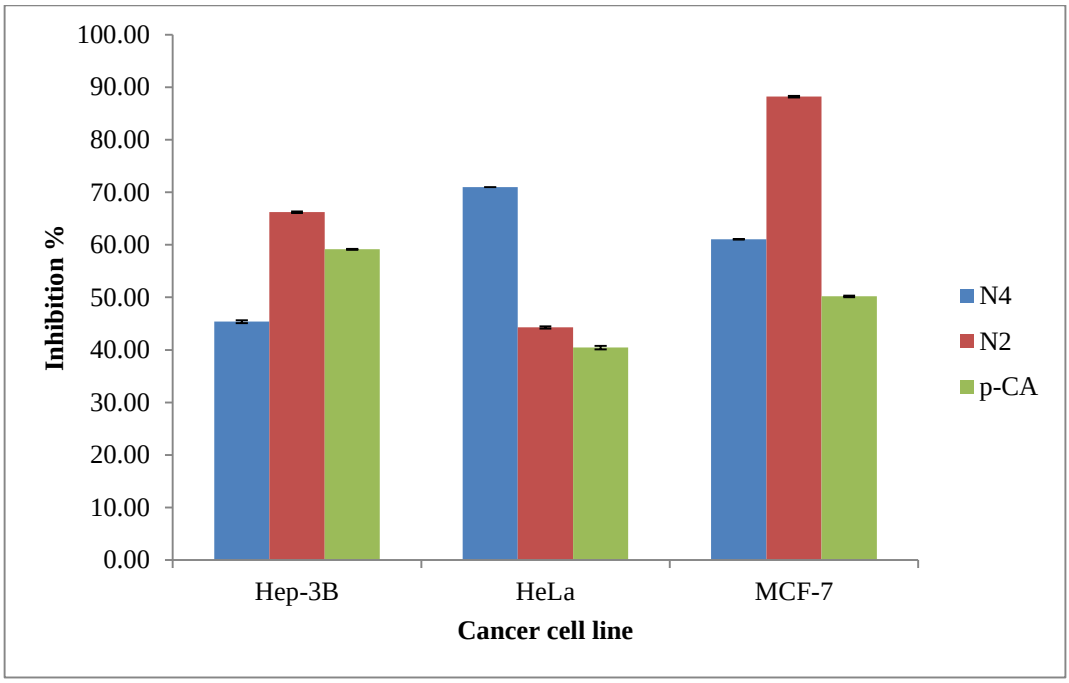

Figure B44

IC_{50} of J16 and Thymol

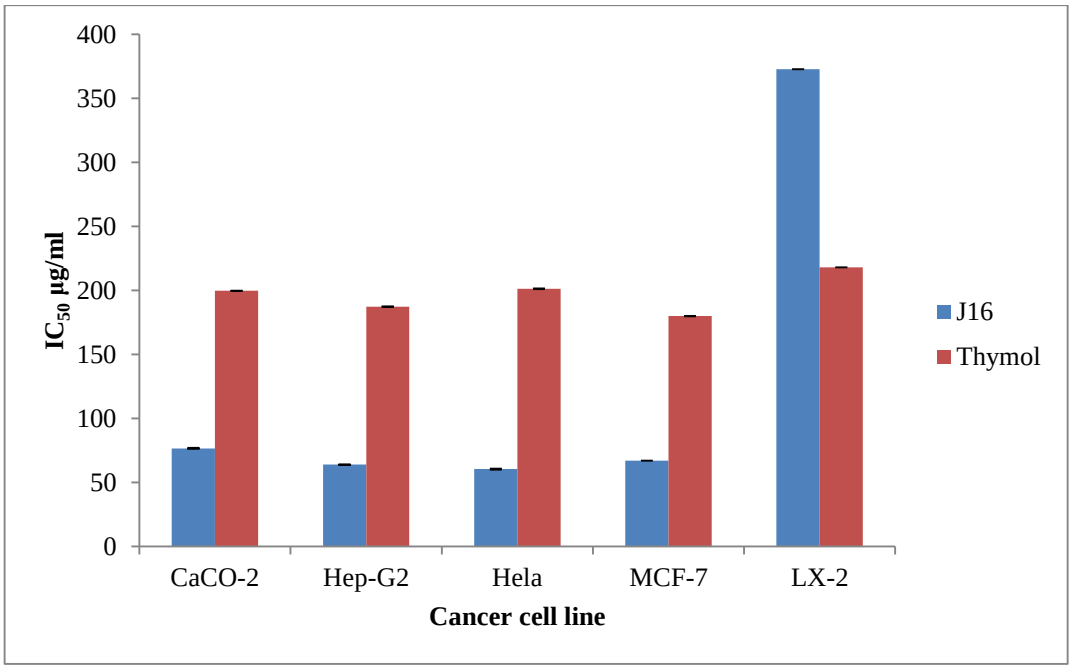

Figure B45

IC_{50} of J10 and Thymol

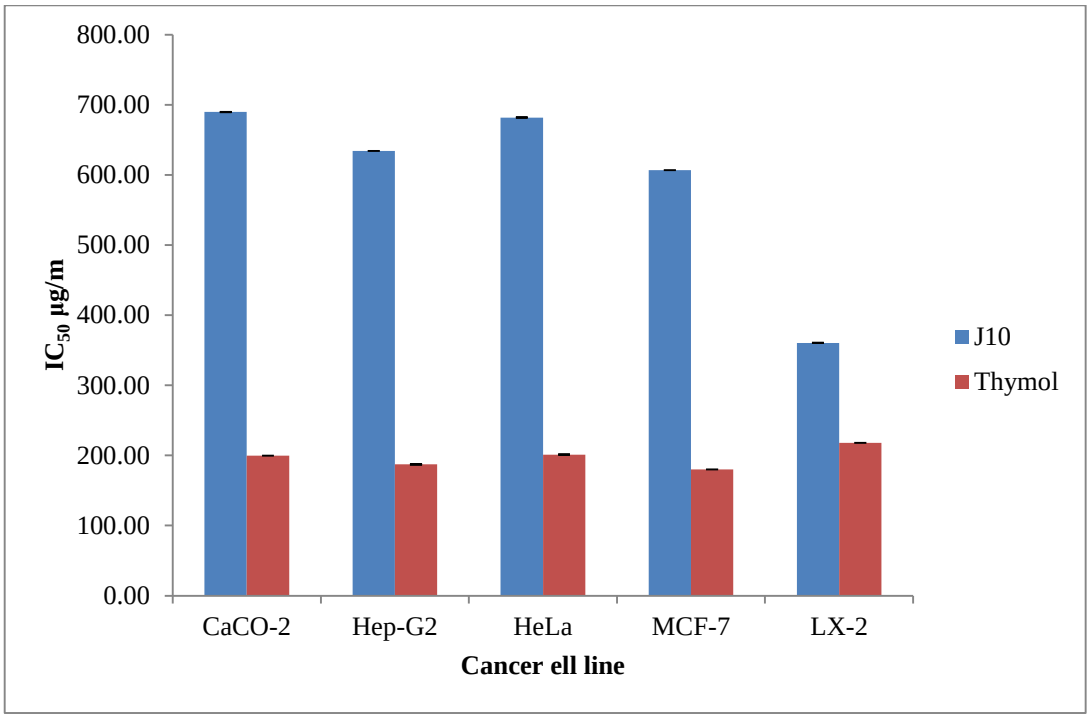

Figure B46

IC_{50} of J11 and Thymol

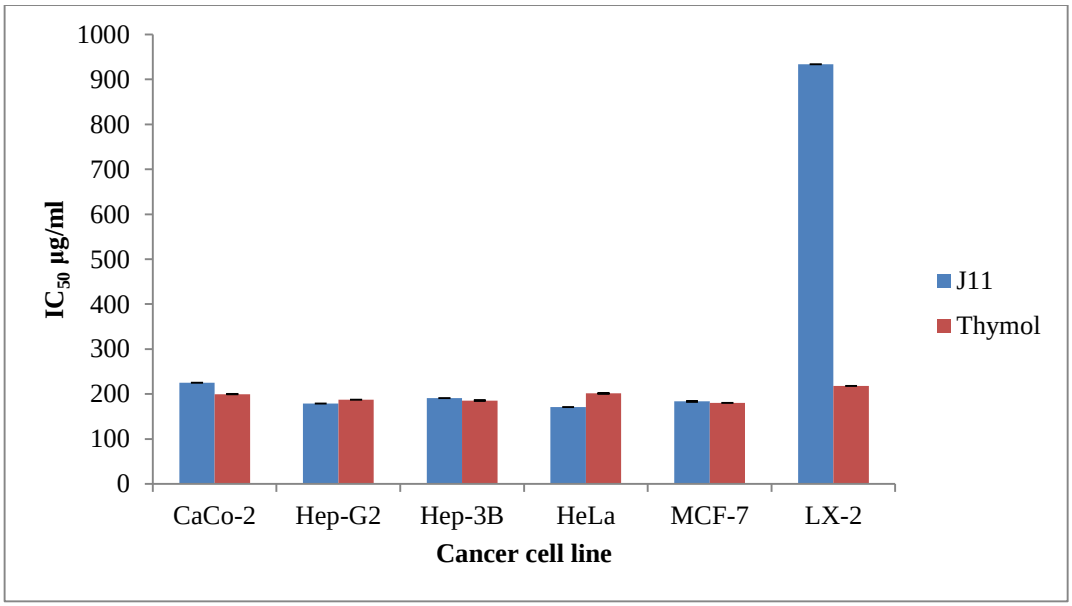

Figure B47

IC_{50} of J12 and Thymol

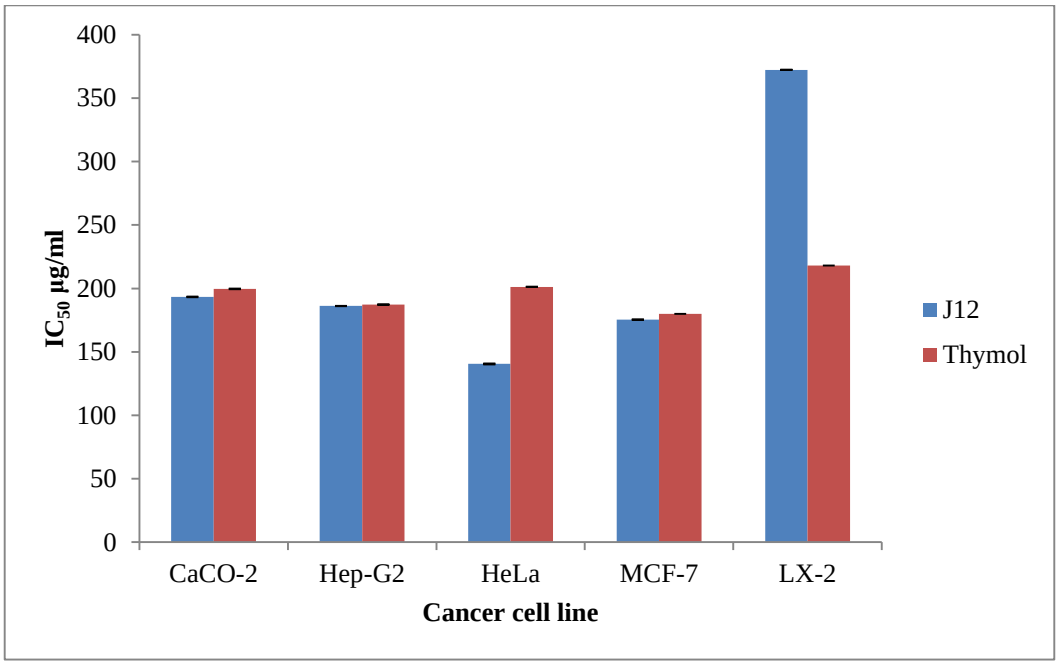

Figure B48

IC_{50} of Thymol and esters

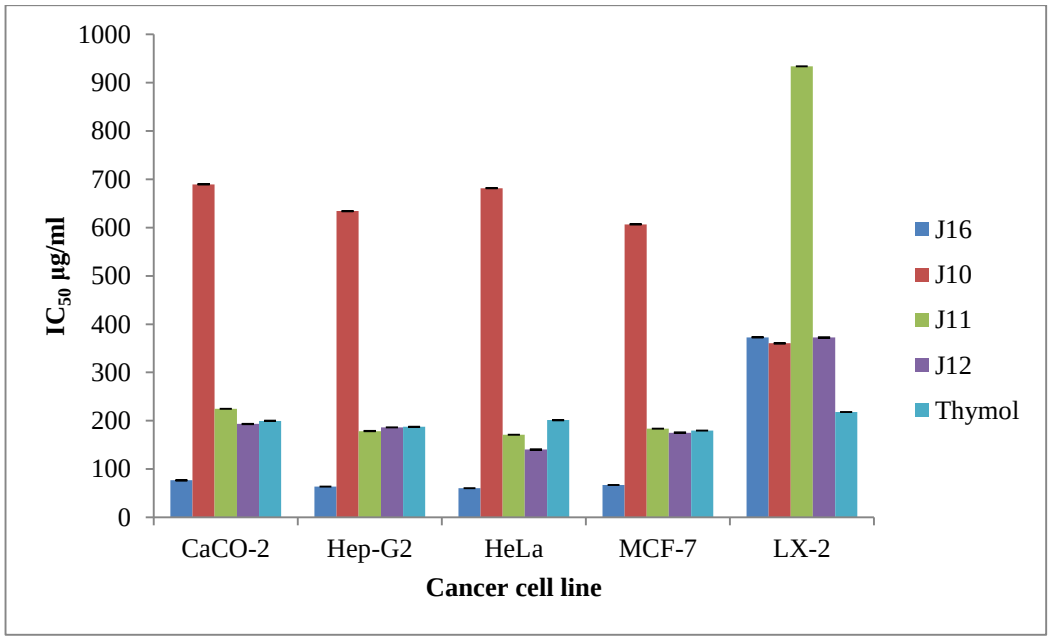

Figure B49

Antimicrobial activity of cis-jasmone amines

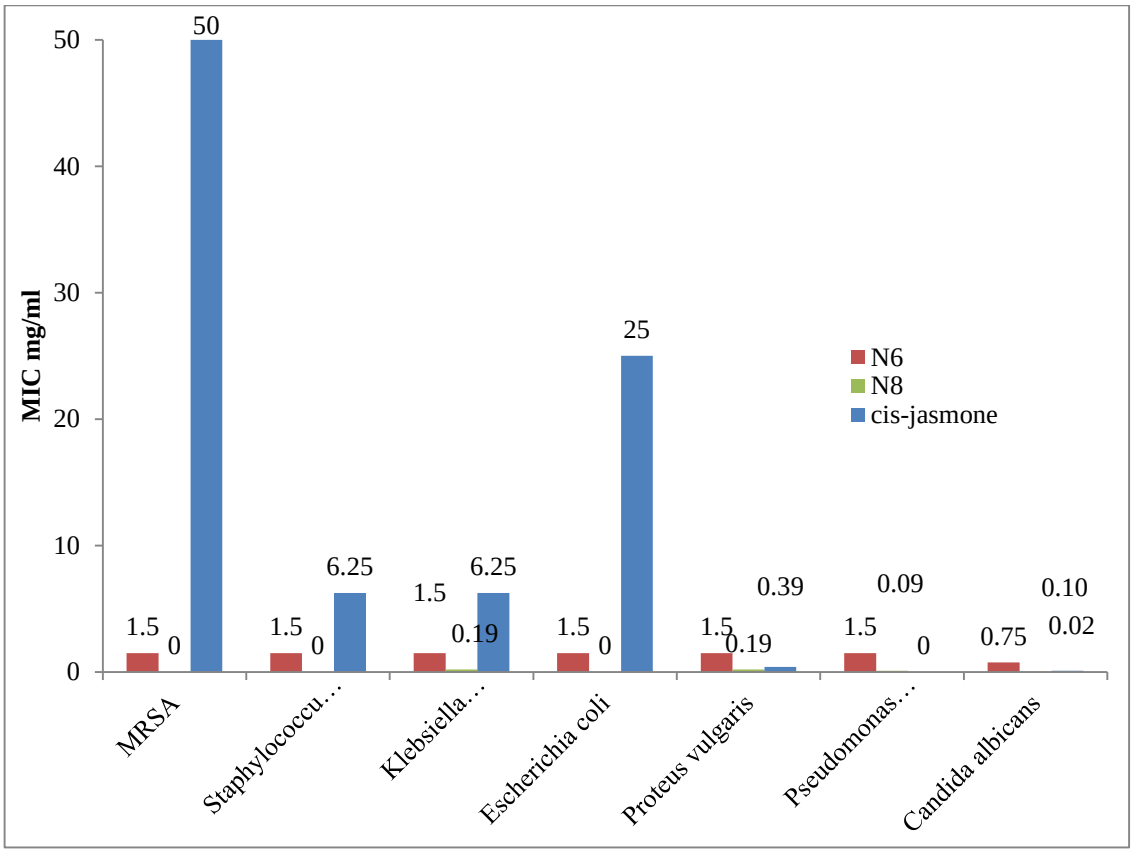

Figure B50

Antimicrobial activity of Thymol Esters

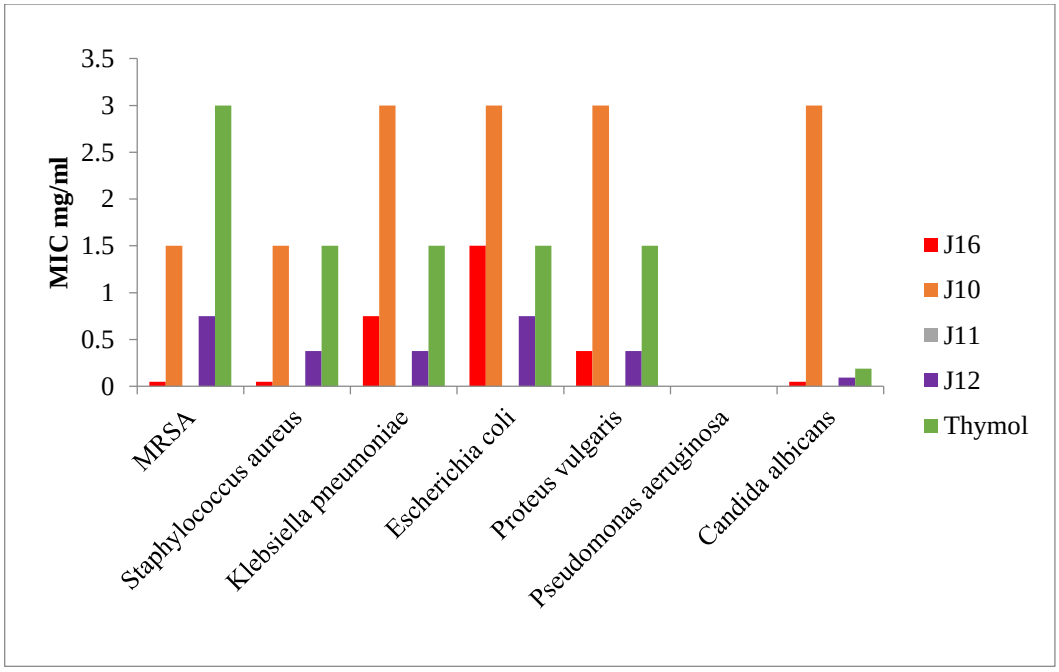

جامعة النجاح الوطنية
كلية الدراسات العليا

تفعيل المركبات الطبيعية المضادة للسرطان (*cis*-Jasmone، *p*-Coumaric acid، Citronellol و Thymol) التحضير والتوصيف والنشاط السام للخلايا

إعداد
نهايه محمد يوسف سلامه

إشراف
أ. د. محمد عبد الله النوري
أ. د. نضال جردات

قدمت هذه الأطروحة استكمالاً لمتطلبات الحصول على درجة الدكتوراه في الكيمياء،
بكلية الدراسات العليا في جامعة النجاح الوطنية في نابلس – فلسطين.

2024

تفعيل المركبات الطبيعية المضادة للسرطان (*cis*-Jasmone، *p*-Coumaric acid، Citronellol و Thymol) التحضير والتوصيف والنشاط السام للخلايا

إعداد

نهايه محمد يوسف سلامه

إشراف

أ. د. محمد عبد الله النوري

أ. د. نضال جردات

الملخص

يعد تفعيل المركبات الطبيعية التي تظهر ذ شاطًا بيولوجيًا أحد أكثر الطرق كفاءة لتخليق المواد الذ شطة بيولوجيًا لتحسين آثارها الدوائية أو لاستكشاف طرق علاجية جديدة.

تهدف هذه الدراسة إلى تحضير مشتقات جديدة من المركبات النشطة بيولوجيا بما في ذلك السيترونيلول، حمض الكوماريك، *cis*-jasmone، والثيمول عن طريق تعديل مجموعاتها الوظيفية واختبار ذ شاطاتها البيولوجية الجديدة فيما إذا كان هناك تحسن أو انخفاض في هذه الأنشطة.

طرق تحضـــير مركبات جديدة مثل الاســـترات والأميدات والأنهيدريدات والأمينات من خلال تفاعلات تكثيف الكحولات مع الأحماض الكربوكســـيلية، وبطريقة الإضـــافة مايكل. تم التعرف على المركبات الجديدة عن طريق تحليل FT-IR و .NMRتم استخدام اختبار MTS لتقييم نشاطهم المضاد للسرطان. تم استخدام طريقة تخفيف المرق لتقييم نشاطها المضاد للميكروبات.

أظهرت بعض المشتقات الجديدة من المنتجات الطبيعية أنشطة مضادة للسرطان ومضادة للميكروبات أكثر فعالية من المركب الطبيعي البادئ، بينما أظهرت البعض الآخر فعالية أقل من المركب الطبيعي البادئ الذي تم استخدامه لتحضير مشتقات جديدة، ولكنه يحافظ بشكل أفضل على خط الخلايا الطبيعي.

تم تحضير المشتقات المحضرة حديثا بنجاح والتحقق من بنيتها عن طريق التحليل الطيفي. تم اختبار أنشطتهم البيولوجية ضد خطوط السرطان والسلالات الميكروبية المختلفة. من بين استرات الستروئيلول كان J15 هو الأكثر فعالية ضد سرطان الكبد Hep-G2 وكان J14 *p*-CA ester أقوى عامل مضاد للسرطان ضد خطوط الخلايا السرطانية CaCo-2 و Hep-G2 و HeLa و MCF-7 ، كما أظهر J14 نشاطًا أعلى بشكل مميز ضد جميع الكائنات الحية الدقيقة باستثناء *Pseudomonas aeruginosa*. أظهر أميد J19 *p*-CA نشاطًا مضادًا للميكروبات ضد الإشريكية القولونية، والمتقلبة الشائع، و *P. aeruginosa*، و *C. albicans*كان أنهيدريد N2 *p*-CA هو الأقوى ضد خطوط خلايا Hep-3B و MCF-7بينما كان N4 هو الأقوى ضد خطوط خلايا HeLa. من بين أمينات*cis*-jasmone ، كان N6هو الأكثر فعالية ضد خطوط HeLa و B16-F1cell.أظهر الأمين N8 أعلى نشاط مضاد للميكروبات بشكل مميز ضد*Klebsiella pneumoniae* ، *P.* vulgaris، *P. aeruginosa*، و *C. albicans*كان استر الثيمول J16 هو الأقوى ضد CaCo-2 و Hep-G2و HeLaو MCF-7،و B16-F1وأظهر أعلى نشاط بشكل مميز ضد جميع الكائنات الحية الدقيقة باستثناء ضد *Escherichia coli* حيث كان استر الثيمول J12 كان الأكثر فعالية.

الكلمات المفتاحية: مركبات طبيعية مضادة للسرطان، سيترونيلول، الثيمول، *cis*-Jasmone، *p*-CA.